Chapter – 2

Synthesis, Characterization and Anticancer Activity of Some 2-hydroxy-1,4-Napthoquinone (Lawsone) Based Mannich Bases

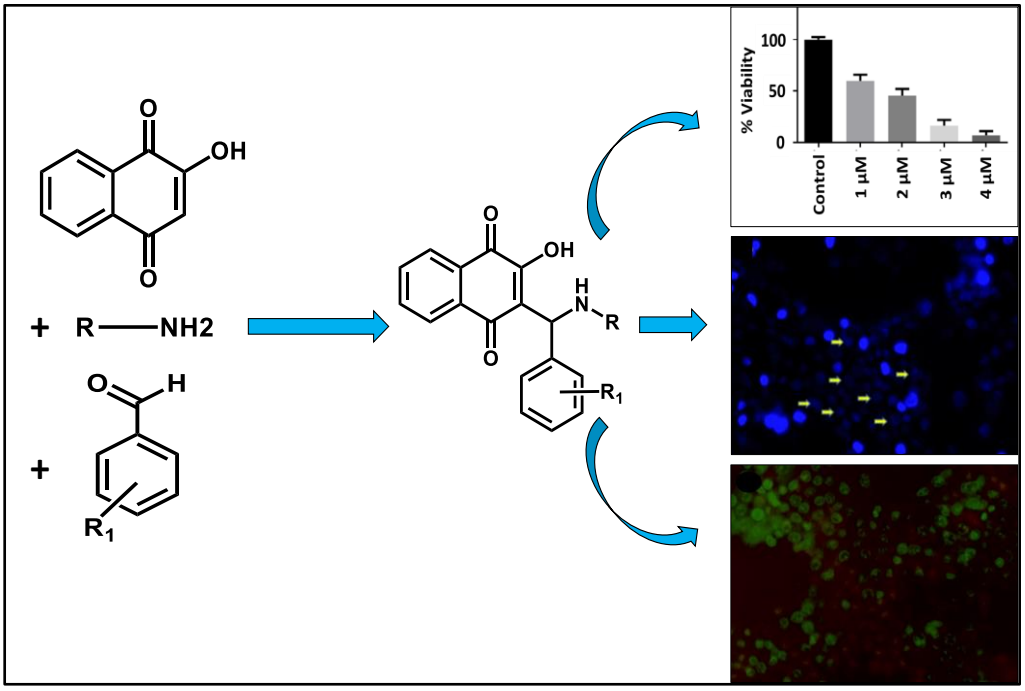

Published in *Synthetic Communications*, 2020, *50*, 1724-1735

2.1 Introduction

Cancer is a major health problem worldwide and the second most common cause of death[1]**.** The strategies used for combating cancer generally include specialized surgical operations, radiation therapy, and chemotherapy. Despite continued research efforts toward the development of anticancer (chemotherapeutic) drugs, cancer remains a primary cause of death[2]. However, due to toxicity and drug resistance problems encountered with many currently available treatments, a great deal of effort has been devoted to the exploration and screening of new drugs for combating cancer which is one of the paramount goals in medicinal chemistry.

Quinone containing natural products has a notable pharmacophoric element as reported by the National Cancer Institute. It exhibits an array of pharmacological properties and it is one of the important subunits found in many drugs such as doxorubicin, daunorubicin, mitoxantrone, and mitomycin-C which have been used for clinical trials for cancer therapy[3]**.** Due to the intimate relationship between quinones and the biochemical processes of cells, these compounds have been extensively explored in the synthesis of several bioactive compounds with antitumor activities [4]**.**

Naphthoquinones are members of the quinone family, as was mentioned in **Chapter 1**. There have been reports of a variety of biological activities, including anticancer, antibacterial, antiparasitic, and antioxidant, in both natural and synthetic derivatives of naphthoquinone[5]**.** There are several known naturally occurring naphthoquinone derivatives, including Lawsone, Plumbagin, Juglone, Menadione, Thymoquinone, Lapachol, and Parvaquone [6]. Among all these naphthoquinones, Lawsone (2-hydroxy-1, 4-naphthoquinone) is one of the simplest naturally occurring naphthoquinones which is obtained from dry powdered leaves of the henna plant (*Lawsonia inermis*) and showed weak toxicity both to hepatocytes and various tumor cell lines [7].

However, introducing nitrogen atom in lawsone or naphthoquinone enhances its anticancer activities [8]. Nitrogen-containing derivatives and metal complexes are known to have enhanced biological activity. 2-hydroxy (3-aminomethyl)-1,4- naphthoquinone and its Pt^{2+}complexes derived from lawsone were reported to have cellular accumulation and topoisomerase against cancer cells [9]. Similarly, ruthenium (II) complexes of lawsone are known for inhibiting tumor cell lines by apoptosis[10]. Quinonoid compounds derived from lawsone are known to have cytotoxic evolution against cancer cells [5].

One of the strategies for introducing nitrogen atom in lawsone is the formation of its Mannich base via mannich reaction. Mannich bases sometimes referred to as compounds that carry beta-amino ketone, are the final product of the Mannich reaction. The mannich reaction, a nucleophilic addition reaction that forms carbon-carbon bonds, is a crucial step in the synthesis of a wide range of natural products, medicines, and other substances **(figure 2.1).** The construction of compounds containing nitrogen depends on the Mannich process[11] .

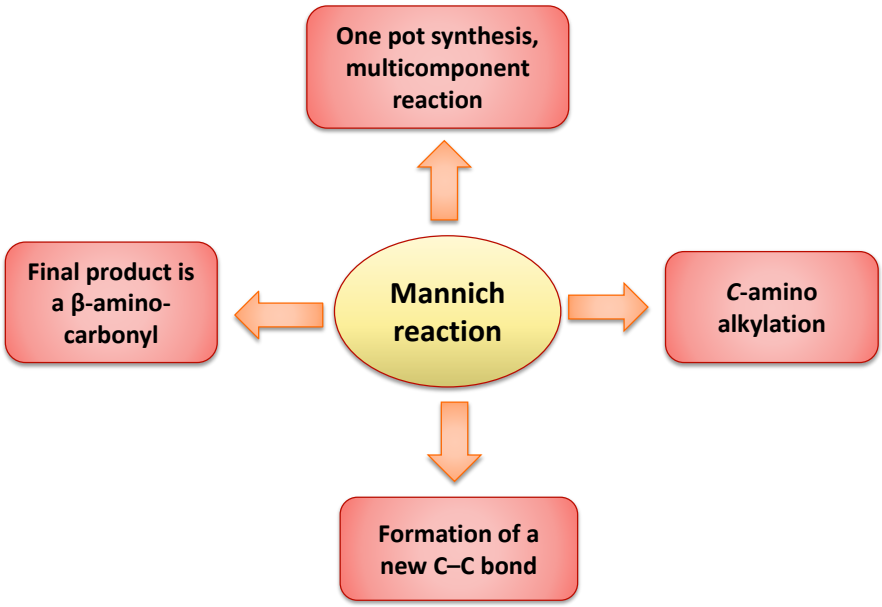

Figure 2.1 Features of Mannich reaction

Ibrahim Al Nasr et al. recently reported lawsone Mannich bases derived from salicylaldehyde or nitro furfural for antiparasitic activity [12]. Similarly series of anticancer active Mannich bases derived from lawsone recently reported [13,14]. Cytotoxicity of Mannich bases has been attributed partially to the α,β-unsaturated ketones liberated by deamination of the hydrogen atom of the amine group [11]. These α,β-unsaturated ketones have a markedly greater affinity for thiols over amino and hydroxyl nucleophiles. This preferential affinity may result in a lack of mutagenicity and carcinogenicity which are associated with certain alkylating agents due to presumed interaction with nucleic acids [15].

In this study, we have successfully explored a series of anticancer active 3-aminomethyl-1,4-naphthoquinone synthesized from lawsone via one-pot mannich reaction to

investigate their cytotoxicity/anticancer activity effects on HepG2 cell line (Human liver carcinoma cell line).

2.2 Results and Discussion

2.2.1 Synthesis of mannich bases derived from lawsone

Mannich bases were synthesized from the reaction of lawsone with various amine and aldehydes using ethanol as a solvent on stirring at room temperature **(scheme 2.1).** The reaction was monitored by TLC, pet ether and ethyl acetate (5:5) used as a mobile phase for TLC. Products were recrystallized in hot ethanol. The yield of the compounds is in 54% to 85% range and the formation of compounds was confirmed by ^{1}H NMR, ^{13}C NMR, FT-IR, and Mass spectroscopy as discussed in **section 2.2.2.** Since we have used the classical method to synthesize Mannich base from lawsone without catalyst and ethanol as solvent, it follows the classical route of mechanism. It primarily forms the iminium ion by condensation of amine and aldehyde. Subsequently, the nucleophile lawsonate attacks the iminium ion (analogous to the enolate) to give a Mannich base [16].

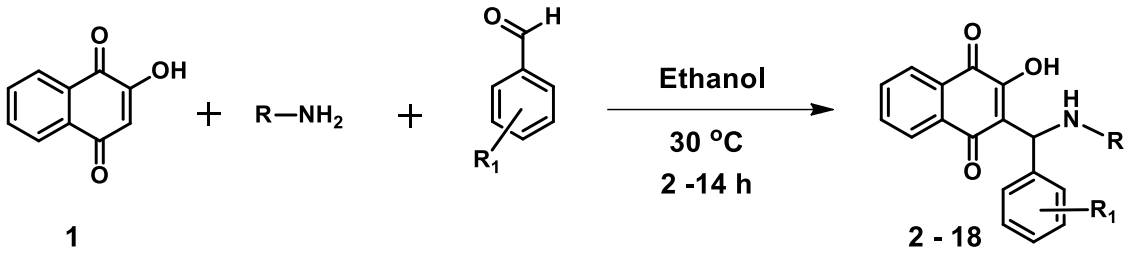

Scheme 2.1 Schematic for the synthesis of mannich bases derived from lawsone

All synthesized compounds are stable in solid state but tend to undergo decomposition in solution (DMSO, Ethanol, Methanol, and Chloroform) after a long period of time as reported in the literature [14].

2.2.2 Spectral characterization

The FT-IR spectra of the compounds show a broad band from 3450 to 3300 cm^{-1} corresponding to the hydroxy group and secondary amine (-NH) of lawsone mannich base. The band in the range of 3050-3180 cm^{-1} is assigned to the =C-H stretching of the aromatic ring. Several weak bands were observed in the range of 2400-2900 cm^{-1} attributed to aromatic and aliphatic C-H groups. The strong band of carbonyl group was

observed around 1680-1695 cm^{-1}. The bending frequency of δ_{N-H} was observed at 1530 cm^{-1}. The strong ν_{c-o} band 1280 cm^{-1} was attributed to the naphthoquinone group. In the case of the Mannich base containing nitro group, symmetric and asymmetric stretching frequency for NO_2 was also observed at 1593 cm^{-1} and 1349 cm^{-1} respectively.

In ^{1}H NMR spectra of the compounds, four hydrogens of naphthoquinone appear in the δ 7-8 ppm region as double doublet (dd), doublet of double doublet (ddd), and triplet of doublet (td). The protons of aromatic aldehyde also appear in the expected region (δ 7-8.5 ppm). The values of the coupling constant (J) are in well agreement with a literature report [17]. The aliphatic hydrogens appear in δ 0.8 to 2.8 ppm as multiplets or triplets. A singlet is observed in the range of δ 5.4-6.1 ppm due to the formation of a new bond between aldehyde, amine, and lawsone. The broad peak between δ 9-10 ppm was also observed due to hydrogen bonding between hydroxy group (-OH) and secondary amine (-NH) of Mannich Base.

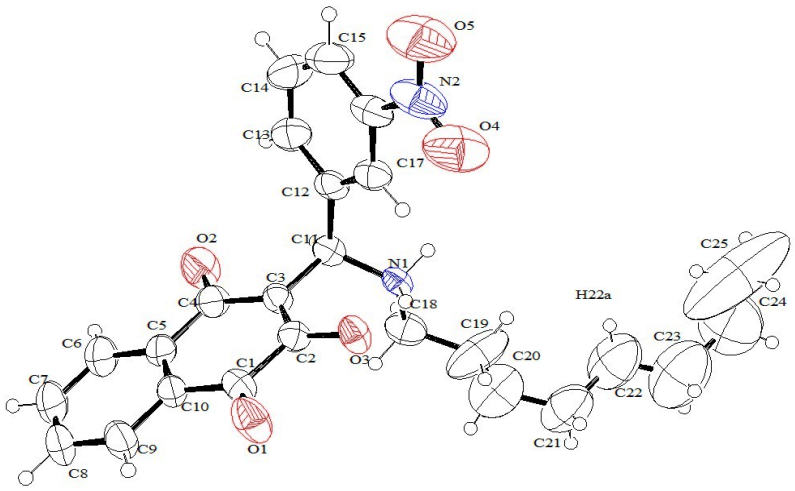

Figure 2.2 ORTEP diagram of compound 2 with atom numbering scheme. Displacement ellipsoids are drawn at the 50% probability.

The ^{13}C NMR spectra exhibited peaks at δ 184, and 179 ppm corresponding to the naphthoquinone carbonyl group. While the carbon close to the carbonyl group was observed near δ 171, and 155 ppm. One ternary carbon peak was observed around δ 54 ppm due to newly formed C-C bond. Aliphatic protons were seen between δ 14 and 46 ppm, while all other aromatic carbons were seen in the aromatic area between δ 110 and 134 ppm.

Mass spectra of all synthesized compounds were recorded and the [M+1] values of all compounds matched with theoretical values. All spectroscopic data confirm the structure of compounds. All spectra are provided in **section 2.6**

Table 2.1 Crystal data and structure refinement of 2

Empirical formula	$C_{25}H_{26}N_2O_5$	Z	4
Formula weight	434.48	μ/mm^{-1}	0.087
Temperature/K	293(2)	F(000)	920.0
Crystal system	monoclinic	Crystal size/mm^3	0.40× 0.3 × 0.25
Space group	$P2_{1/1}$	Radiation	MoKα (λ = 0.71073)
a/Å	15.359(3)	2Θ range for data collection/°	6.648 to 58.28
b/Å	8.9761(17)	Reflections collected	25816
c/Å	18.292(4)	Independent reflections	5469
α/°	90.00	Data/restraints/parameters	5469/0/290
β/°	113.47(2)	Goodness-of-fit on F^2	1.315
γ/°	90.00	Final R indexes	R_1 = 0.1259, wR_2 = 0.2623
Volume/ $Å^3$	2313.1(9)	Peak and hole	0.63 and -0.29 $Å^{-3}$

One of compound **2** was crystallized from ethanol to obtain a crystal suitable for single crystal diffraction. The monoclinic (space group $P2_{1/1}$) crystal of the **2** exhibits the structure as seen in its ORTEP diagram **(figure 2.2).** The crystal data and structure refinement data of **2** are depicted in **table 2.1.** Single crystal and all spectroscopic data confirm the synthesized mannich bases crystalize in monoclinic crystal system and structure of compounds.

2.2.3 Biological evaluation and Structure Activity Relationship (SAR)

The synthesized compounds were screened for MTT assay[18] and half inhibitory concentration (IC_{50}) values for the compounds were determined. The general structure of compounds is shown in **figure 2.3.** All compounds were screened at 1, 2, 3, 4, 5, and

10μM concentrations. The IC_{50} values in μM concentration were determined from the MTT assay and presented in **table 2.2.** The results obtained in a cytotoxicity assay for Mannich bases of lawsone analogs accounted for decreased cell viability in a dose-dependent manner. The parent compound Lawsone did not exhibit significant cytotoxic activity at the concentrations used for the studies. The anticancer drug Doxorubicin hydrochloride was taken as a positive control. As shown in **Table 2.2**, all synthesized compounds showed promising activity except **11** (IC_{50} 389.40 μM), while **10** is not active. MTT graph of the most active compounds are shown in **figure 2.4**.

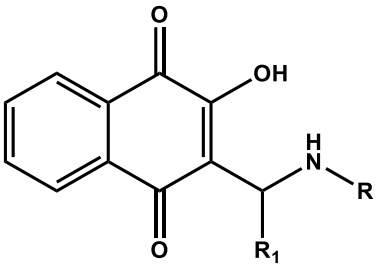

Figure 2.3 General structure of the compound

Table 2.2 Table of compounds with their IC_{50} value and structure

Comp.	R	R_1	IC_{50} (μM)
2	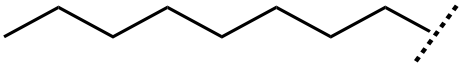	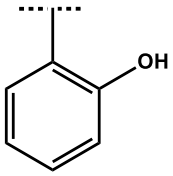	1.68
3	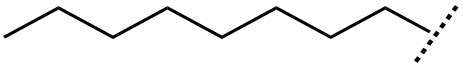	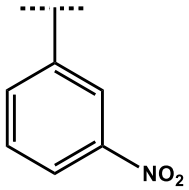	8.41
4	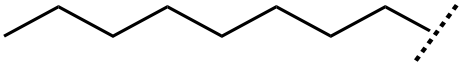	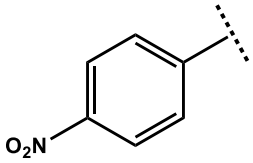	12.43
5	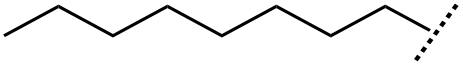	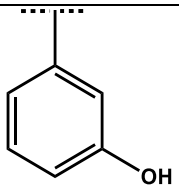	14.43

6	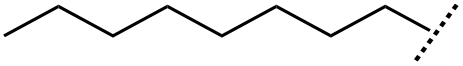	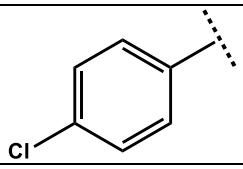	56.82
7	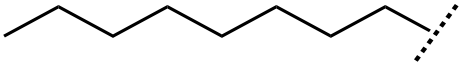	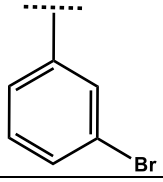	37.19
8	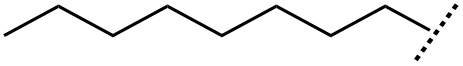	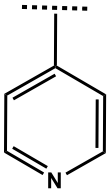	4.56
9	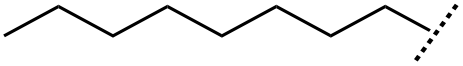	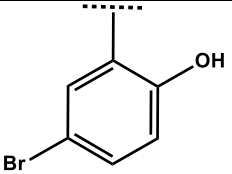	1.64
10	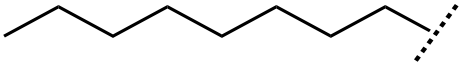	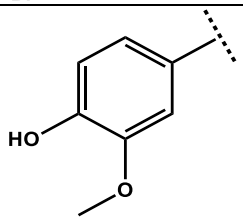	Not Active
11	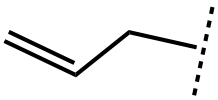	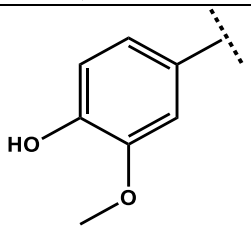	389.40
12	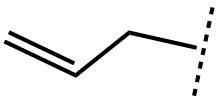	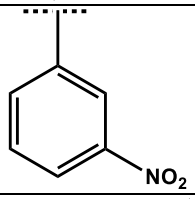	11.01
13	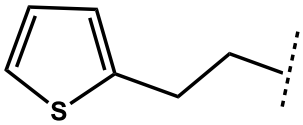	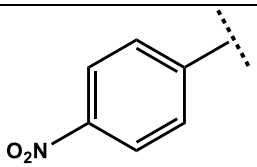	7.29
14	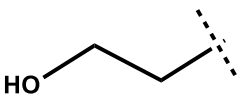	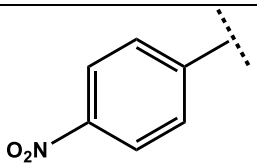	4.98
15	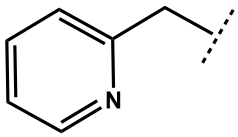	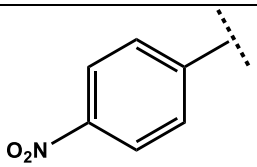	4.65

16	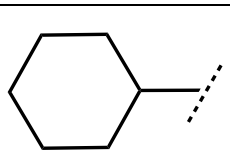	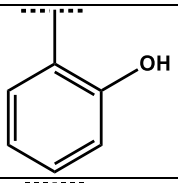	3.38
17	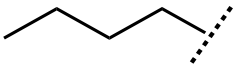	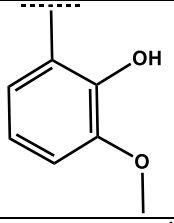	3.86
18	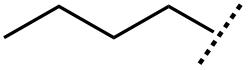	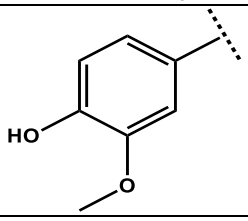	4.98
Doxorubicin			1.30

The results of the MTT assay showed that the activity of MBs is mostly dependent on the nature of the substituent at the R and R1 position. Compound **2** (1.68 μM, derived from salicylaldehyde) and **9** (1.64μM, derived from 5-Bromo salicylaldehyde) are the most active compounds with octyl chain substitution at R and hydroxyl group in the phenyl ring at R1. Substitution of cyclic (cyclohexyl**, 16**) or heterocyclic rings such as pyridine **(15)** and thiophene **(13)** at the R position does not show any significant changes in the activity. However, **13**, **15,** and **16** have IC_{50} lower than 5 μM.

Substitution on the aromatic ring of the R1 position is also important for anticancer potential. Aryl ring substituted with electron withdrawing groups like Nitro, Chloro, and Bromo **(3, 4, 6, and 7)** along with octyl chain leads to a decrease in activity. The compound with a shorter chain **(11)** is found to be the most inactive compound with IC_{50} 389.40 μM among all the MBs derivatives.

Overall, the compounds with an aliphatic substituent at the R position and hydroxyl substituted phenyl ring at the R1 position are associated with the highest activities. The effective IC_{50} concentration for **2, 8, 9, 15,** and **16** are 1.68μM, 4.56 μM, 1.63 μM, 4.64 μM, and 3.68 μM respectively. These compounds showed higher anticancer potential against HepG2 cells among screened compounds and were used for further experimentations.

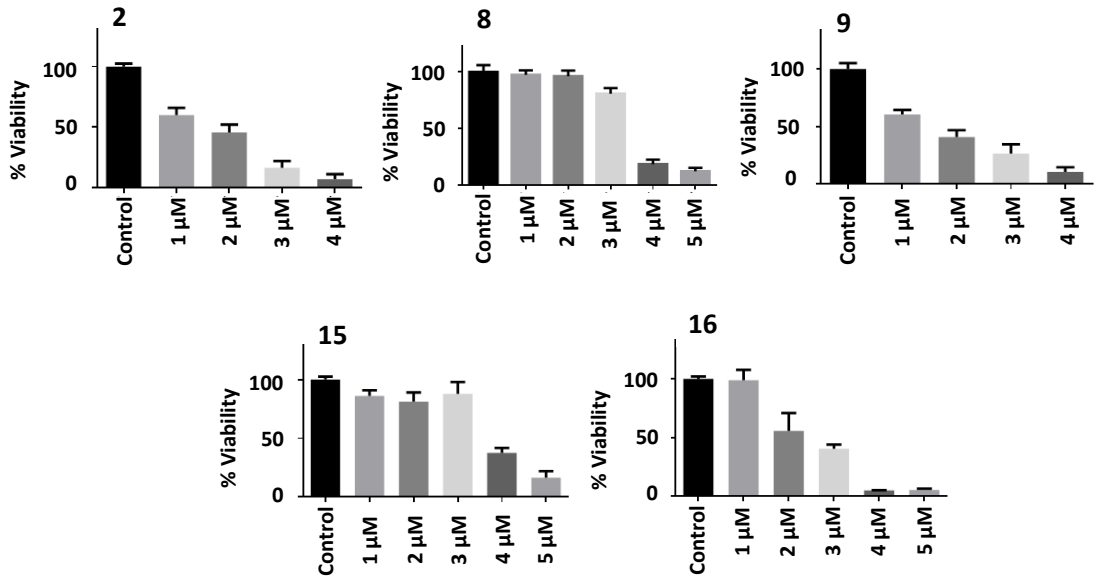

Figure 2.4 Graph of %viability against concentration for MTT assay of 2, 8, 9, 15, and 16.

Detection for nuclear condensation was done using DAPI staining[19]. Nuclear condensation was evident in all the compounds at different intensities. Compound **2** and **15** showed a higher amount of nuclear condensation among all. The same is shown in **figure 2.5**, marked with yellow arrows. We performed a DNA ladder assay to observe apoptosis induced DNA damage. However, not much shearing was observed in any of the compounds except for compound **16,** as shown in **figure 2.6**.

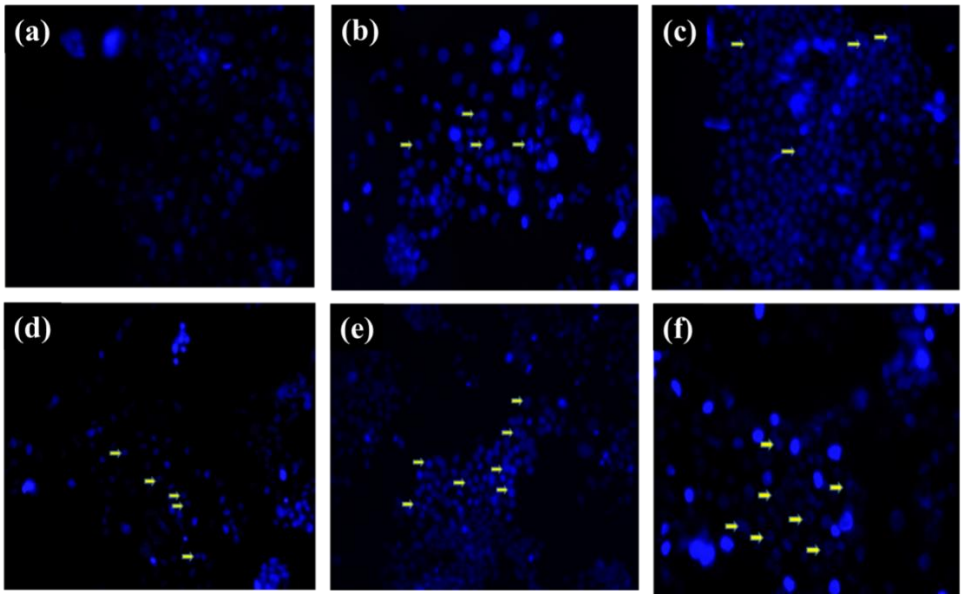

Figure 2.5 DAPI staining for analysis of nuclear condensation and morphology for compounds (a) Control (b) 2 (c) 8 (d) 9 (e) 15 and (f) 16 at their IC_{50} values for 24 h (arrows indicate condensation/fragmentation/distortion of nuclei as compared to the control)

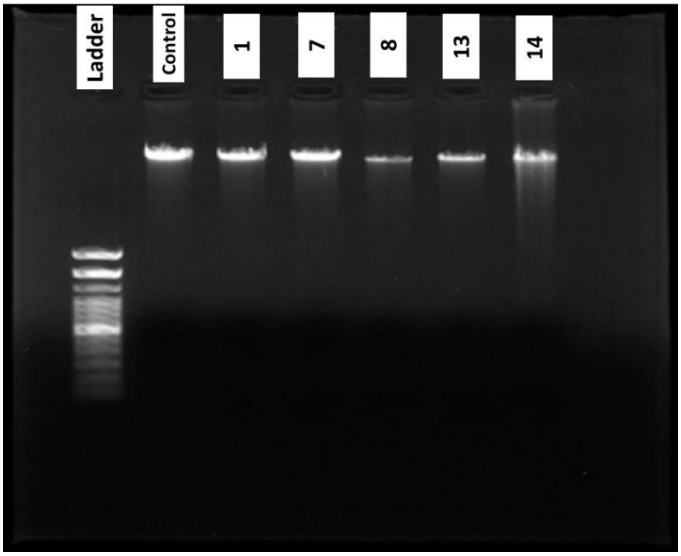

Figure 2.6 DNA ladder assay. Gel electrophoresis was done for DNA isolated from HepG2 cells treated with the mentioned compounds.

The results of AO/EB staining for compounds are shown in **figure 2.7**. An interesting observation drawn from the AO/EB staining was a morphological change in cellular structures observed in **15**. The cells were rounded up in comparison to their natural morphology suggesting a higher number of cells progressing towards apoptosis. The same was evidenced by more red stained cells in **figure 2.7d**. All the compounds showed apoptosis but **2, 15,** and **16** showed higher levels of apoptotic cells.

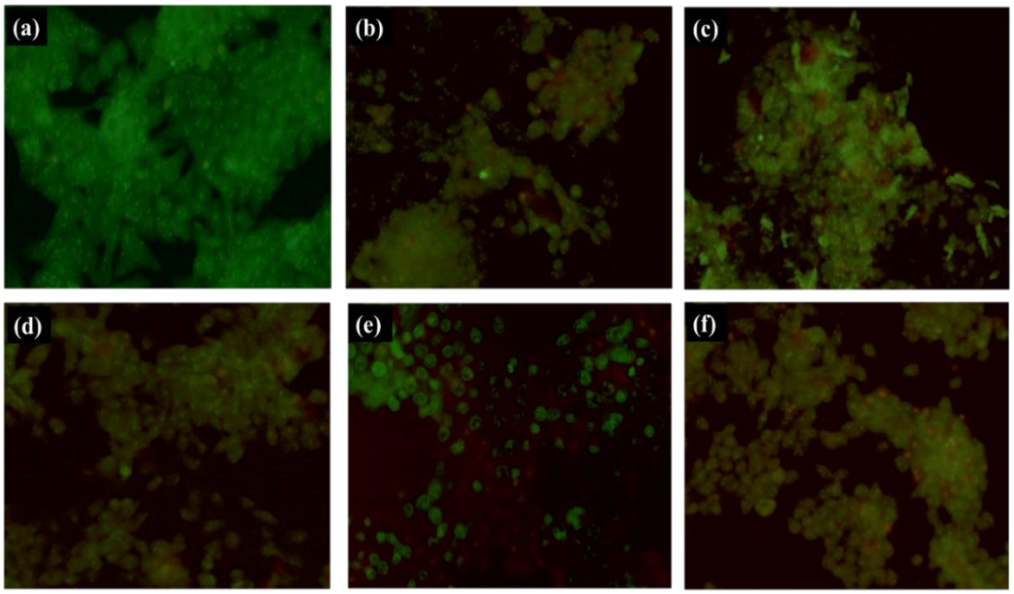

Figure 2.7 AO/EB staining for the compounds (a) Control (b) 2 (c) 8 (d) 9 (e) 15 and (f) 16 at their IC_{50} values for 24 h. (The green cells indicate live cells whereas red ones show apoptotic ones)

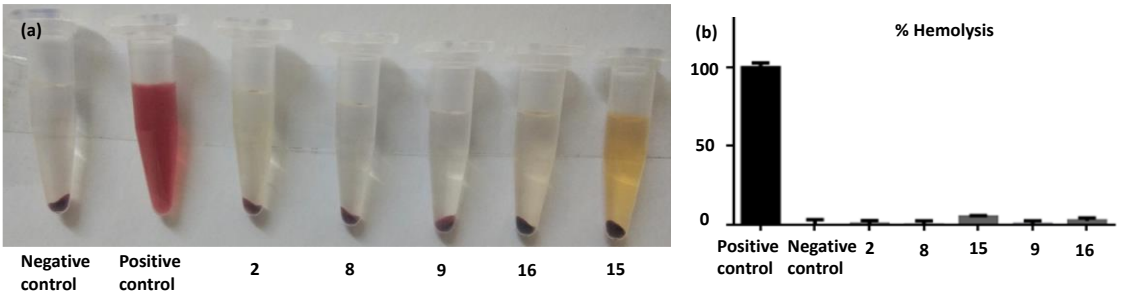

Figure 2.8 (a) Hemolysis assay performed with each compound (b) graphical representation of calculated % hemolysis

Another important aspect of the biological study is the hemolysis assay [20]. A therapeutant when administered into the body, first encounters the circulatory system and then reaches the target organ. This makes it inevitable to test the compound for its effect on the red blood cells of the body. Here we performed a hemolysis assay, where RBCs were exposed to the synthesized compounds for 3h at physiological body temperature (37^{o}C). It can be concluded from the results that none of the compounds led to significant damage to the RBCs as shown in **figure 2.8.**

2.3 Experimental

2.3.1 Material and methods

Lawsone was purchased from Sigma-Aldrich, India. All other reagents (Aldehydes and Amines) were purchased from Sigma-Aldrich, Spectrochem, and SRL chemicals, Mumbai, India. All the reagents were used without further purification. All melting points were recorded by a scientific open capillary method and are uncorrected. IR spectra (KBr pellets) were recorded using Bruker Alpha FT-IR Spectrometer. Elemental analysis was recorded on a Thermo Finnigan Flash 11-12 series. ^{1}H &^{13}C NMR spectra were recorded in DMSO-*d6* solvent using Bruker Avance (400 MHz) spectrometer. Chemical shift is reported in parts per million (ppm) downfield from TMS and coupling constants (*J*) are reported in Hertz (Hz). Proton count multiplicities are reported as singlet (s), doublet (d), triplet (t), multiplet (m), doublet of doublet (dd), triplet of doublet (td). Mass spectra were determined by Water Acquity Ultra Performance LC with SQ detector. The reaction progress was monitored by TLC in ultraviolet light. Solvents have been purified as per the literature process. Merck TLC plates were used to monitor the reaction progress.

2.3.2 General procedure for the synthesis of Mannich Bases (MB) of lawsone and spectral data

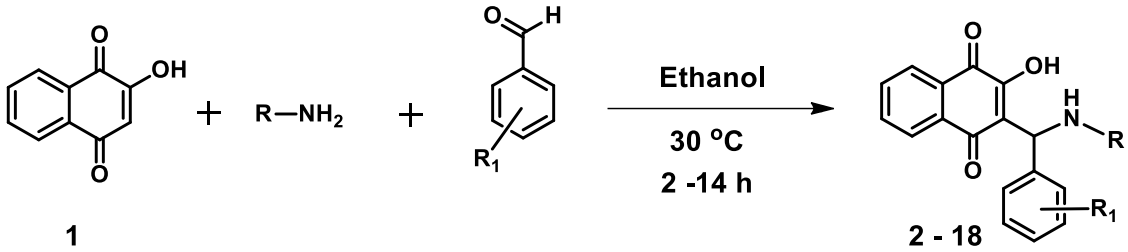

Scheme 2.1 Schematic for the synthesis of mannich bases derived from lawsone

The compounds from **2-18** were synthesized according to the reported literature procedure [17]. Briefly, to a suspension of **1** (2 mmol) in ethanol (6 mL), respective amine (2.4 mmol) was added and allowed to stir for 15 minutes. After the formation of lawsonate in the solution the aldehyde (2.4 mmol) was added to the reaction mixture and the resulting reaction mixture was left on stirring at room temperature. In less than an hour, the reactants get dissolved and the product started to separate from the reaction mixture as a solid. The reaction time depends on the substrate. The progress of the reaction was monitored by TLC. The obtained solid product was filtered and washed with water, ethanol followed by diethyl ether. The crude product was recrystallized in ethanol and dried in a vacuum oven. The general schematic for synthesis is shown in **scheme 2.1.**

2-hydroxy-3-((2-hydroxyphenyl)(octylamino)methyl)naphthalene-1,4-dione (2)

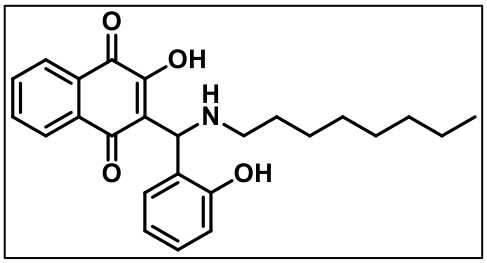

Orange solid; Yield: 74%; M.P: 152 °C -155 °C

^{1}H NMR (DMSO-*d6*, 400 MHz) δ (ppm): 7.87 (dd, *J*=8.2 Hz, *J*=1.2 Hz, 2H), 7.71 (td, *J*=8.2 Hz, *J*=1.2 Hz 1H), 7.62 (td, *J*=8.2Hz, *J*=1.2 Hz, 1H), 7.31 (dd, *J*=6.0 Hz, *J*=1.6 Hz, 1H), 7.14 (td, *J*=8.8 Hz, *J*=0.8 Hz, 1H), 6.87 (dd, *J*=6.8 Hz, *J*=0.8 Hz,1H), 6.74 (td, *J*=8 Hz, *J*=0.8 Hz,1H), 5.72 (s, 1H), 2.89 (t, *J*=7.4 Hz,2H), 1.59 (q, 2H), 1.19 (m, 10H), 0.81 (m, 3H) **(figure S2.1)**, **^{13}C NMR** (DMSO-*d6*, 100 MHz) δ (ppm):14.37, 22.48, 26.04, 26.30, 28.83, 28.87, 31.58, 46.30, 54.42, 110.29, 116.27, 119.46, 123.96, 125.56, 125.91, 129.03, 129.90, 131.52, 131.98, 134.24, 155.82, 171.93, 179.88, 184.42 **(figure**

S2.2) IR (KBr) cm^{-1}: 3254 (N-H), 3068 (=C-H), 2955 (C-H), 2928 (C-H), 1680 (C=O), 1592 (C=C), 1516 (δ N-H), 1276 (C-O), 1099 (C-N) **(figure S2.3), ESI/MS** 408.7[M+1]$^{+}$calculated for $C_{25}H_{29}NO_4$. **(figure S2.4)**, Anal. Calculated for: C, 73.69; H, 7.17; N, 3.44; O, 15.70; Found C, 73.80; H, 7.10; N, 3.39.

2-hydroxy-3-((3-nitrophenyl)(octylamino)methyl)naphthalene-1,4-dione (3)

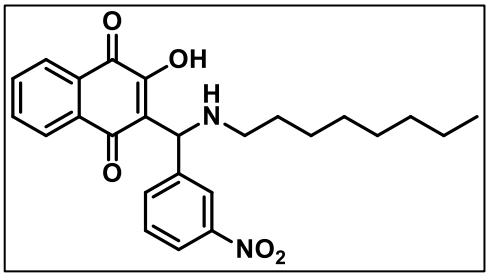

Orange solid; Yield: 74%; M.P: 162 ºC

^{1}H NMR (DMSO-*d6*, 400 MHz) δ (ppm): 8.15 (dt, *J*=3.4 Hz, *J*=0.8 Hz, 1H), 7.89 (d, 1H), 7.82 (dd, *J*=3.4 Hz, *J*=0.8 Hz, 1H), 7.91 (dd, *J*=3.4 Hz, *J*=0.8 Hz, 1H), 7.70 (td, *J*=7.6 Hz, *J*=1.2 Hz, 1H), 7.64 (t, 1H), 7.58 (td, *J*=7.6 Hz, *J*=1.2 Hz, 1H), 5.67 (s, 1H), 2.89 (t, 2H), 1.61 (q, 2H), 1.2 (m, 10H), 0.81 (t, 3H) **(figure S2.5)**, **^{13}C NMR** (DMSO-*d6*, 100 MHz) δ (ppm): 13.81, 21.91, 25.34, 25.74, 28.26, 28.28, 31.01, 45.60, 57.61, 110.15, 122.41, 122.62, 125.04, 125.36, 129.76, 130.86, 131.46, 133.70, 134.33, 134.48, 140.65, 147.50, 170.66, 178.26, 184.07 **(figure S2.6)**, **IR (KBr) cm^{-1}**: 3429 (O-H), 3071 (=C-H), 2927 (C-H), 1677 (C=O), 1613 (C=C), 1589 (N=O), 1533 (δ N-H), 1351 (N=O), 1274 (C-O), 1094 (C-N) **(figure S2.7)**, **ESI/MS** 437.0 [M+1]$^{+}$ calculated for $C_{25}H_{28}N_2O_5$. **(figure S2.8)**,Anal. Calculated for: C, 78.79; H, 6.47; N, 6.42; O, 18.33; Found C, 68.70; H, 6.50; N, 6.40.

2-hydroxy-3-((4-nitrophenyl)(octylamino)methyl)naphthalene-1,4-dione (4)

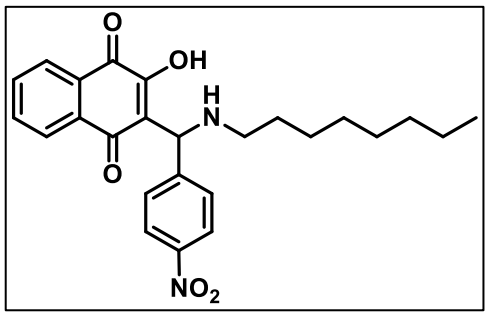

Orange solid; Yield: 68%; M.P: 152 ºC

^{1}H NMR (DMSO-*d6*, 400 MHz) δ (ppm): 8.22 (d, 2H), 7.90 (dd, *J*=1.2 Hz, *J*=0.8, 1H), 7.82 (m, 3H), 7.70 (td, *J*=7.4 Hz, *J*=1.2 Hz, 1H), 7.59 (td, *J*=7.4 Hz, *J*=1.2 Hz, 1H), 5.66

(s, 1H), 2.92 (t, 2H), 1.61 (q, 2H), 1.23 (s, 10H), 0.80 (t, 3H) **(figure S2.10)**, **^{13}C NMR** (DMSO-*d6*, 100 MHz) δ (ppm): 13.75, 21.89, 25.35, 28.25, 28.27, 30.99, 45.58, 57.62, 110.02, 123.28, 125.03, 125.34, 128.42, 130.886, 131.39, 133.68, 134.42, 145.85, 146.61, 170.49, 178.29, 184.02 **(figure S2.11)**, **IR (KBr) cm^{-1}**: 3429 (O-H), 3071 (=C-H), 2927 (C-H), 1677 (C=O), 1613 (C=C), 1589 (N=O), 1533 (δ N-H), 1351 (N=O), 1274 (C-O), 1094 (C-N) **(figure S2.12)**, **ESI/MS** 437.96 $[M+1]^+$ calculated for $C_{25}H_{28}N_2O_5$ **(figure S2.9)**, Anal. Calculated for: C, 78.79; H, 6.47; N, 6.42; O, 18.33; Found C, 68.88; H, 6.46; N, 6.48.

2-hydroxy-3-((3 -hydroxyphenyl)(octylamino)methyl)naphthalene-1,4-dione (5)

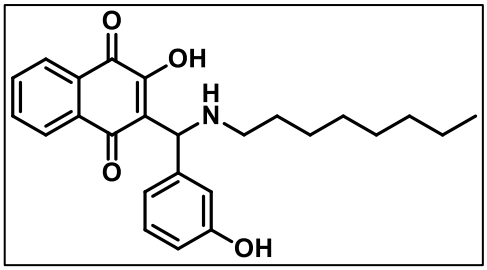

Orange solid; Yield: 75%; M.P: 168 ^{o}C

^{1}H NMR (DMSO-*d6*, 400 MHz) δ (ppm): 9.85 (s, 1H), 8.79 (s. 1H), 7.83 (dd, *J*=4.2 Hz, *J*=0.8, 1H), 7.75 (dd, *J*=4.2 Hz, *J*=0.8 Hz, 1H), 7.63 (td, *J*=8.0 Hz, *J*=1.2 Hz, 1H), 7.52 (td, *J*=8.0 Hz, *J*=1.2 Hz, 1H), 7.07 (t, 1H), 6.96 (m, 2H), 6.60 (dd, *J*=4.8 Hz, *J*=1.6 Hz, 1H), 5.53 (s, 1H), 2.78 (s, 2H), 1.54 (q, 2H), 1.12 (s, 11H), 0.75 (t, 3H) **(figure S2.13)**, **^{13}C NMR** (DMSO-*d6*, 100 MHz) δ (ppm): 13.880, 21.92, 25.34, 25.76, 28.26, 28.28, 31.01, 45.47, 58.71, 110.99, 114.59, 114.76, 118.24, 124.96, 125.21, 129.16, 130.74, 131.39, 133.60, 134.51, 139.81, 157.22, 170.44, 178.40, 184.22**(figure S2.14)**, **IR (KBr) cm^{-1}**: 3179 (=C-H), 2954 (C-H), 2931 (C-H), 1679 (C=O), 1520 (δ N-H), 1276 (C-O), 1082 (C-N) **(figure S2.15)**, **ESI/MS** 408.91 $[M+1]^+$ calculated for calculated for $C_{25}H_{29}NO_4$ **(figure S2.16)**, Anal. Calculated for: C, 73.69; H, 7.17; N, 3.44; O, 15.70; Found C, 73.76; H, 7.12; N, 3.46.

2-((4-chlorophenyl)(octylamino)methyl)-3-hydroxynaphthalene-1,4-dione (6)

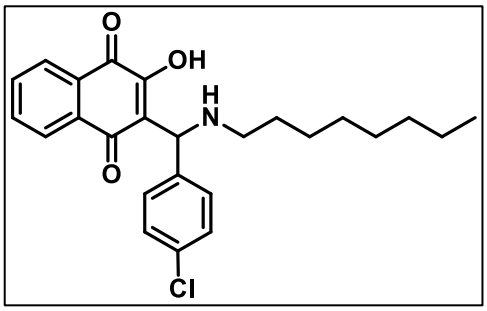

Bright orange solid; Yield: 81.96%; M.P: 159 ^{o}C

^{1}H NMR (DMSO-*d6*, 400 MHz) δ (ppm): 7.89 (dd, *J*=4.2 Hz, *J*=0.8 Hz, 1H), 7.81 (dd, *J*=4.2 Hz, *J*=0.8 Hz, 1H), 7.69 (td, *J*=8.2 Hz, *J*=1.2 Hz, 1H), 7.58 (m, 3H), 7.41 (d, 2H), 5.49 (s, 1H), 2.84 (t, 2H), 1.58 (q, 2H), 1.2 (m, 10H), 0.82 (t, 3H) **(figure S2.17)**, **^{13}C NMR** (DMSO-*d6*, 100 MHz) δ (ppm): 13.79, 21.93, 25.38, 25.78, 28.27, 28.30, 31.02, 45.56, 57.87, 110.73, 125.01, 125.29, 128.11, 129.51, 130.81, 131.39, 132.32, 133.66, 134.46, 137.52, 170.4, 178.42, 184.18 **(figure S2.18)**, **IR (KBr) cm^{-1}**: 3451 (O-H), 3329 (N-H), 3063 (=C-H), 2926 (C-H), 1673 (C=O), 1614 (C=C), 1526 (δ N-H), 1273 (C-O), 1089 (C-N), 731 (C-Cl) **(figure S2.19)**, **ESI/MS** 426.98 $[M+1]^{+}$, 428.93 $[M+3]^{+}$ calculated for $C_{25}H_{28}NO_3Cl$ **(figure S2.20)**, Anal. Calculated for: C, 73.69; H, 7.17; N, 3.44; O, 15.70; Cl, 8.32; Found C, 73.76; H, 7.12; N, 3.46.

2-((3-bromophenyl)(octylamino)methyl)-3-hydroxynaphthalene-1,4-dione (7)

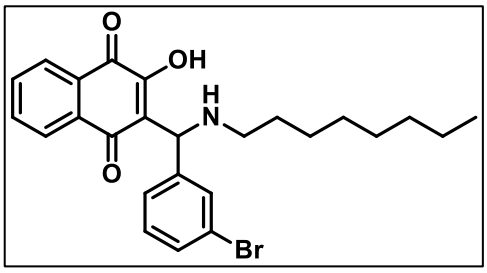

Yellow solid; Yield: 57%; M.P: 140 ^{o}C

^{1}H NMR (DMSO-*d6*, 400 MHz) δ (ppm): 9.66 (s, 1H), 8.96 (s. 1H), 7.91 (dd, *J*=4.4 Hz, *J*=1.2, 1H), 7.83 (dd, *J*=4.4 Hz, *J*=1.2 Hz, 2H), 7.70 (td, *J*=8.2 Hz, *J*=1.2 Hz, 1H), 7.57 (td, *J*=8.2 Hz, *J*=1.2 Hz, 1H), 7.5 (td, *J*=3.6 Hz, *J*=0.8 Hz, 1H),7.30 (t, 1H), 5.49 (s, 1H), 2.85 (t, 2H), 1.60 (q, 2H), 1.21 (s, 10H), 0.81 (t, 3H) **(figure S2.21)**, **^{13}C NMR** (DMSO-*d6*, 100 MHz) δ (ppm):13.79, 21.91, 25.33, 25.75, 28.25, 28.28, 31.0, 45.57, 57.87, 110.42, 121.33, 125.02, 125.31, 126.67, 130.07, 130.36, 130.50, 130.81, 131.40, 133.66, 134.45, 141.16, 170.47, 178.37, 184.13 **(figure S2.22)**, **IR (KBr) cm^{-1}**: 3445 (O-H), 3067 (=C-H), 2958 (C-H), 2928 (C-H), 1669 (C=O), 1614 (C=C), 1539 (δ N-H), 1274

(C-O), 1075 (C-N), 595 (C-Br) **(figure S2.23)**, **ESI/MS** 471.03 $[M+1]^+$, 473.03 $[M+3]^+$ calculated for $C_{25}H_{28}NO_3Br$ **(figure S2.24)**, Anal. Calculated for: C, 68.83; H, 6.0; N, 2.98; O, 10.20; Br, 16.99; Found C, 68.72; H, 6.08; N, 3.02.

2-hydroxy-3-((octylamino)(pyridin-4-yl)methyl)naphthalene-1,4-dione (8)

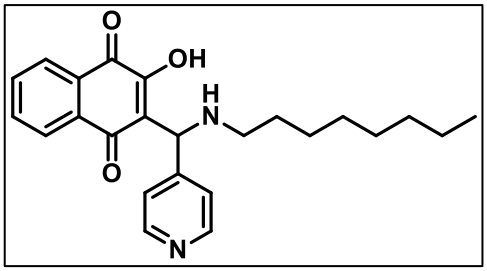

Yellow solid; Yield: 75.5%; M.P: 140 °C

^{1}H NMR (DMSO-*d6*, 400 MHz) δ (ppm): 9.55 (s, 1H), 9.14 (s. 1H), 8.52 (dd, *J*=3.0 Hz, *J*=1.6, 1H), 7.90 (dd, *J*=3.0 Hz, *J*=1.6 Hz, 1H), 7.81 (dd, *J*=4.4 Hz, *J*=1.2 Hz, 1H), 7.69 (td, *J*=8.2 Hz, *J*=1.2 Hz, 1H), 7.57 (td, *J*=8.2 Hz, *J*=1.2 Hz, 1H),7.54 (dd, *J*=3.0 Hz, *J*=1.6 Hz, 2H) , 5.55 (s, 1H), 2.88 (t, 2H), 1.61 (q, 2H), 1.22 (s, 10H), 0.80 (t, 3H) **(figure S2.25)**, **^{13}C NMR** (DMSO-*d6*, 100 MHz) δ (ppm): 13.82, 21.93, 25.26, 25.73, 28.26, 28.28, 31.01, 45.40, 56.97, 109.67, 121.98, 125.03, 125.36, 130.84, 131.44, 133.69, 134.50, 146.87, 149.48, 170.67, 178.18, 184.02 **(figure S2.26)**, **IR (KBr) cm^{-1}**: 3437 (O-H), 3067 (=C-H), 2924 (C-H), 2856 (C-H), 1679 (C=O), 1534 (δ N-H), 1272 (C-O), 1080 (C-N) **(figure S2.27)**, **ESI/MS** 393.7 $[M+1]^+$ calculated for $C_{24}H_{28}N_2O_3$ **(figure S2.28)**, Anal. Calculated for: C, 73.44; H, 7.19; N, 7.14; O, 12.43; Found C, 73.46; H, 7.15; N, 7.10.

2-((5-bromo-2-hydroxyphenyl)(octylamino)methyl)-3-hydroxynaphthalene-1,4-dione (9)

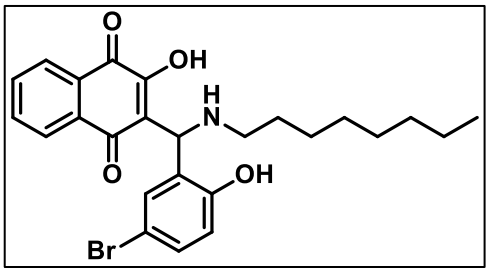

Red solid; Yield: 60%; M.P: 155 °C

^{1}H NMR (DMSO-*d6*, 400 MHz) δ (ppm): 7.90 (dd, *J*=4.2 Hz, *J*=1.2, 1H), 7.85 (dd, *J*=4.2 Hz, *J*=1.2, 1H), 7.72 (dd, *J*=4.4 Hz, *J*=1.2 Hz, 1H), 7.62 (td, *J*=8.2 Hz, *J*=1.2 Hz, 1H),

7.52 (d, 1H),7.30 (dd, *J*=5.6 Hz, *J*=2.4 Hz, 1H) , 5.68 (s, 1H), 2.86 (t, 2H), 1.58 (q, 2H), 1.22 (s, 11H), 0.80 (s, 3H) **(figure S2.31)**, **^{13}C NMR** (DMSO-*d6*, 100 MHz) δ (ppm): 13.82, 21.94, 25.43, 25.75, 28.29, 28.32, 31.03, 45.80, 53.15, 109.64, 109.98, 118.04, 125.06, 126.43, 130.75, 131.04, 131.42, 131.84, 133.74, 134.28, 154.65, 171.35, 179.29, 183.79 **(figure S2.32)**, **IR (KBr) cm^{-1}**: 3432 (O-H), 3103 (N-H), 3064 (=C-H), 2955 (C-H), 2925 (C-H), 1677 (C=O), 1590 (C=C), 1520 (δ N-H), 1277 (C-O), 1165 (C-N) **(figure S2.29)**, **ESI/MS** 486.6 $[M+1]^+$, 488.6 $[M+3]^+$ calculated for $C_{24}H_{28}NO_4Br$ **(figure S2.30)**, Anal. Calculated for: C, 61.73; H, 5.80; N, 2.88; O, 13.16; Br, 13.16; Found C, 61.70; H, 5.83; N, 2.97.

2-((octylamino)(4-hydroxy-3-methoxyphenyl)methyl)-3-hydroxynaphthalene-1,4-dione (10)

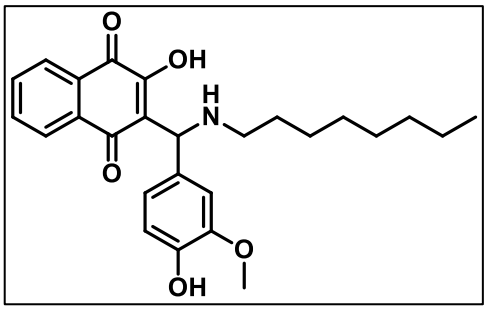

Orange solid; Yield: 59%; M.P: 159 ^{o}C

^{1}H NMR (DMSO-*d6*, 400 MHz) δ(ppm): 9.77 (s, 1H), 9.09 (s, 1H), 8.75 (s, 1H), 7.9 (td, *J*=8.2 Hz, 1H), 7.68 (td, *J*=8.2 Hz, 1H), 7.59 (d, 1H), 7.56 (d, 1H), 7.21 (d, 1H), 6.72 (t, *J*=16 Hz, 1H), 5.38 (s, 1H), 3.73 (s,3H), 2.81 (t, *J*=7 Hz, 2H), 1.55-1.60 (m, 2H), 1.18-1.21 (s, 10H), 0.81 (t, *J*=7.4 Hz, 3H) **(figure S2.33)**, **^{13}C NMR** (DMSO-*d6*, 100 MHz) δ (ppm): 14.38, 22.49, 25.90, 26.33, 28.83, 28.84, 31.58, 45.90, 56.10, 59.26, 111.99, 112.93, 115.54, 121.25, 125.54, 125.75, 129.75, 131.29, 131.93, 134.18, 135.09, 146.98, 147.69, 170.99, 179.01, 184.88 **(figure S2.34)**, **IR (KBr) cm^{-1}**: 3308 (O-H) , 3191 (N-H), 2959 (C-H), 2933 (C-),1679 (C=O), 1589 (C=C), 1516 (δ N-H), 1276 (C-O), 1082 (C-O). Anal. Calculated for: C, 70.90; H, 6.90; N, 3.31; O, 18.89; Found C, 70.78; H, 6.15; N, 3.60.

2-((allylamino)(4-hydroxy-3-methoxyphenyl)methyl)-3-hydroxynaphthalene-1,4-dione (11)

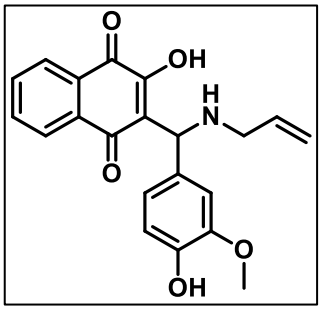

Red solid; Yield: 47%; M.P: 168 ^{o}C

^{1}H NMR (DMSO-*d6*, 400 MHz) δ (ppm): 9.15 (s, 2H), 7.90 (dd, *J*=4.2 Hz, *J*=0.8, 1H), 7.81 (dd, *J*=4.2 Hz, *J*=0.8, 1H), 7.69 (td, *J*=8.2 Hz, *J*=1.2 Hz, 1H), 7.57 (td, *J*=8.2 Hz, *J*=1.2 Hz, 1H), 7.18 (s, 1H), 6.94 (dd, *J*=5.0 Hz, *J*=2.0 Hz, 1H), 6.70 (d, 1H), 5.88 (m, 1H), 5.39 (s, 1H), 5.32 (m, 2H), 3.73 (s, 3H), 3.49 (d, 2H) **(figure S2.35)**, **^{13}C NMR** (DMSO-*d6*, 100 MHz) δ (ppm): 47.37, 55.59, 57.83, 111.28, 112.46, 115.07, 120.79, 122.10, 124.99, 125.19, 129.07, 129.41, 130.70, 131.47, 133.60, 134.60, 146.47, 147.19, 170.45, 178.39, 184.36 **(figure S2.36)**, **IR (KBr) cm^{-1}**: 3261 (N-H), 2993 (=C-H), 2958 (C-H), 2931 (C-H), 1675 (C=O), 1610 (C=C), 1523 (δ N-H), 1269 (C-O), 1069 (C-N) **(figure S2.37)**, **ESI/MS** 366.78 $[M+1]^{+}$ calculated for $C_{21}H_{19}NO_5$ **(figure S2.38)**, Anal. Calculated for: C, 69.03; H, 5.24; N, 3.83; O, 21.89; Found C, 68.95; H, 5.29; N, 3.90.

2-((allylamino)(3-nitrophenyl)methyl)-3-hydroxynaphthalene-1,4-dione (12)

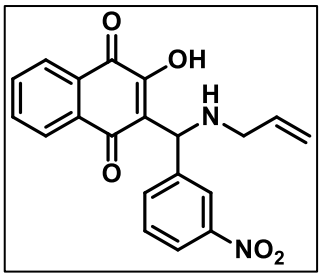

Yellow solid; Yield: 88%; M.P: 162 ^{o}C

^{1}H NMR (DMSO-*d6*, 400 MHz) δ (ppm): 9.59 (s, 2H), 8.50 (s, 1H), 8.15 (dd, *J*=5.2 Hz, *J*=1.2, 1H), 7.96 (d, 1H), 7.91(dd, *J*=4.2 Hz, *J*=0.8, 1H), 7.82 (dd, *J*=4.2 Hz, *J*=0.8 Hz, 1H), 7.70 (td, *J*=8.2 Hz, *J*=1.2 Hz, 1H), 7.64 (t, 1H), 7.58 (td, *J*=8.0 Hz, *J*=1.2 Hz, 1H), 5.9 (m, 1H), 5.66 (s, 1H), 3.57 (m, 2H) **(figure S2.39)**, **^{13}C NMR** (DMSO-*d6*, 100 MHz) δ (ppm): 47.64, 56.72, 110.12, 122.43, 122.48, 122.67, 125.08, 125.38, 129.16, 129.82, 130.89, 131.47, 133.72, 134.35, 134.48, 140.44, 147.52, 170.60, 178.32, 184.13 **(figure**

S2.40), **IR (KBr) cm^{-1}**: 3436 (O-H), 3067 (=C-H), 2924 (C-H), 1679 (C=O), 1612 (C=C), 1589 (N=O), 1534 (δ N-H), 1352 (N=O), 1274 (C-O), 1090 (C-N) **(figure S2.41)**, **ESI/MS** 365.81 $[M+1]^+$ calculated for $C_{20}H_{16}N_2O_5$ **(figure S2.42)**, Anal. Calculated for: C, 65.93; H, 4.43; N, 7.69; O, 21.96; Found C, 65.86; H, 4.51; N, 7.75.

2-hydroxy-3-((4-nitrophenyl)((2-(thiophen-2-yl)ethyl)amino)methyl)naphthalene-1,4-dione (13)

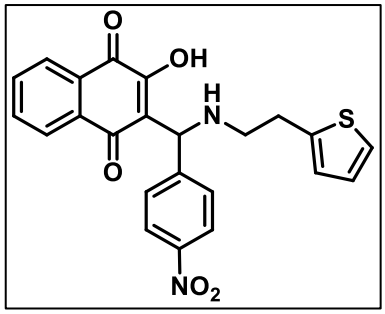

Orange solid; Yield: 80%; M.P: 156 ^oC

^{1}H NMR (DMSO-*d6*, 400 MHz) δ (ppm): 9.62 (s, 2H), 8.22 (d, 2H), 7.82 (m, 3H), 7.70 (td, *J*=8.0 Hz, *J*=1.2, 1H), 7.57 (td, *J*=8.0 Hz, *J*=1.2 Hz, 1H), 7.35(dd, *J*=3.0 Hz, *J*=1.2 Hz, 1H), 6.94 (m, 2H), 5.76 (s, 1H), 3.17 (m, 4H) **(figure S2.43)**, **^{13}C NMR** (DMSO-*d6*, 100 MHz) δ (ppm): 27.13, 30.55, 33.52, 61.63, 123.86, 125.14, 125.93, 126.70, 127.19, 128.00, 128.81, 130.96, 131.94, 133.76, 138.79, 141.80, 145.10, 148.45, 150.65, 160.13, 182.15, 183.76 **(figure S2.44)**, **IR (KBr) cm^{-1}**: 3433 (O-H), 3087 (=C-H), 2960 (C-H), 2927 (C-H), 1746 (C=O), 1679 (C=O), 1586 (N=O), 1518 (δ N-H), 1347 (N=O), 1280 (C-O), 1122 (C-N) **(figure S2.45)**, **ESI/MS** 435.95 $[M+1]^+$ calculated for $C_{23}H_{18}N_2O_5S$ **(figure S2.46)**, Anal. Calculated for: C, 63.58; H, 4.18; N, 6.45; O, 18.41; S, 7.38; Found C, 63.64; H, 4.20; N, 6.42.

2-hydroxy-3-(((2-hydroxyethyl)amino)(4-nitrophenyl)methyl)naphthalene-1,4-dione (14)

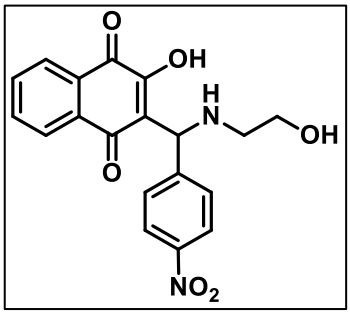

Orange solid; Yield: 56%; M.P: 147 °C

^{1}H NMR (DMSO-*d6*, 400 MHz) δ (ppm): 9.52 (s, 2H), 8.22 (d, 2H), 7.90 (dd, *J*=4.4 Hz, *J*=0.8 Hz, 2H), 7.82 (m, 3H), 7.70 (td, *J*=8.0 Hz, *J*=1.2 Hz, 1H), 7.57 (td, *J*=8.0 Hz, *J*=1.2 Hz, 1H), 5.75 (s, 1H), 5.11 (s, 1H), 3.64 (m, 2H), 3.03 (m, 2H) **(figure S2.47)**, **^{13}C NMR** (DMSO-*d6*, 100 MHz) δ (ppm): 47.86, 56.46, 57.78, 110.29, 123.45, 125.09, 125.43, 128.54, 130.56, 131.38, 133.79, 134.42, 145.64, 146.71, 170.52, 178.30, 184.06 **(figure S2.48)**, **IR (KBr) cm^{-1}**: 3498 (O-H), 3406 (N-H), 3070 (=C-H), 2949 (C-H), 1677 (C=O), 1590 (N=O), 1527 (δ N-H), 1348 (N=O), 1274 (C-O), 1110 (C-N) **(figure S2.49)**, **ESI/MS** 369.81 $[M+1]^+$ calculated for $C_{19}H_{26}N_2O_6$ **(figure S2.50)**, Anal. Calculated for: C, 61.96; H, 4.38; N, 7.61; O, 26.06; Found C, 62.02; H, 4.36; N, 7.68.

2-hydroxy-3-((4-nitrophenyl)((pyridin-2-ylmethyl)amino)methyl)naphthalene-1,4-dione (15)

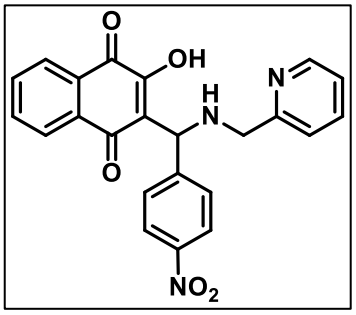

Orange solid; Yield: 78%; M.P: 139 °C

^{1}H NMR (DMSO-*d6*, 400 MHz) δ (ppm): 8.63 (s, 1H), 8.21 (d, 2H), 7.90 (dd, *J*=4.4 Hz, *J*=0.8 Hz, 1H), 7.82 (m, 4H), 7.69 (td, *J*=1.6 Hz 1H), 7.58 (td, *J*=1.6 Hz 1H), 7.39 (m, 2H), 5.84 (s, 1H), 4.35 (m, 2H) **(figure S2.51)**, **^{13}C NMR** (DMSO-*d6*, 100 MHz) δ (ppm): 49.02, 57.89, 110.05, 123.53, 125.16, 125.76, 128.72, 130.92, 131.43, 133.77, 134.39, 137.14, 145.39, 146.83, 148.83, 148.91, 152.14, 170.61, 178.42, 183.92 **(figure S2.52)**, **IR (KBr) cm^{-1}**: 3435 (O-H), 3108 (=C-H), 3070 (=C-H), 2925 (C-H), 1681 (C=O), 1593 (N=O), 1526 (δ N-H), 1349 (N=O), 1277 (C-O), 1111 (C-N) **(figure S2.53)**, **ESI/MS** 416.83 $[M+1]^+$ calculated for $C_{23}H_{17}N_3O_5$ **(figure S2.54)**, Anal. Calculated for: C, 66.50; H, 4.13; N, 10.12; O, 19.26; Found C, 66.57; H, 4.10; N, 10.15.

2-((cyclohexylamino)(2-hydroxyphenyl)methyl)-3-hydroxynaphthalene-1,4-dione (16)

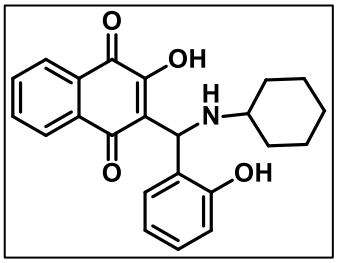

Light orange solid, Yield: 75%; M.P: 184 ^{o}C

^{1}H NMR (DMSO-*d6*, 400 MHz) δ (ppm): 7.88 (td, *J* =7.8 Hz, *J*=1.2 Hz, 2H), 7.72 (td, *J*= 1.6 Hz, *J*=8. Hz, 1H), 7.62 (td, *J*=1.6 Hz,8.2 Hz, 1H),7.26 (dd, *J*=4.2 Hz, *J*=1.6 Hz, 1H), 7.17 (td, *J*= 8.6 Hz, *J*=2.0 Hz 1H), 6.89 (dd, *J*=0.8 Hz, 1H), 6.73 (td, *J*=1.2 Hz,8.0 Hz, 1H), 5.91 (s, 1H), 2.95 (s, 1H), 1.73 (m, 3H) ,1.54 (d, 1H), 1.39 (m, 2H), 1.16 (m, 3H) **(figure S2.55)**, **^{13}C NMR** (DMSO-*d6*, 100 MHz) δ (ppm): 23.63, 23.66, 23.75, 24.73, 28.32, 30.15, 30.23, 51.40, 54.78, 109.49, 115.42, 118.87, 1123.03, 125.03, 12.36, 128.76, 129.55, 130.98, 131.51, 133.69, 134.27, 155.29, 171.55, 179.39, 183.85 **(figure S2.56)**, **IR (KBr) cm^{-1}**: 3266 (O-H), 3076 (N-H), 2967 (C-H), 1680 (C=O), 1591 (C=C), 1518 (δ N-H), 1278 (C-O) **(figure S2.57)**, **ESI/MS** 378.6 $[M+1]^{+}$ calculated for $C_{23}H_{23}NO_4$ **(figure S2.58)**, Anal. Calculated for: C, 73.19; H, 6.14; N, 3.71; O, 16.96; Found C, 73.27; H, 6.10; N, 3.75.

2-((butylamino)(2-hydroxy-3-methoxyphenyl)methyl)-3-hydroxynaphthalene-1,4-dione (17)

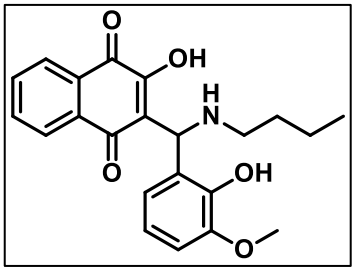

Orange solid; Yield: 56%; M.P: 157^{o}C

^{1}H NMR (DMSO-*d6*, 400 MHz) δ(ppm): 7.87 (dd, *J*=1.2 Hz, *J*=8.6 Hz, 2H), 7.72 (td, *J*=8.2 Hz, 1H),7.60 (td, *J*=8.2 Hz, 2H), 6.70 (t, *J*=16 Hz, 1H), 5.75 (s, 1H), 3.78 (s,3H), 2.88 (t, *J*=7 Hz, 2H), 1.54-1.63 (m, 2H), 1.23-1.34 (m, 2H), 0.831(t, *J*=7.4 Hz, 3H) **(figure S2.60)**, **^{13}C NMR** (DMSO-*d6*, 100 MHz) δ (ppm):13.39, 19.16, 27.61, 45.54, 53.70, 55.81, 110.07, 111.93, 118.72, 120.09, 124.03, 125.0, 125.36, 130.99, 131.37, 133.72, 134.30, 144.48, 147.80, 171.29, 179.34, 183.58 **(figure S2.61)**, **IR (KBr) cm^{-1}**:

3308 (O-H) , 3191 (N-H), 2959 (C-H), 2933 (C-),1679 (C=O), 1589 (C=C), 1516 (δ N-H), 1276 (C-O), 1082 (C-O) **(figure S2.62)**, **ESI/MS** 382.6 $[M+1]^+$ calculated for $C_{22}H_{23}NO_5$ **(figure S2.59)**, Anal. Calculated for: C, 69.28; H, 6.08; N, 3.67; O, 20.96; Found C, 69.37; H, 6.15; N, 3.60.

2-((butylamino)(4-hydroxy-3-methoxyphenyl)methyl)-3-hydroxynaphthalene-1,4-dione (18)

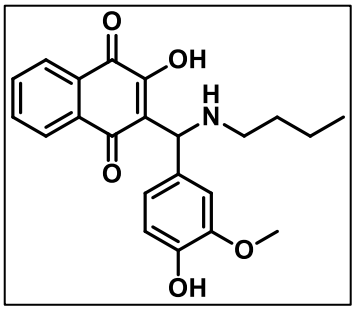

Orange solid; Yield: 56%; M.P: 152ºC

^{1}H NMR (DMSO-*d6*, 400 MHz) δ(ppm): 7.90 (dd, *J*=8.8 Hz, *J*=1.2 Hz, 1H), 7.82 (dd, *J*=8.8 Hz, *J*=1.2 Hz, 1H), 7.70 (td, *J*=8.2 Hz, *J*=1.6 Hz, 1H), 7.58 (td, *J*=8.2Hz, *J*=1.6 Hz, 1H), 7.22 (d, *J*=2Hz, 1H), 6.96 (dd, *J*=5.0 Hz, *J*=2.0 Hz, 1H), 6.72 (td, *J*=8.2Hz, *J*=1.6 Hz, 1H), 5.38 (s,1H), 3.74 (s,3H), 2.82 (t, *J* 7.8 Hz, 2H), 1.61-1.53 (m ,2H), 1.32-1.22 (m,2H) ,0.838 (t, *J* 7.2 Hz ,3H) **(figure S2.63)**, **^{13}C NMR** (DMSO-*d6*, 100 MHz) δ (ppm): 13.39, 19.21, 27.58, 45.17, 55.59, 111.50, 112.46, 115.02, 120.73, 124.98, 125.20, 129.24, 130.73, 131.73, 133.62, 134.55, 146.46, 147.16, 170.43, 178.46, 184.35 **(figure S2.64)**, **IR (KBr) cm^{-1}** : 3272 (O-H) , 3069 (N-H) , 2959 (C-H) , 2932 (C-H) , 1678 (C=O) , 1590 (C=C) , 1520 (δ N-H) , 1273 (C-O) , 1130 (C-O) **(figure S2.65)**, **ESI/MS** 382.84 $[M+1]^+$ calculated for $C_{22}H_{23}NO_5$ **(figure S2.66)**, Anal. Calculated for: C, 69.28; H, 6.08; N, 3.67; O, 20.96; Found C, 69.35; H, 6.12; N, 3.65.

2.3.3 Cell line and culture

HepG2 Cells (Human Liver cancer cell lines) were procured from National Center for Cell Science (NCCS) Pune. Dubecoos Modified Essential Medium (DMEM), Fetus Bovine Serum (FBS), and antimycotic–antibiotic solution were obtained from HiMedia. Cells were cultured in Dulbecco's Modified Eagle's Medium (DMEM) supplemented with 10% Fetal Bovine Serum (FBS) (Gibco) and 1% antimycotic-antibiotic solution (HiMedia). Cells were maintained at 37ºC temperature in the incubator with 5% CO_2. Cells were sub-cultured at about 80% confluency using 0.25% Trypsin Phosphate

Versene Glucose (TPVG) Solution (Himedia). Cell lines were utilized to examine the antitumor activity of testing compounds at varying concentrations.

2.3.4 Cell Viability Assay

IC_{50} values of the synthesized compounds were determined using an MTT assay on the HepG2 cell line. Doxorubicin hydrochloride dosed in different concentrations was used as a positive control for the study. HepG2 cells (10^4 cells/well) were seeded in 96 well plates in 10% DMEM media. 0.1% dimethyl sulfoxide was used to dissolve lawsone and its derivatives. Dilutions of the compounds were prepared in incomplete DMEM media. Dosing was done at about 70% confluency. After 24h incubation 3-(4, 5-dimethylthiazol-2-yl)-2, 5-diphenyl tetrazolium bromide (MTT; 5 mg/ml) was added for 4h. At the end of incubation, MTT was removed from the wells and 150 µL/well of DMSO was added and incubated till formazan crystals dissolved completely. Reading was taken at 570 nm in synergy HTX multimode reader.

2.3.5 Nuclear morphology assessment (DAPI staining)

HepG2 cells were seeded in a 6 well plate (5×10^5). At about 70% confluency the plate was dosed with compounds at their IC_{50} value concentration each. The cells were allowed to incubate for 24h at 37ºC. Post incubation, cells were washed with 1X PBS twice. DAPI stain (1µg/mL) in 1X PBS was added for about 5-10 min at 37ºC. The stain was removed and after 1 wash of 1X PBS, cells were imaged under Floid Imaging Station [21]. Treated cells were examined for condensed and fragmented nuclei.

2.3.6 Assessment of apoptosis (Acridine Orange/Ethidium Bromide (AO/EB) staining)

HepG2 cells were cultured on sterile glass coverslips and were incubated at 37ºC in 5% CO_2 incubator. Cells were further dosed with IC_{50} concentration of compounds. After 24h of incubation cells were stained with 5 µM of AO/EB staining solution. Images were taken on Floid Imaging Station.

2.3.7 Hemolysis assay

Whole blood was collected from a healthy individual in EDTA coated vacutainer tubes, after getting a consent letter. The protocol was approved and experiments were performed in compliance with the relevant laws and guidelines of the Indian medical

association for research on human subjects at blue cross pathology lab (IMA-BMWMC No. 1093), Vadodara, India. The collected blood was diluted with PBS, twice the volume, and centrifuged at 5000 rpm for 10 min to separate the plasma content. The RBC content was used for analysis. Positive control was taken using 800 µL distilled water and 200 µL of RBC content. Similarly, a negative control was set up using 800 µL 1X PBS and 200 µL of RBC content. Likewise, test samples were taken at IC_{50} concentrations and an equal amount of RBCs were added to all of them. All the tubes were incubated at 37°C for 3h. OD was measured at 540 nm and 655 nm [19]. Percentage hemolysis was calculated using the following formula.

$$\% \text{ Hemolysis} = 100 \text{ X } \frac{Sample\ Absorbance\ - Negative\ control\ Absorbance}{Positive\ control\ Absorbance\ - Negative\ control\ Absorbance}$$

2.3.8 DNA ladder assay

For DNA ladder assay, HepG2 cells were seeded in a 6 well plate at about 70% confluency. The cells were dosed with compounds at their IC_{50} concentrations. Cells were collected after 24h by trypsinizing with TPVG solution. The cell pellet was then used for DNA extraction using the GeneJet DNA isolation kit, as per the manufacturer's instructions. DNA fragmentation was quantified by agarose gel electrophoresis, using 2% Agarose Gel [19].

2.4 Conclusion

A small library of lawsone derived mannich bases were synthesized with moderate to high yield via three-component mannich reaction. The structure of the compounds was confirmed by ^{1}H NMR, ^{13}C NMR, FT-IR, Mass spectrometry, and elemental analysis. Synthesized compounds were characterized using various analytical techniques. The IC_{50} values were determined by MTT assay on the HepG2 cell line and structure activity relationship (SAR) was established. The compounds exhibited good to moderate activity and were found to be hemocompatible. The most potent compounds **(2, 8, 9, 15,** and **16)** were subjected to DAPI and AO/EB staining, which indicated that the cytotoxicity was mediated through the induction of apoptosis.

In order to enhance the anticancer activity of mannich bases, it was proposed to synthesize copper and vanadium complexes which are discussed in chapter 3.

2.5 Spectra

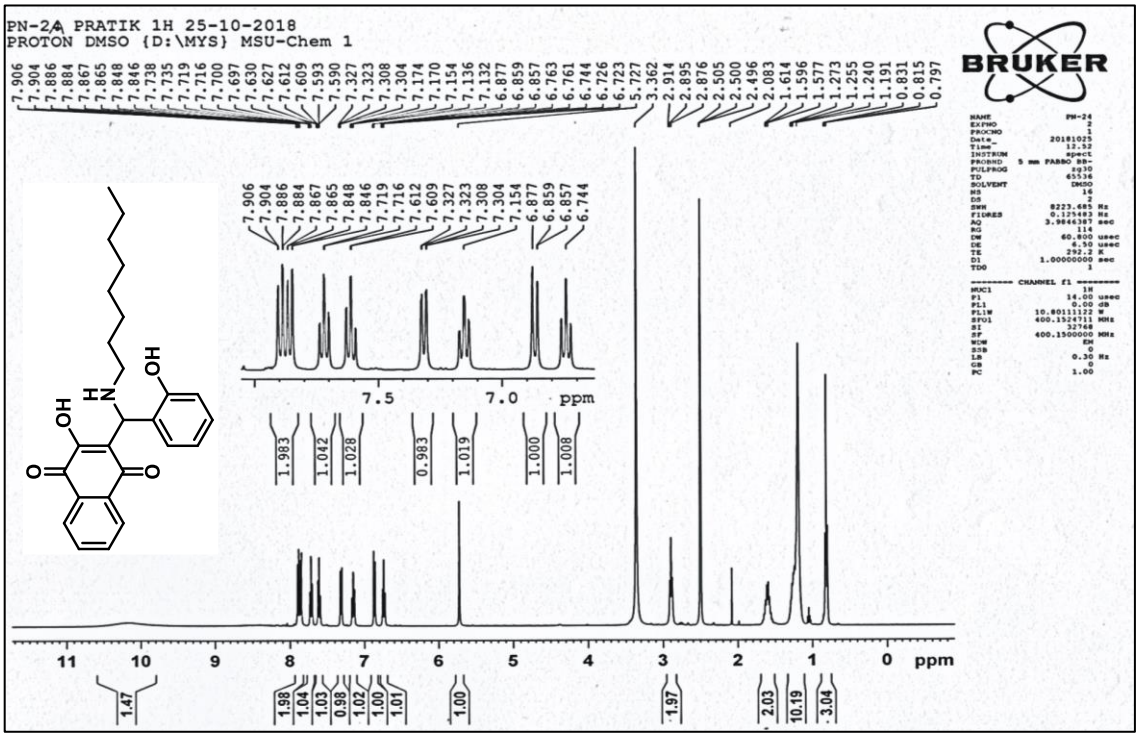

Figure S2.1 ^{1}H NMR spectra of compound **2**

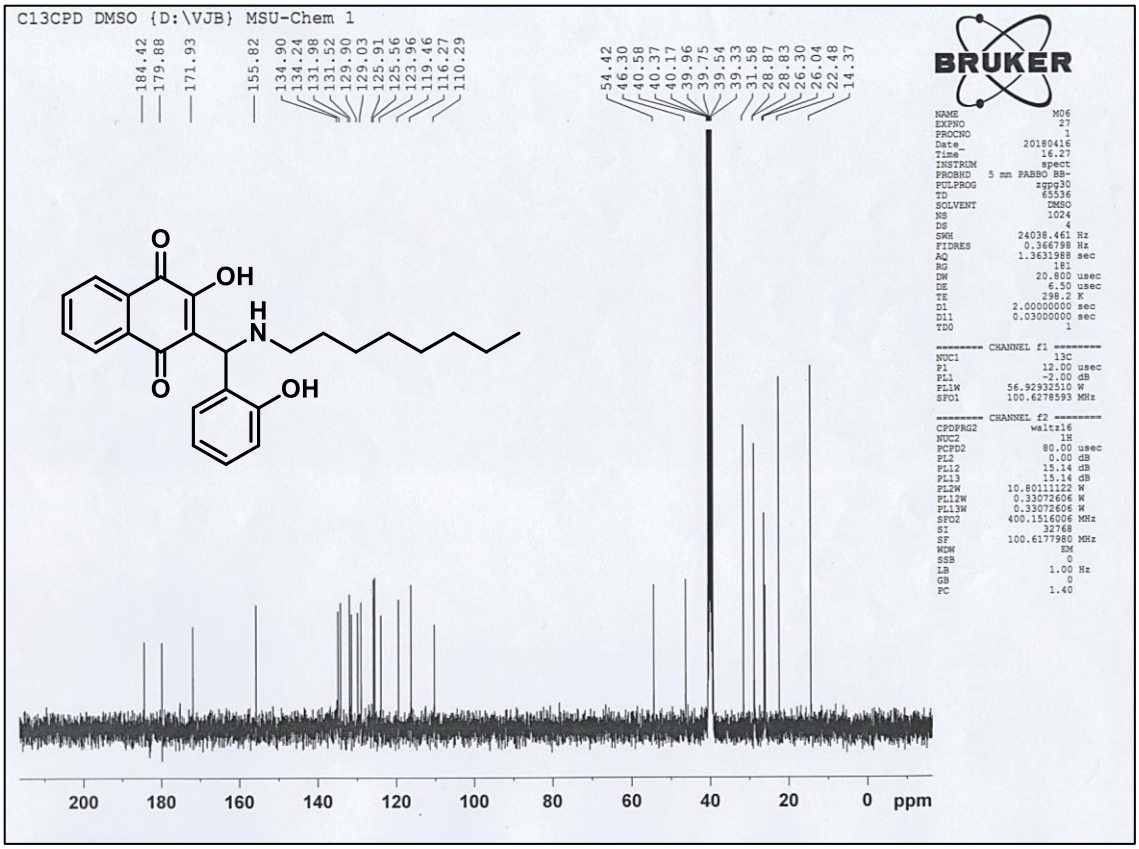

Figure S2.2 ^{13}C NMR spectra of compound **2**

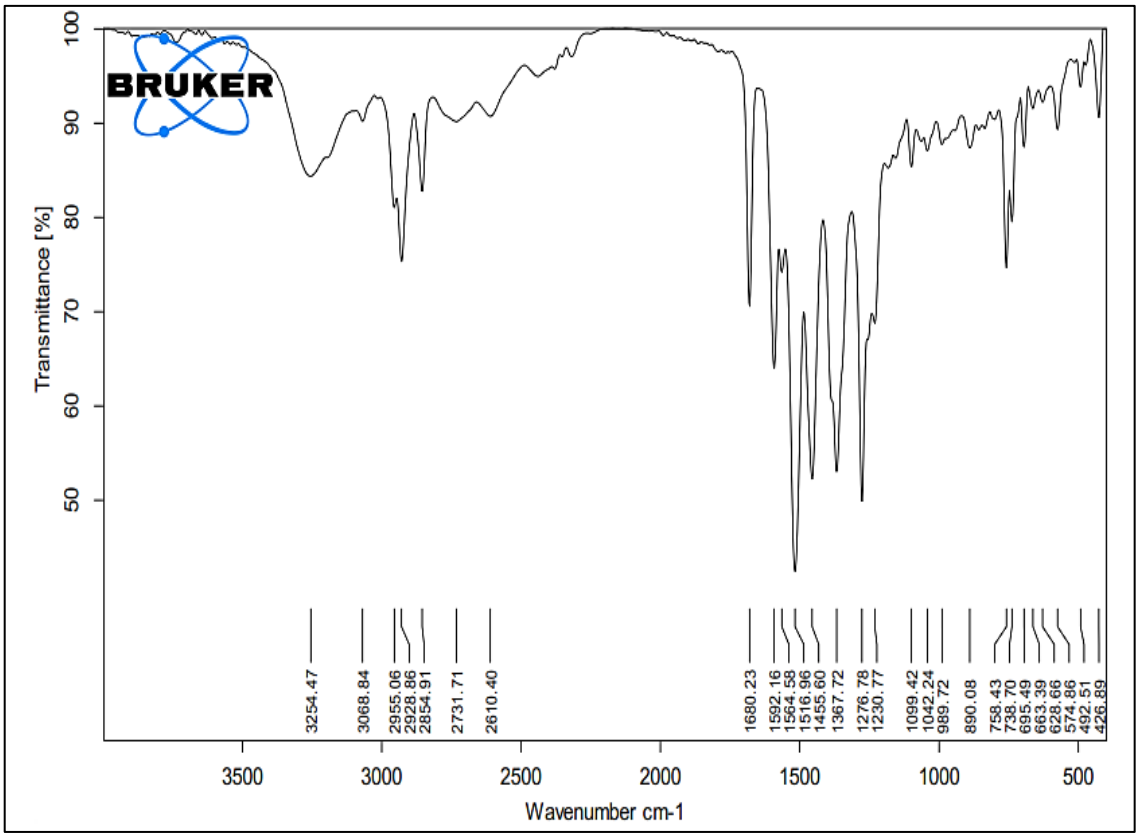

Figure S2.3 FT-IR spectra of compound **2**

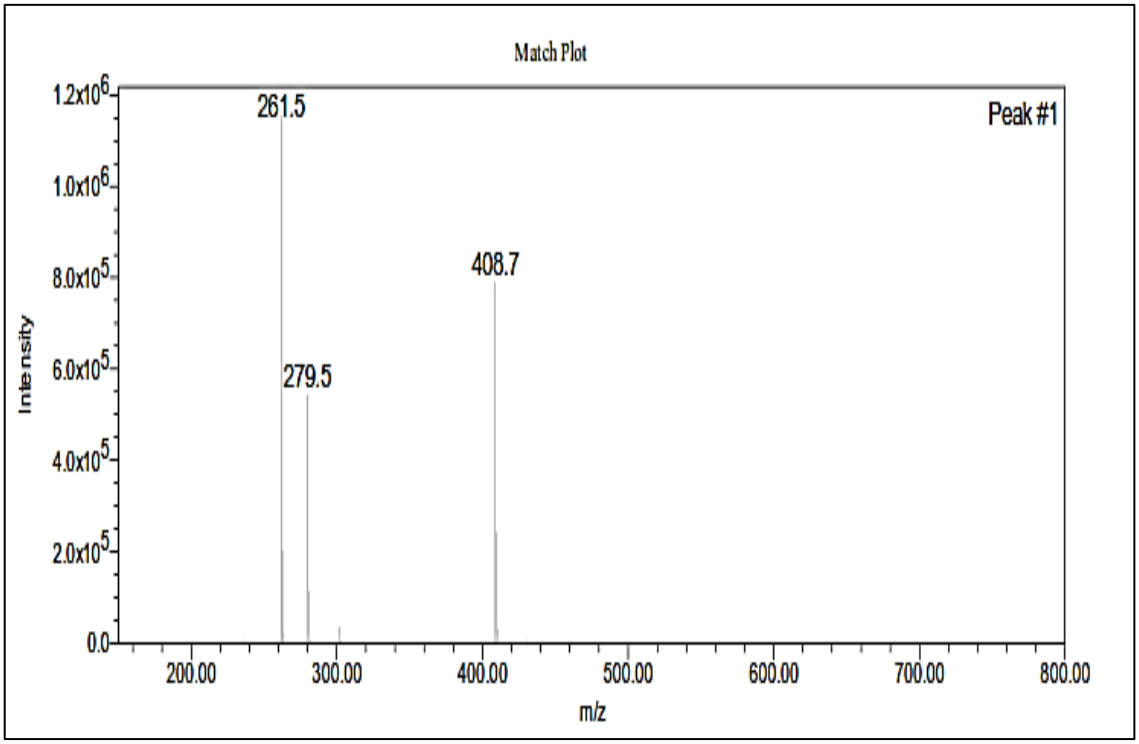

Figure S2.4 ESI-MS spectra of compound **2**

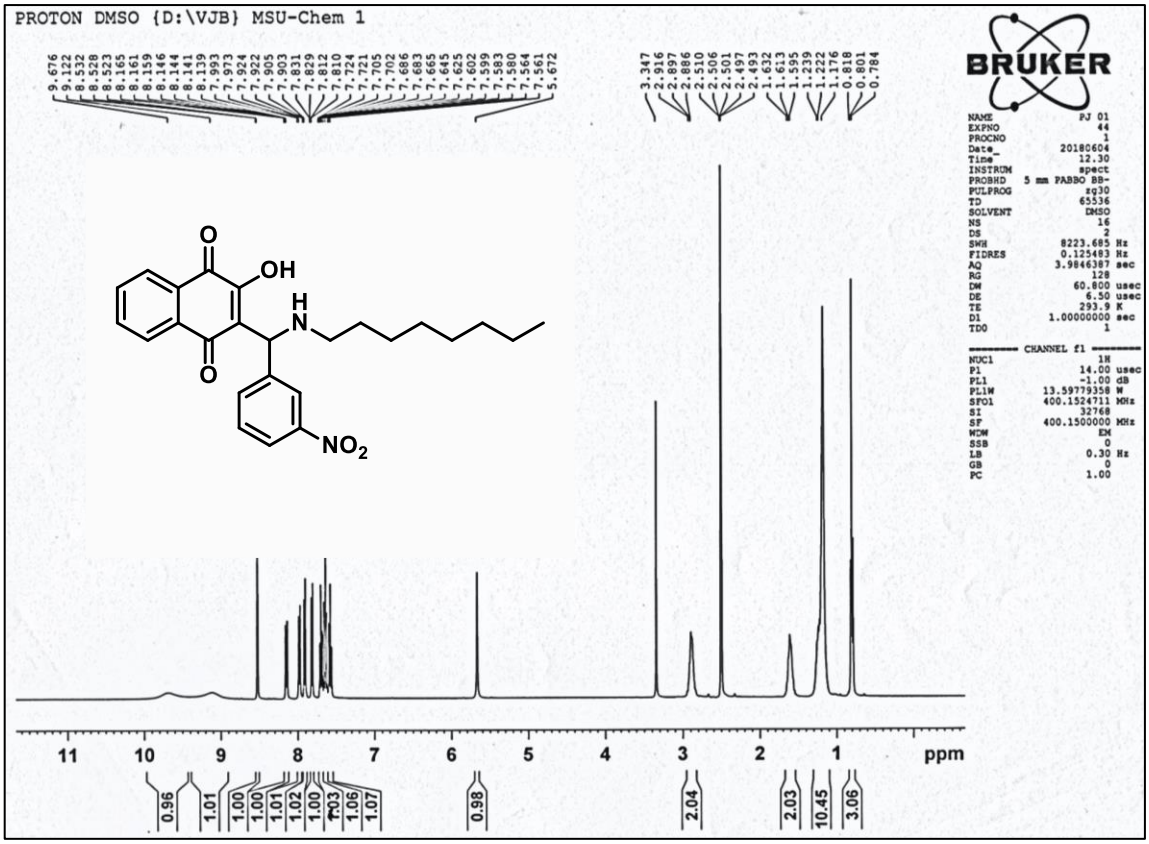

Figure S2.5 ^{1}H NMR spectra of compound **3**

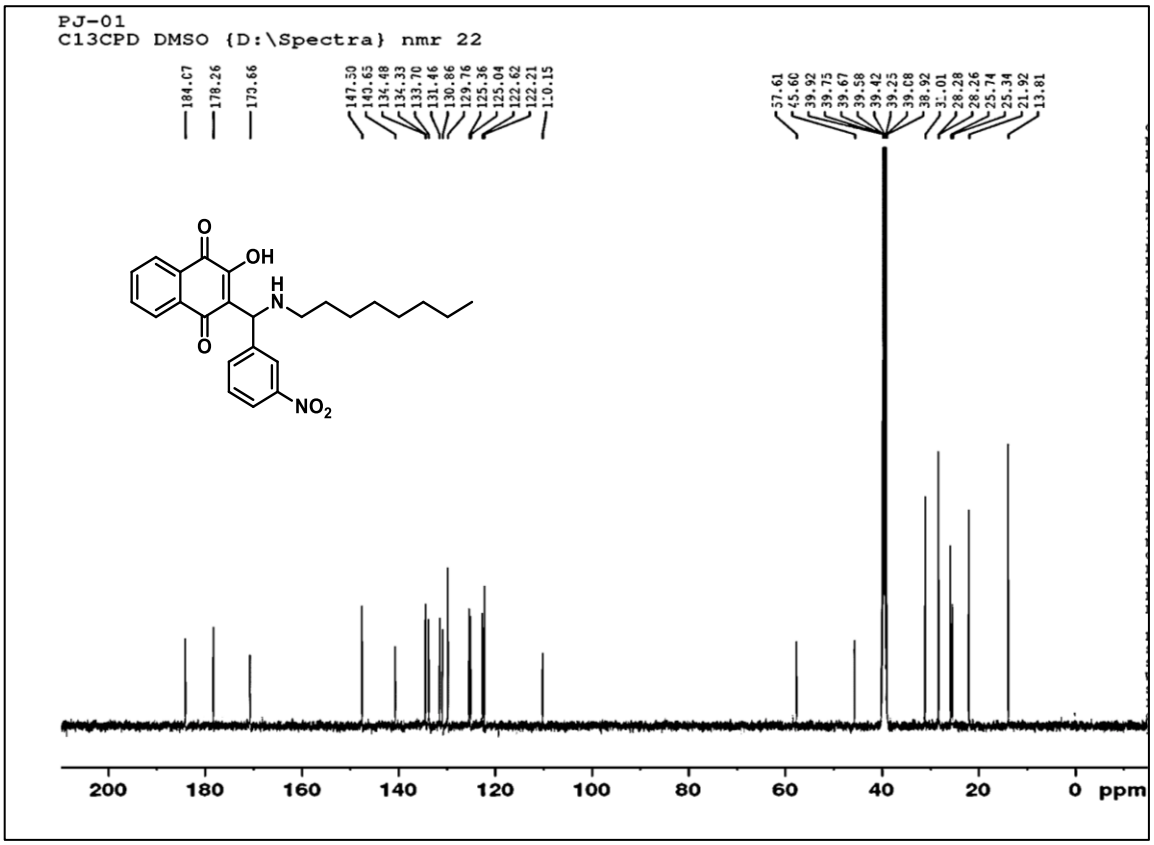

Figure S2.6 ^{13}C NMR spectra of compound **3**

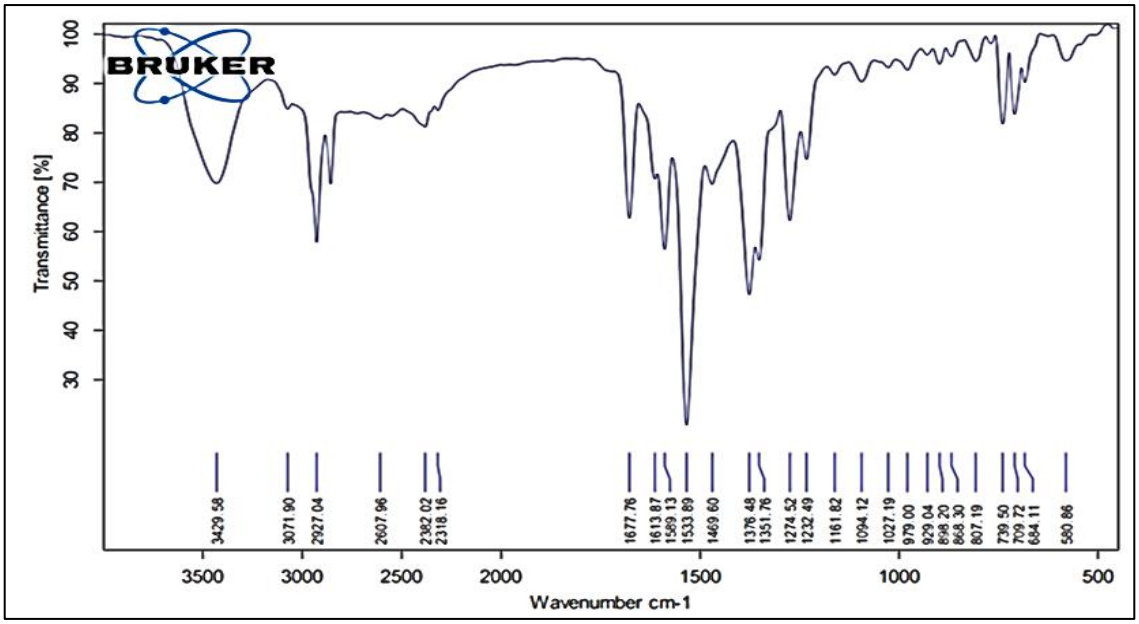

Figure S2.7 FT-IR spectra of compound **3**

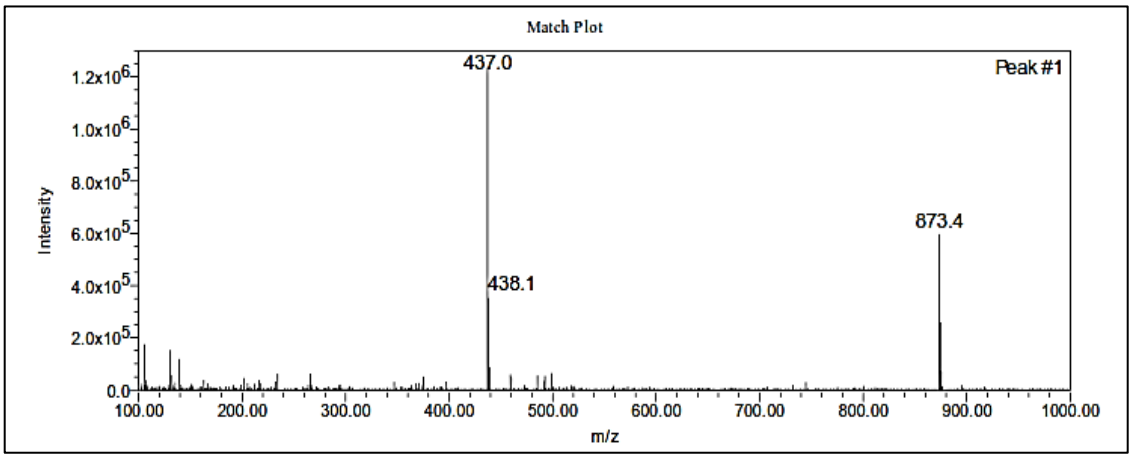

Figure S2.8 ESI-MS spectra of compound **3**

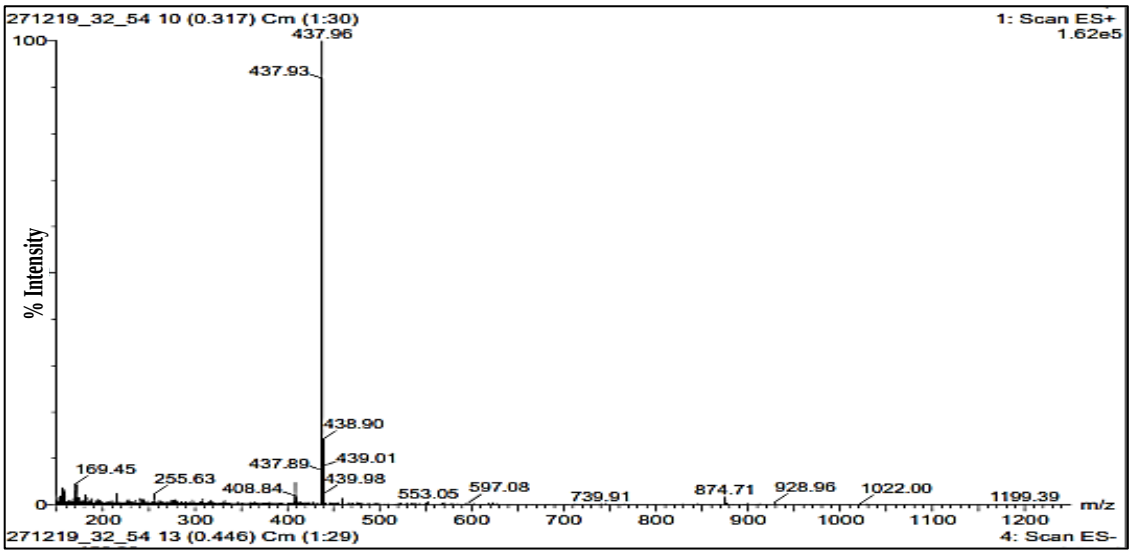

Figure S2.9 ESI-MS spectra of compound **4**

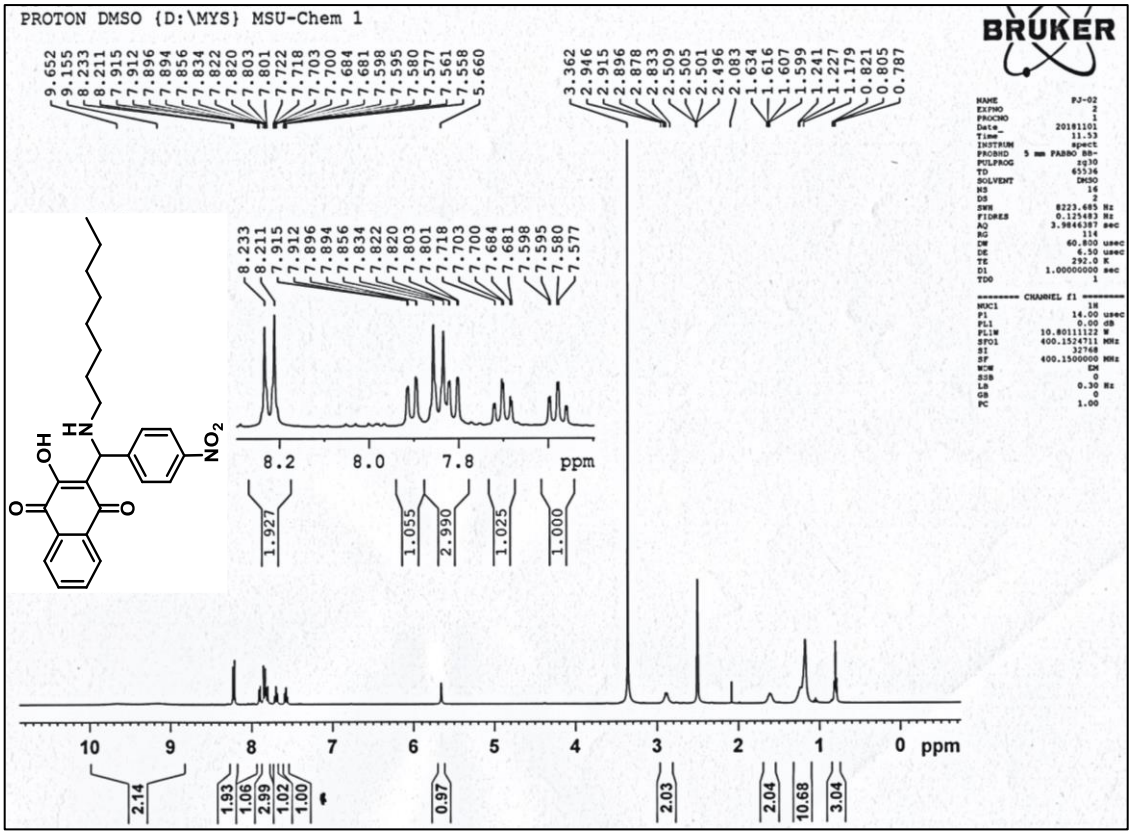

Figure S2.10 ^{1}H NMR spectra of compound **4**

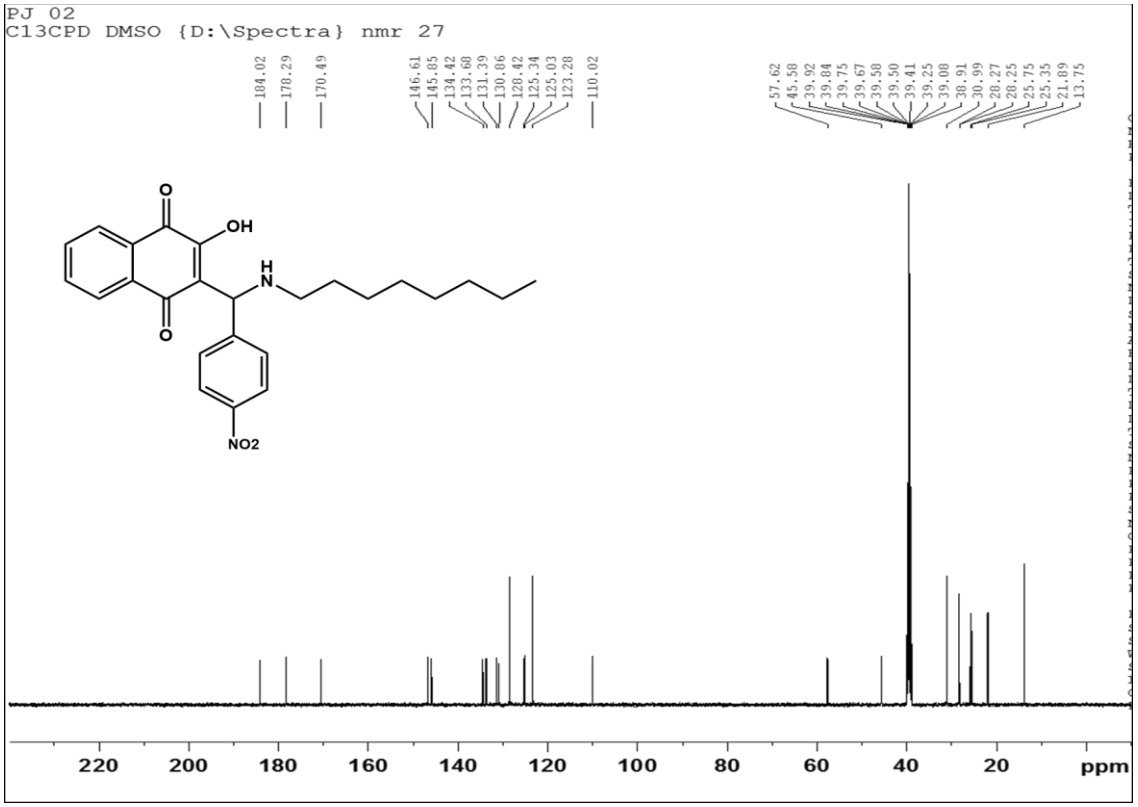

Figure S2.11 ^{13}C NMR spectra of compound **4**

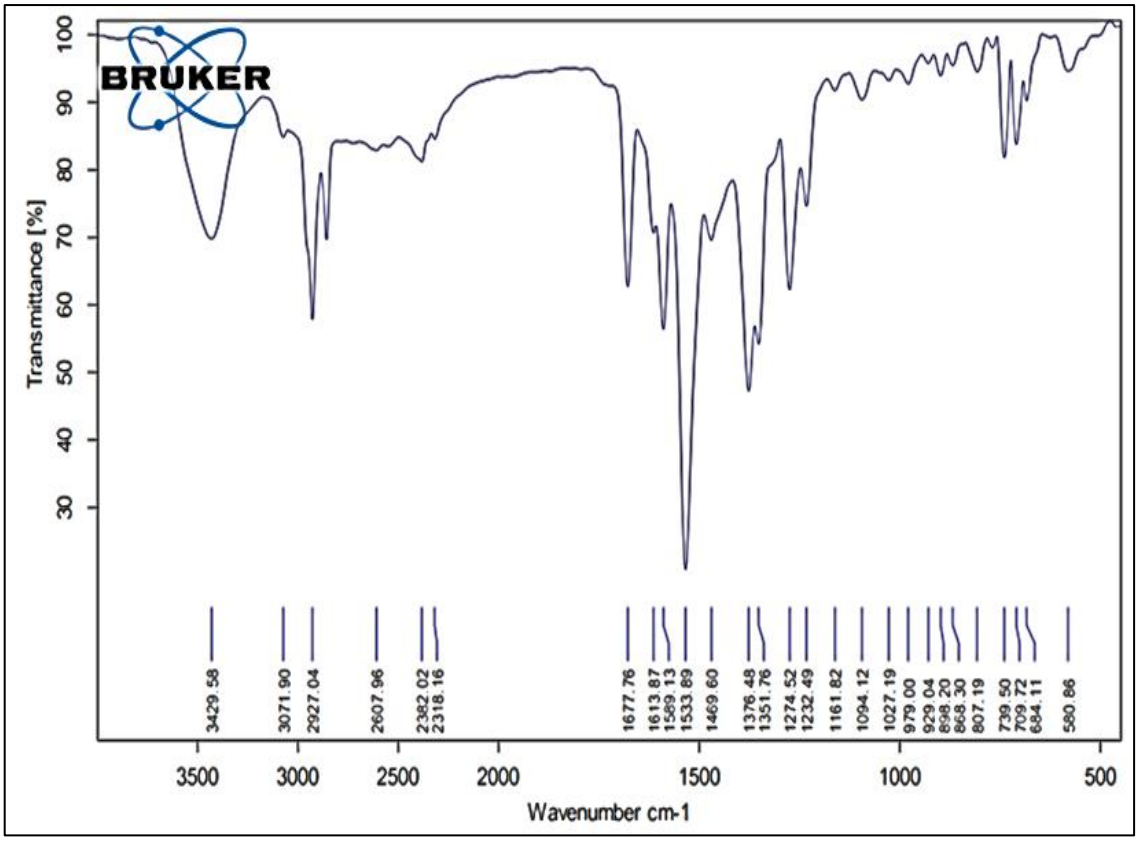

Figure S2.12 FT-IR spectra of compound **4**

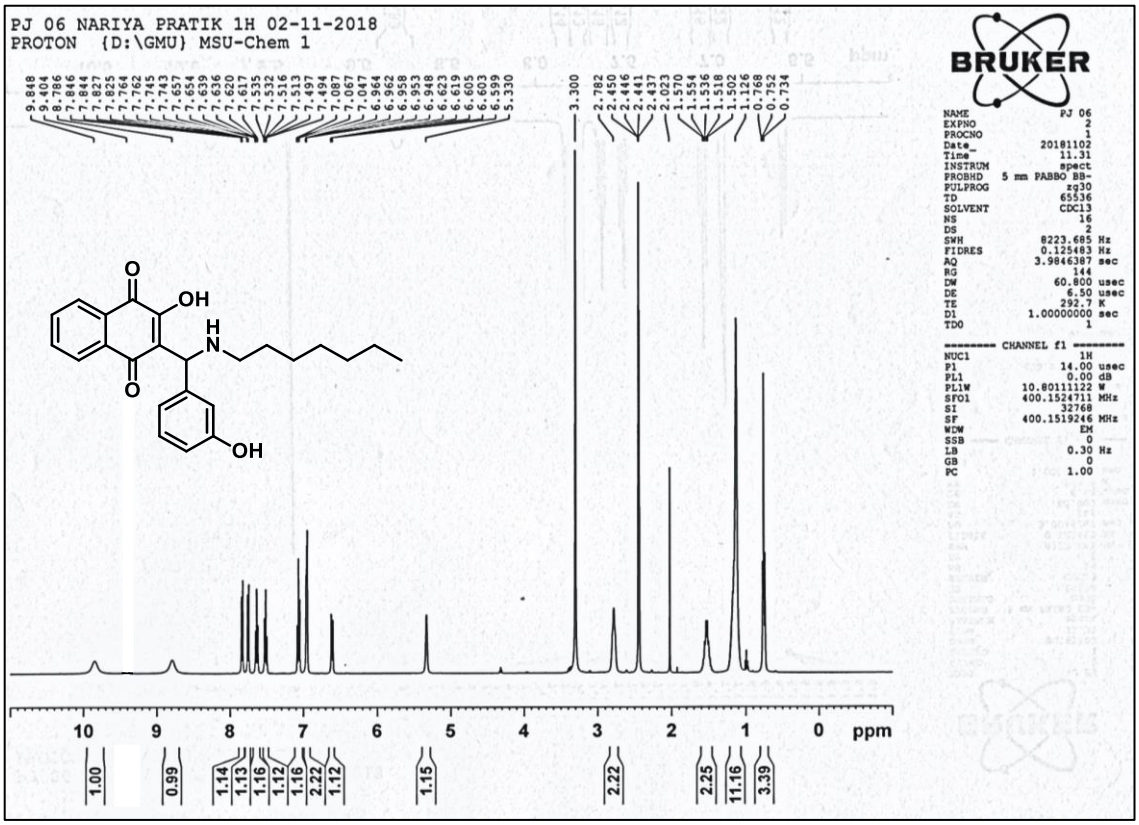

Figure S2.13 ^{1}H NMR spectra of compound **5**

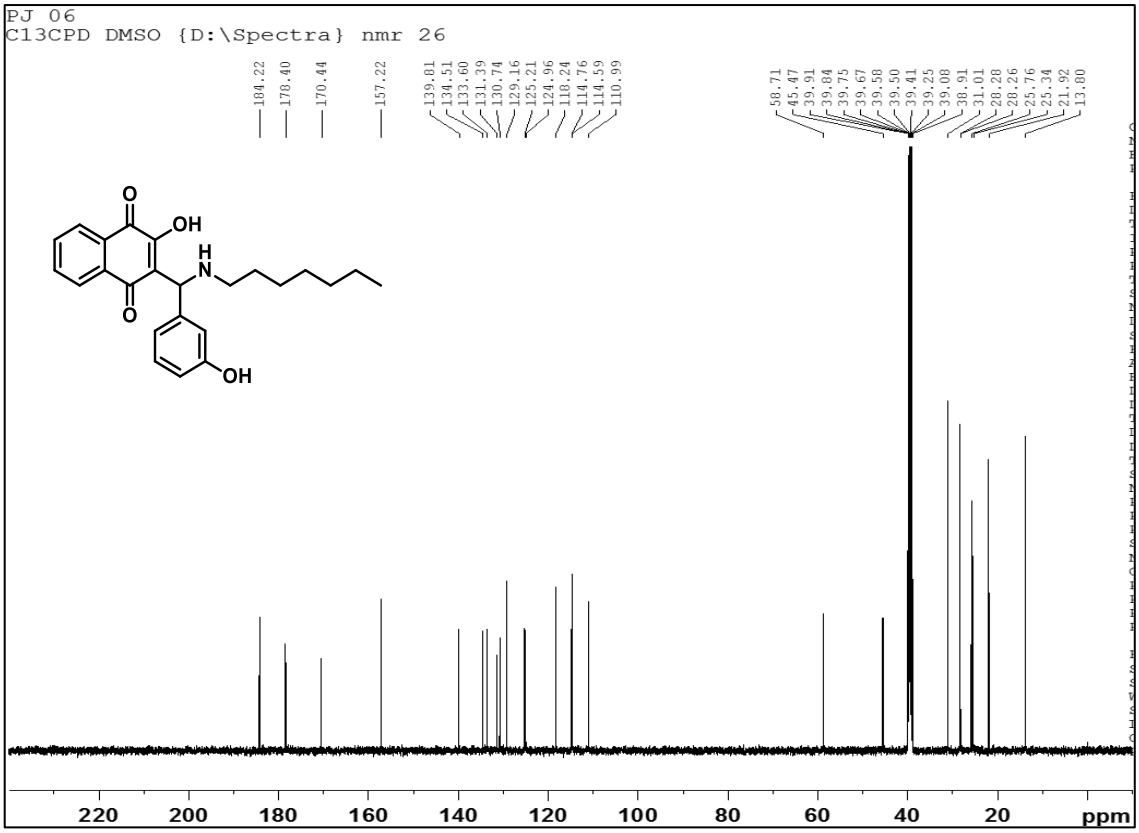

Figure S2.14 ^{13}C NMR spectra of compound **5**

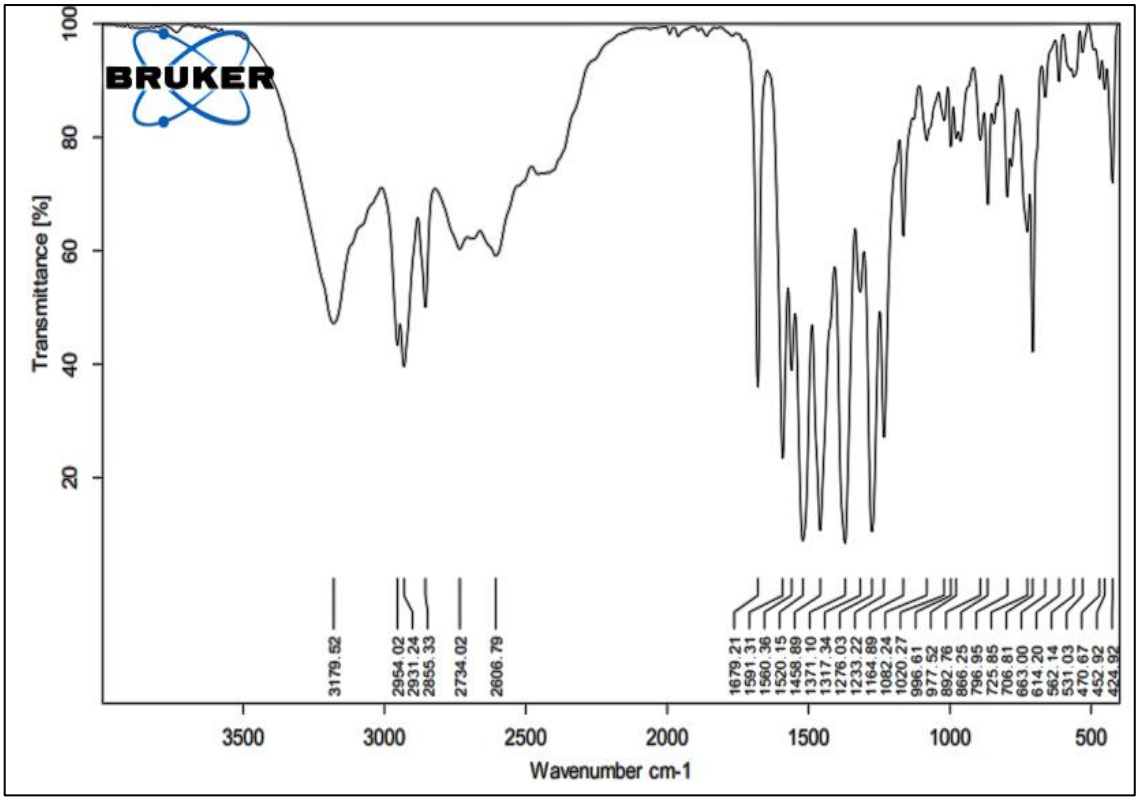

Figure S2.15 FT-IR spectra of compound **5**

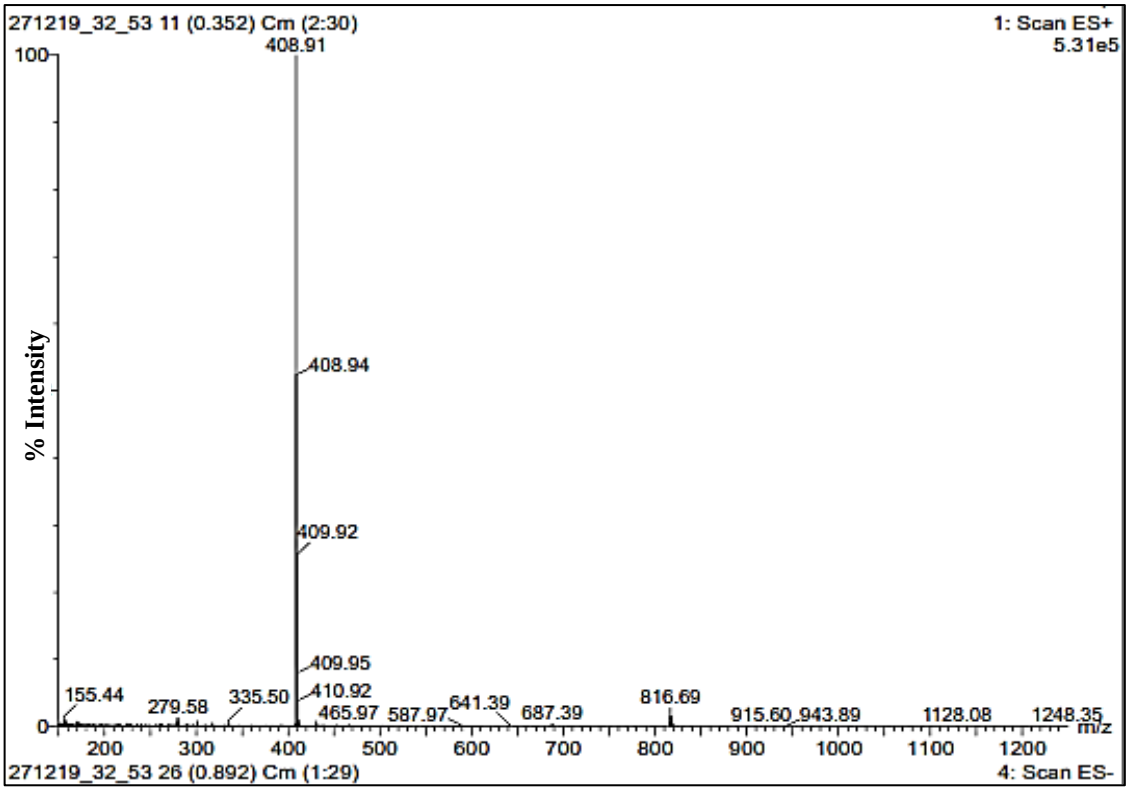

Figure S2.16 ESI-MS spectra of compound **5**

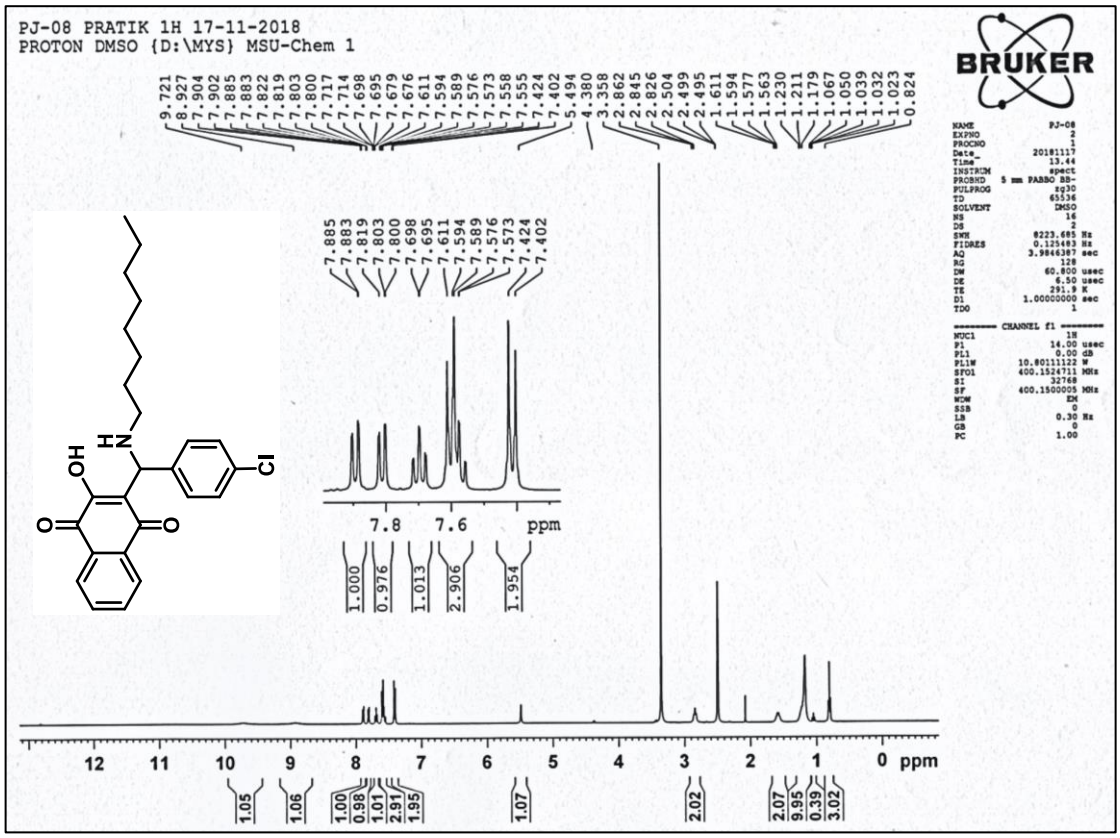

Figure S2.17 ^{1}H NMR spectra of compound **6**

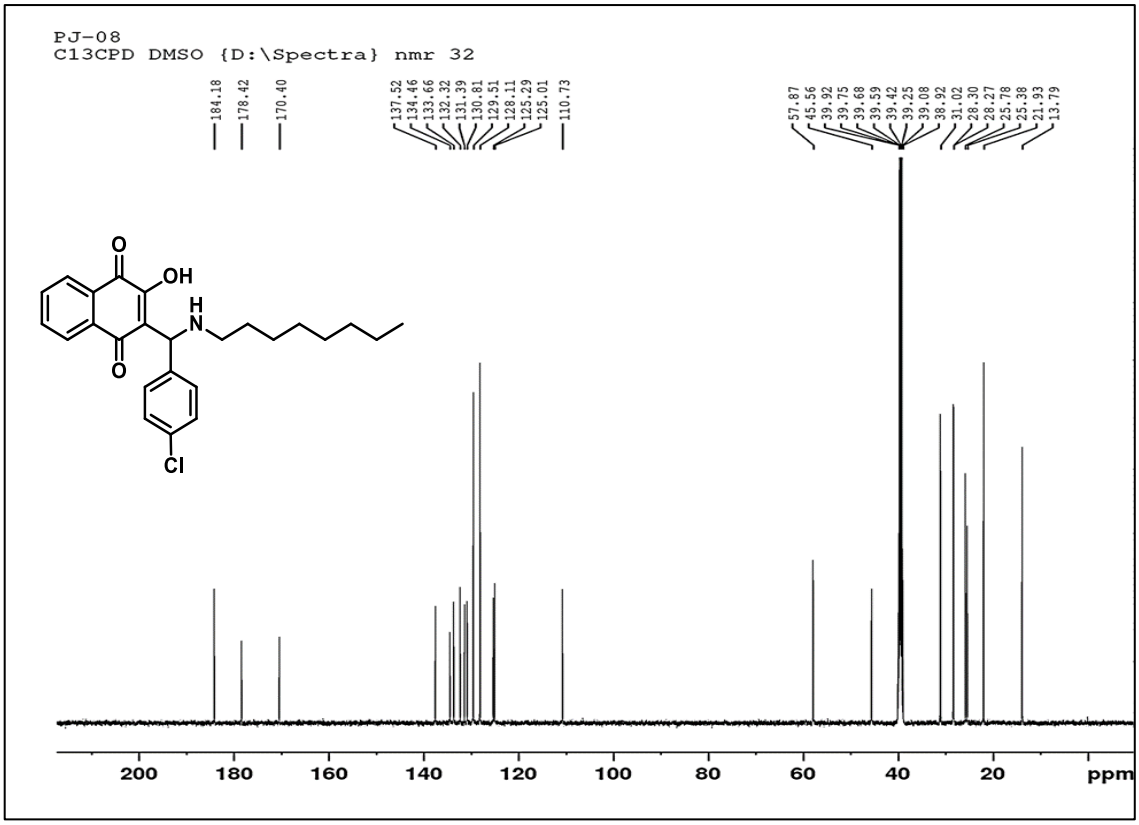

Figure S2.18 ^{13}C NMR spectra of compound **6**

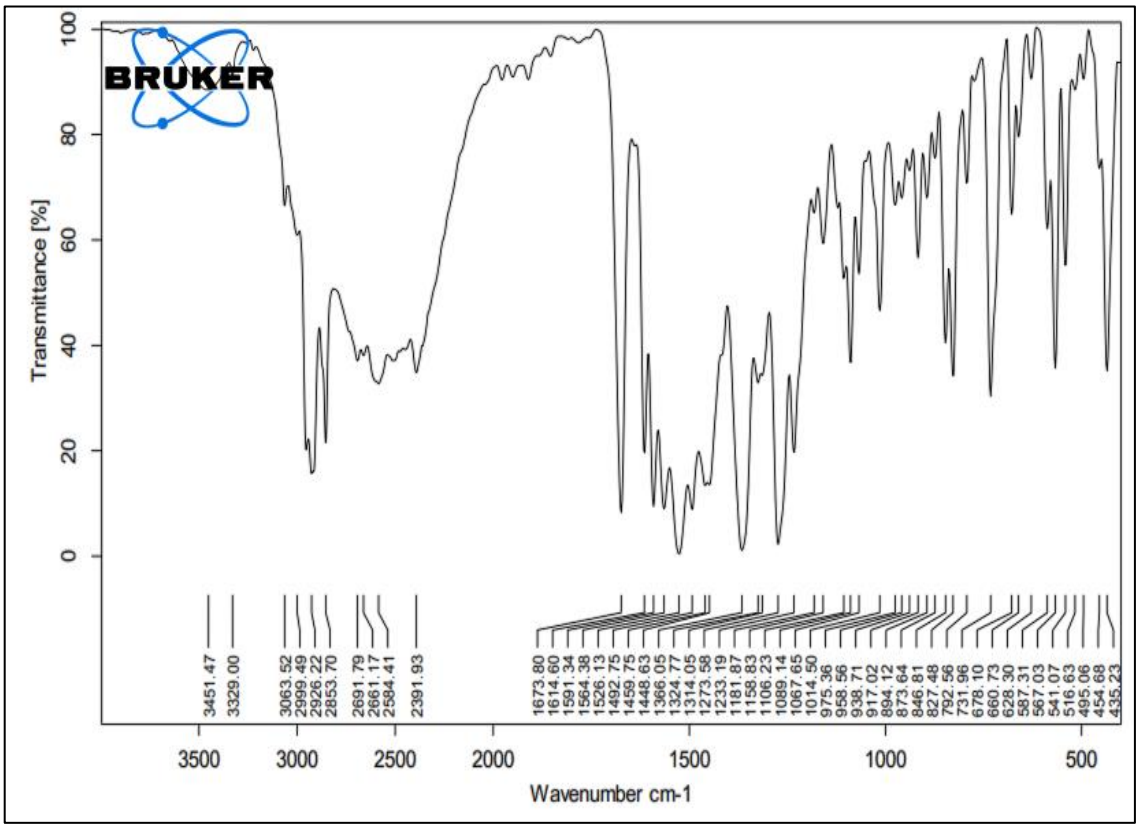

Figure S2.19 FT-IR spectra of compound **6**

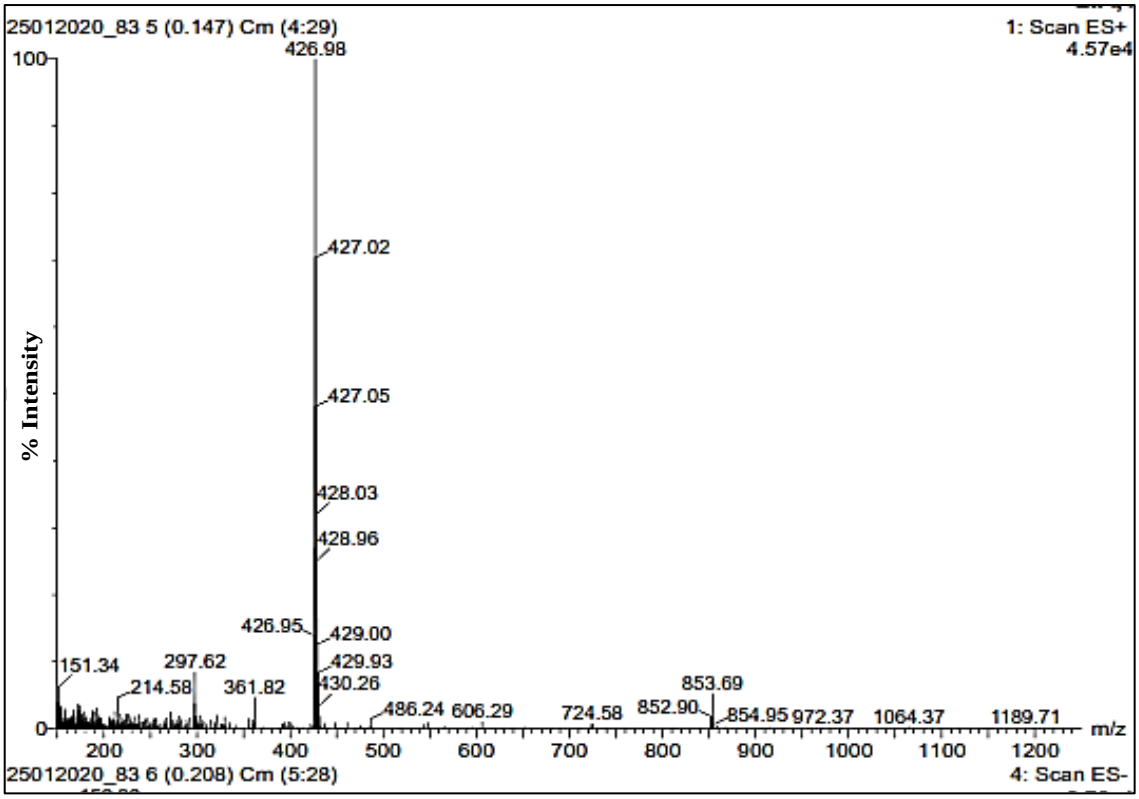

Figure S2.20 ESI-MS spectra of compound **6**

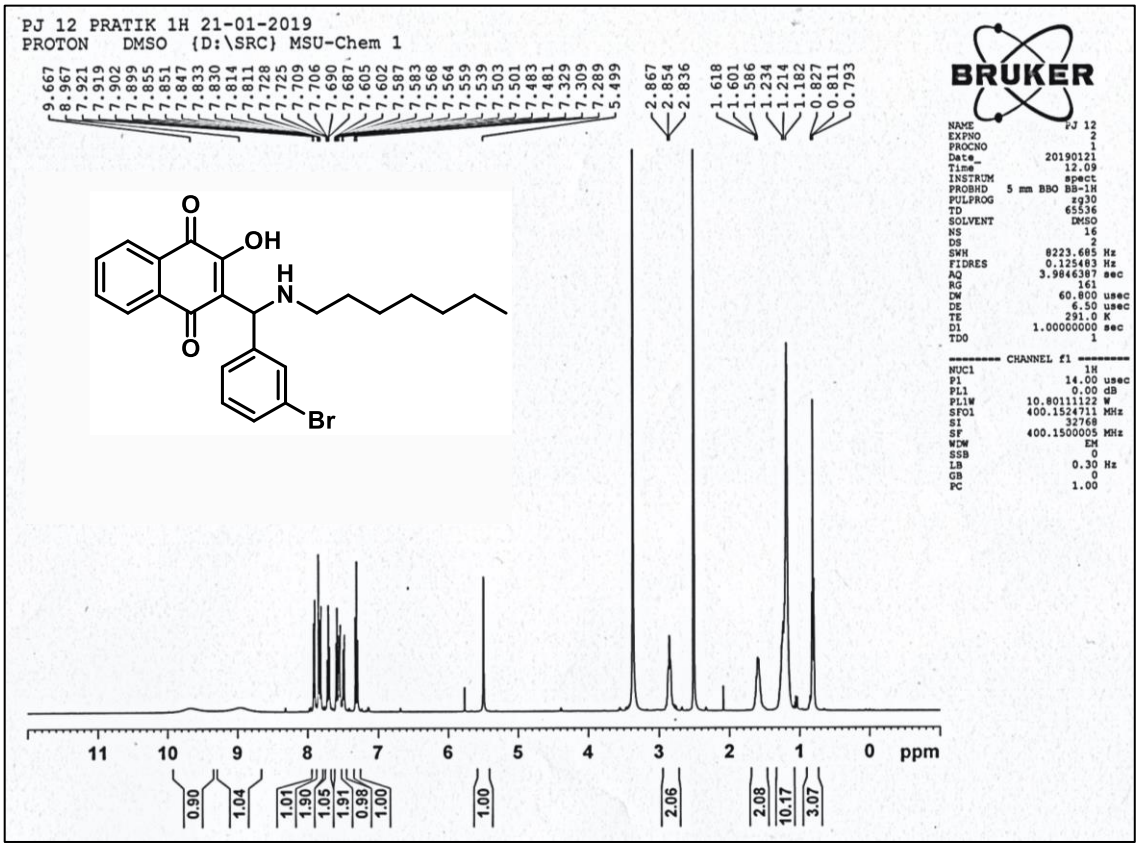

Figure S2.21 ^{1}H NMR spectra of compound **7**

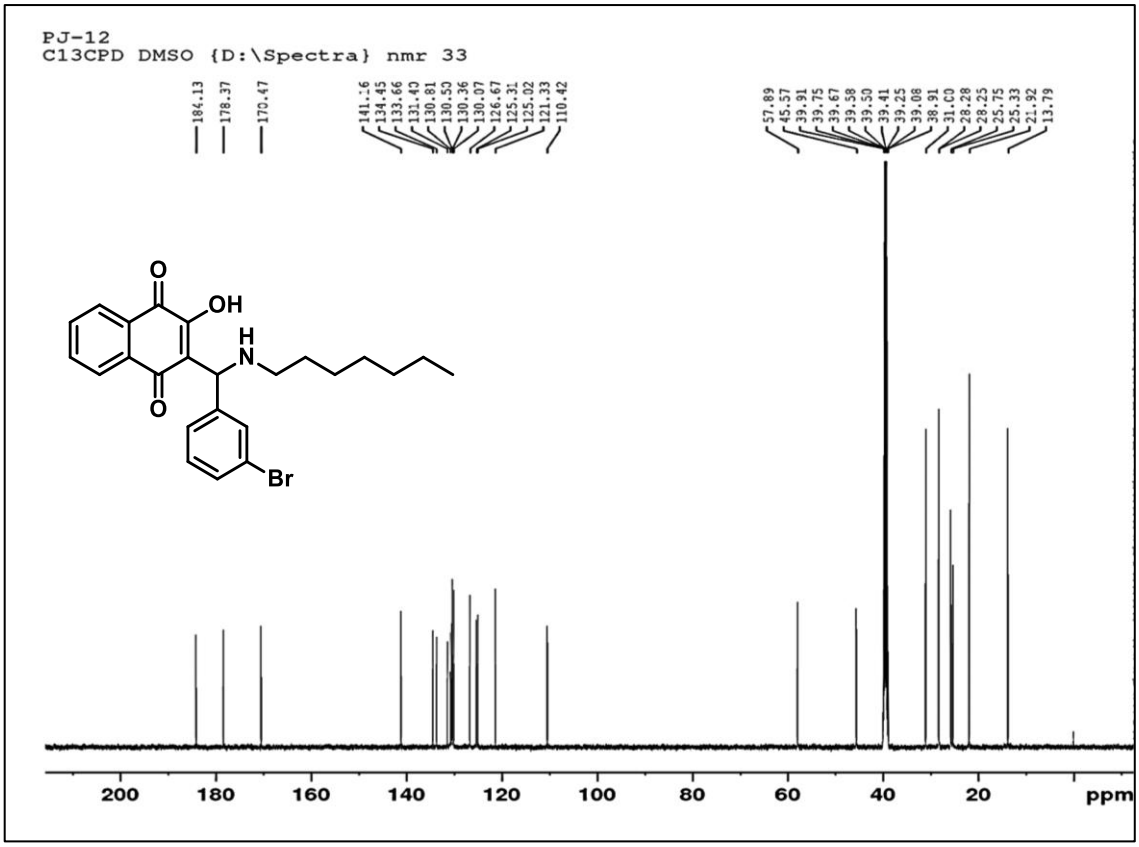

Figure S2.22 ^{13}C NMR spectra of compound **7**

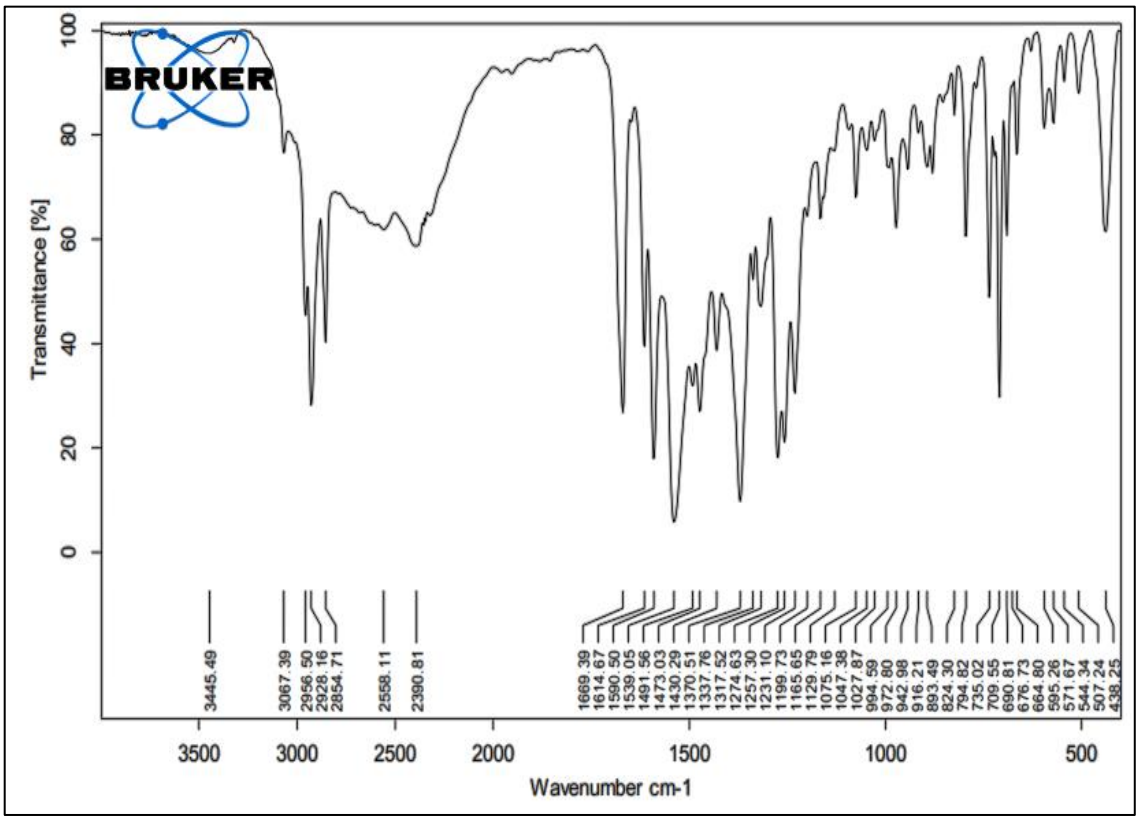

Figure S2.23 FT-IR spectra of compound **7**

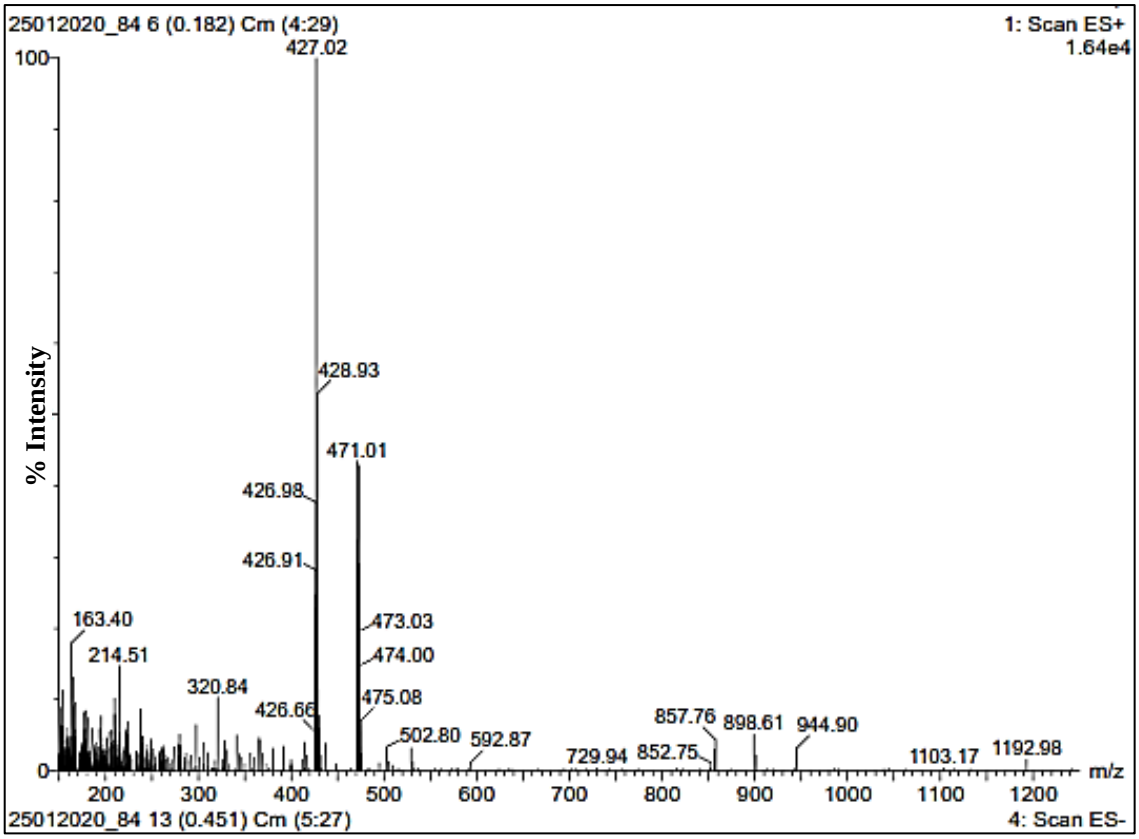

Figure S2.24 ESI-MS spectra of compound **7**

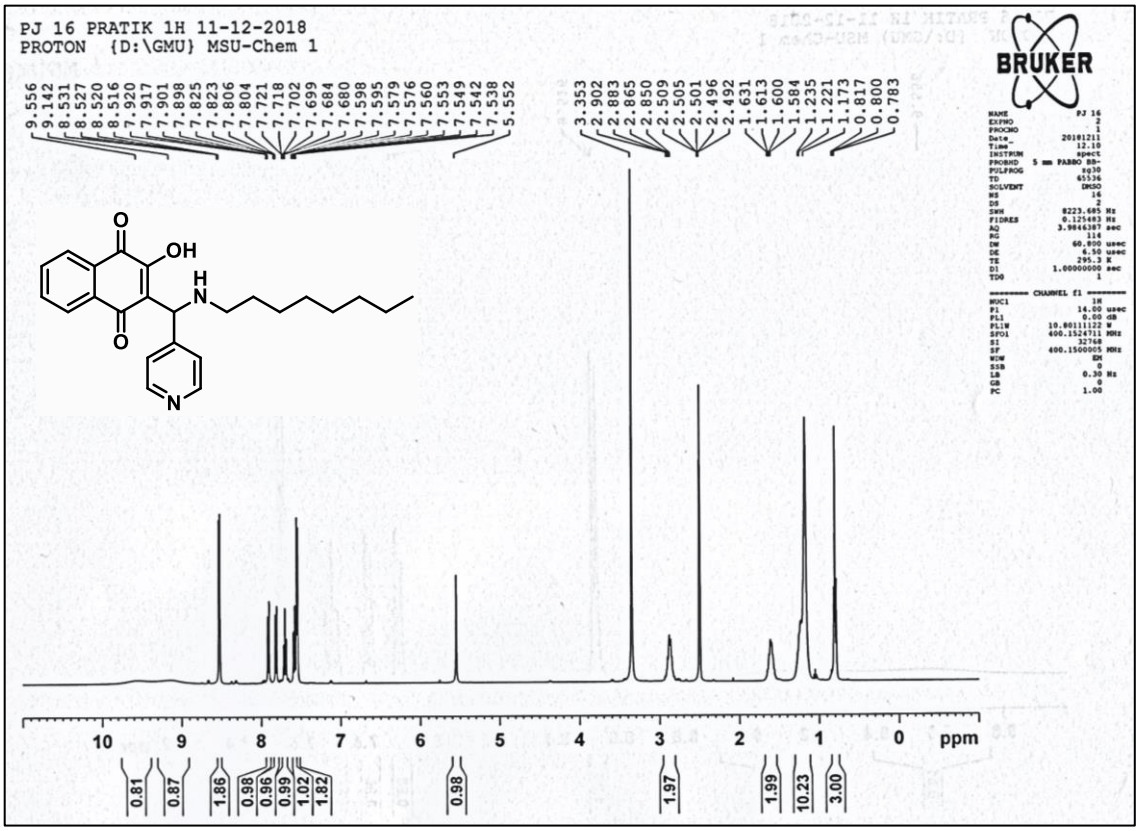

Figure S2.25 ^{1}H NMR spectra of compound **8**

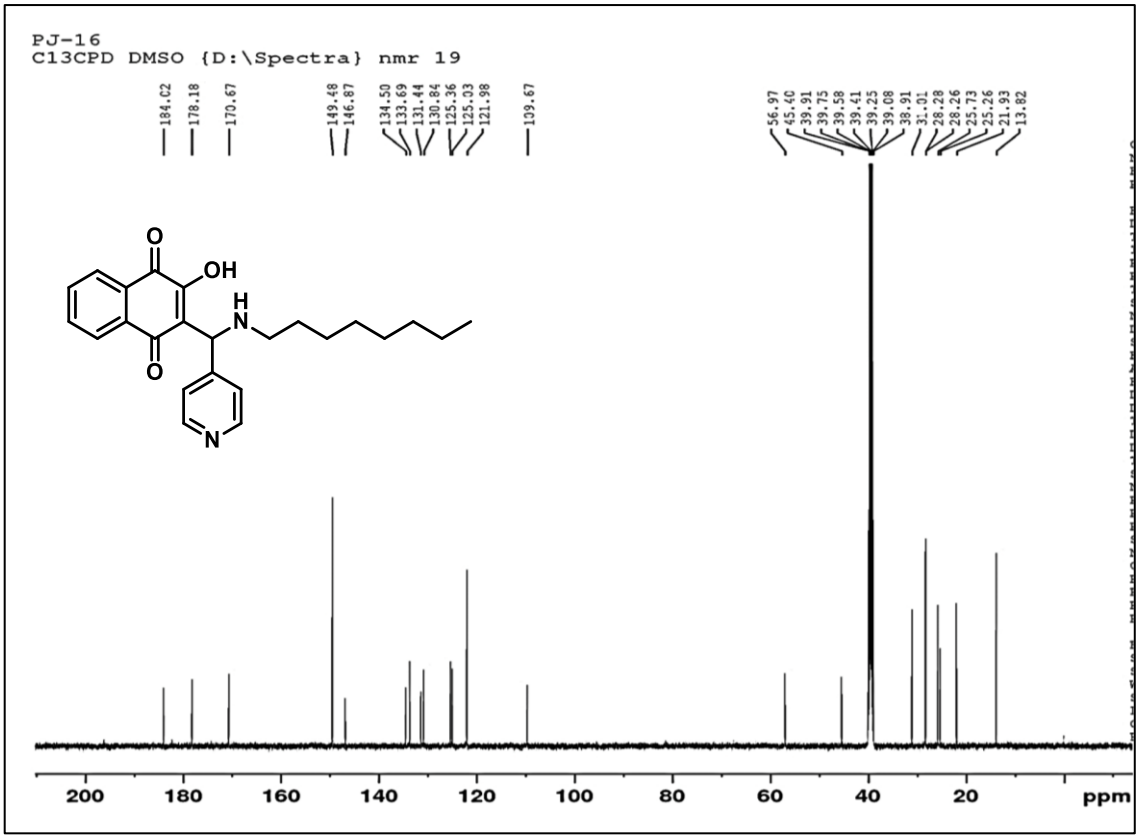

Figure S2.26 ^{13}C NMR spectra of compound **8**

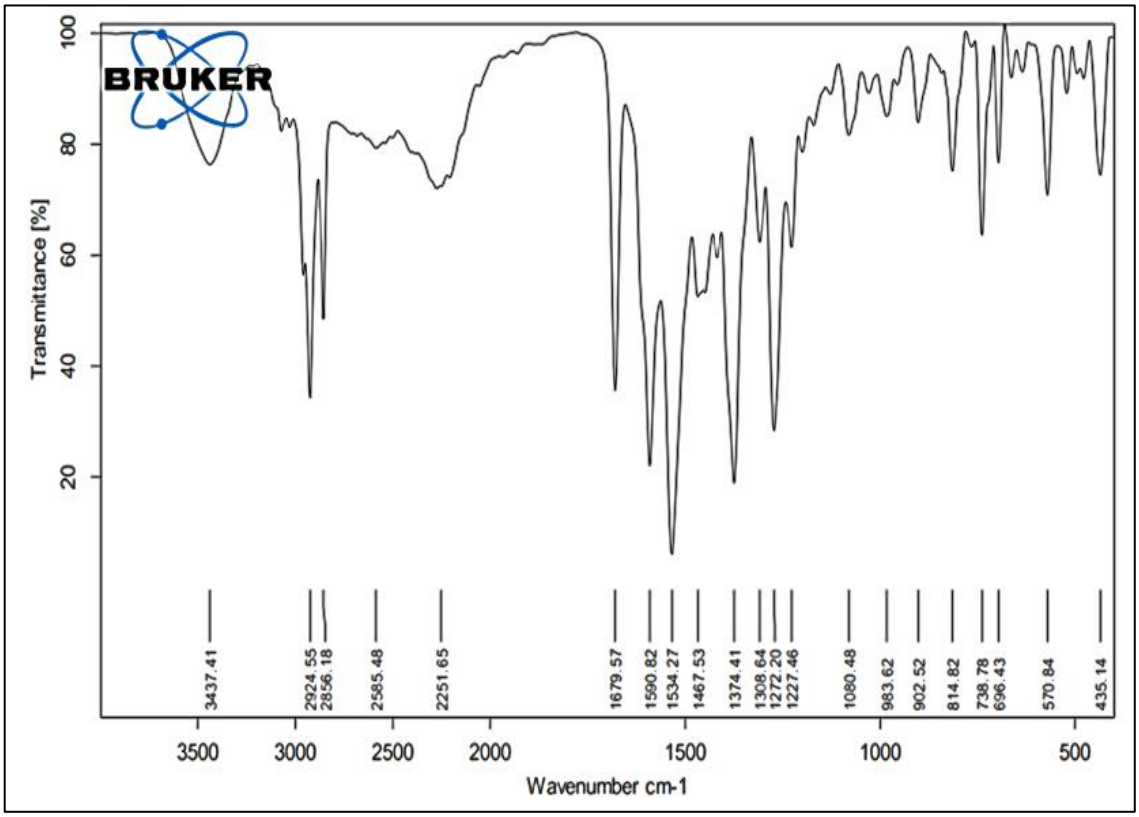

Figure S2.27 FT-IR spectra of compound **8**

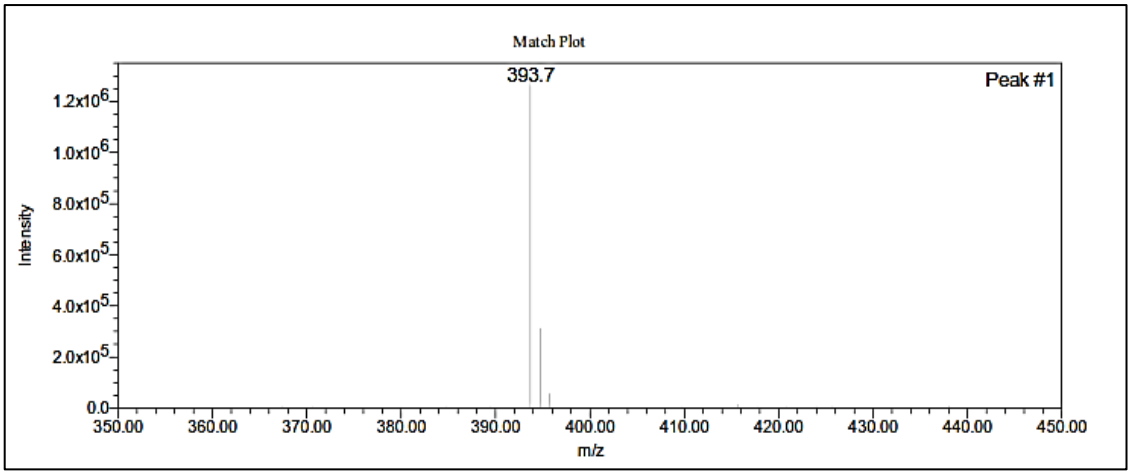

Figure S2.28 ESI-MS spectra of compound **8**

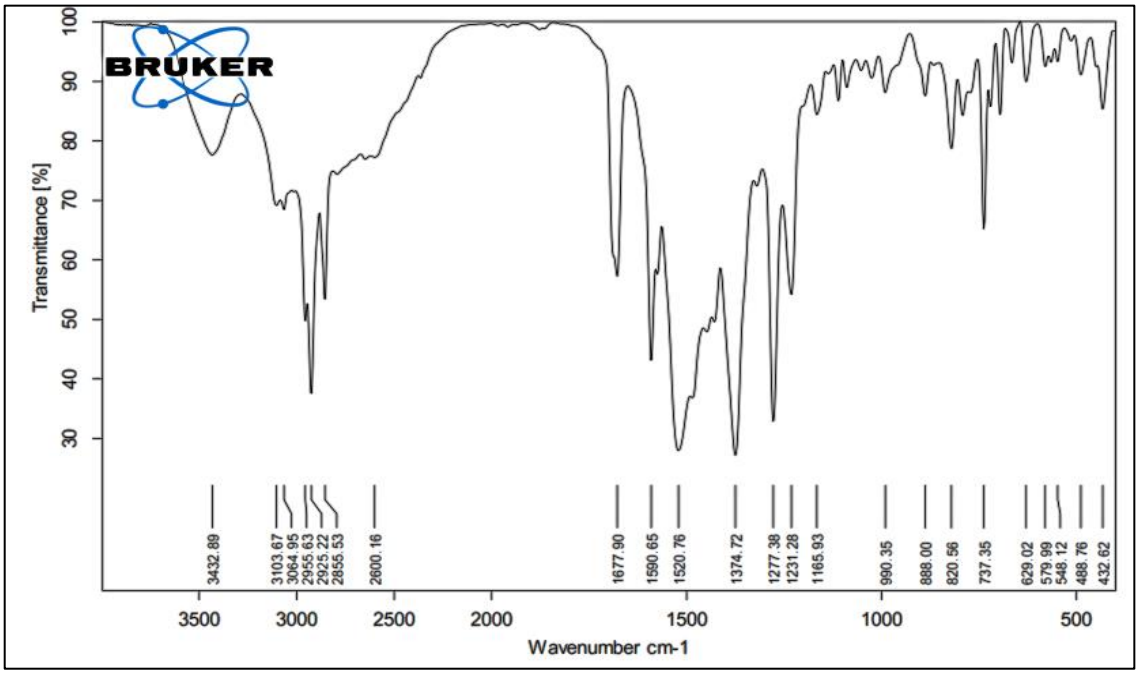

Figure S2.29 FT-IR spectra of compound **9**

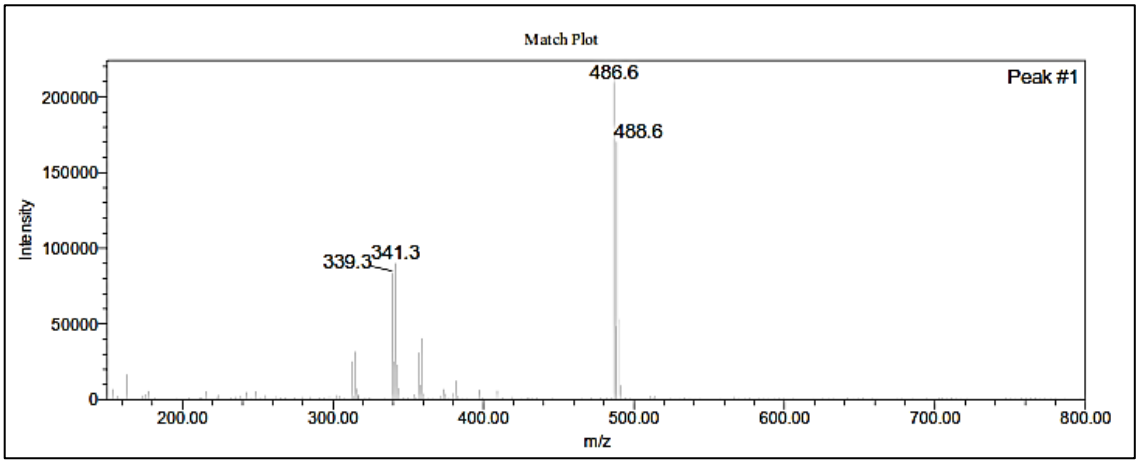

Figure S2.30 ESI-MS spectra of compound **9**

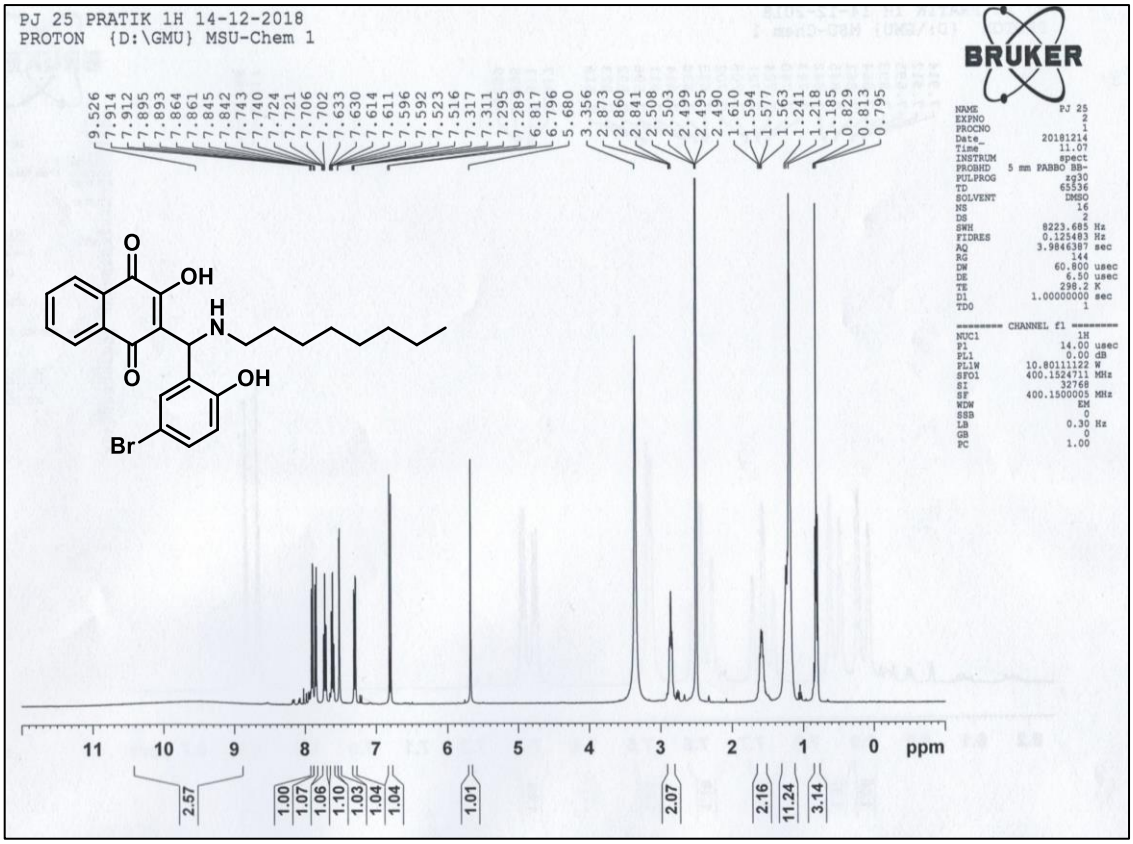

Figure S2.31 ^{1}H NMR spectra of compound **9**

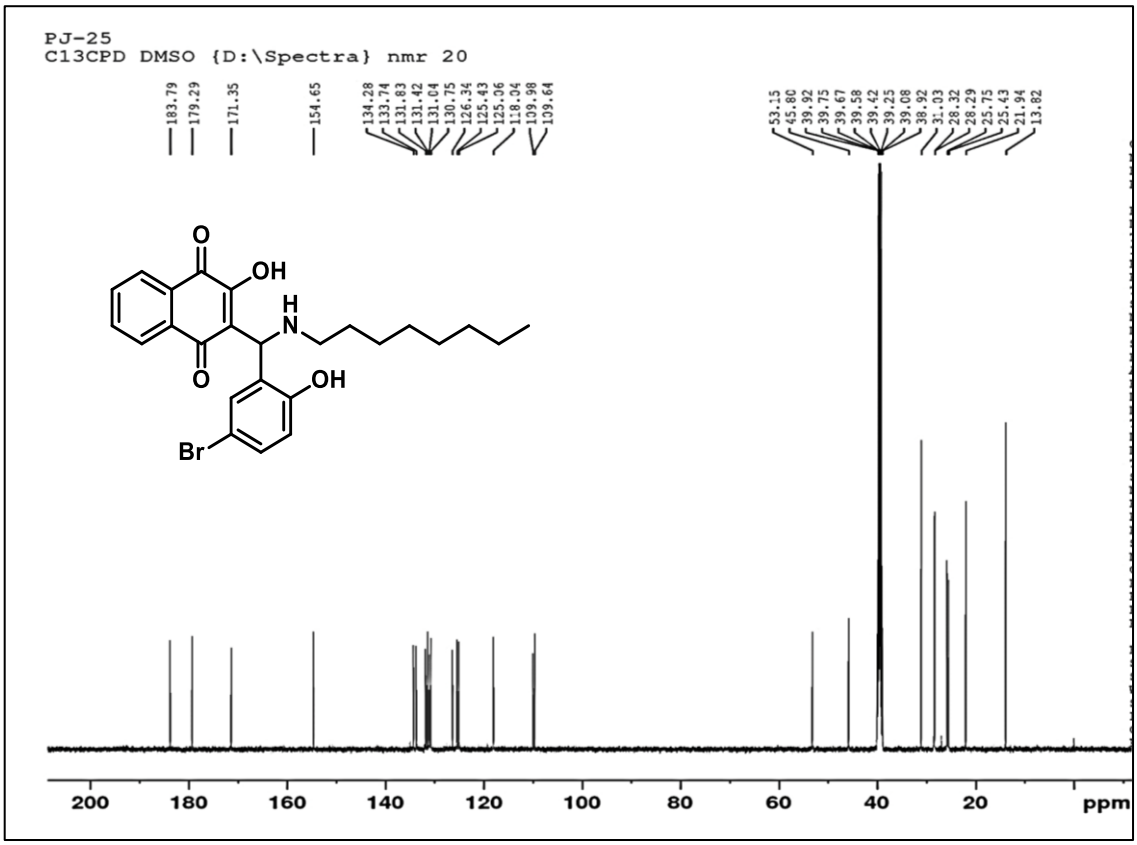

Figure S2.32 ^{13}C NMR spectra of compound **9**

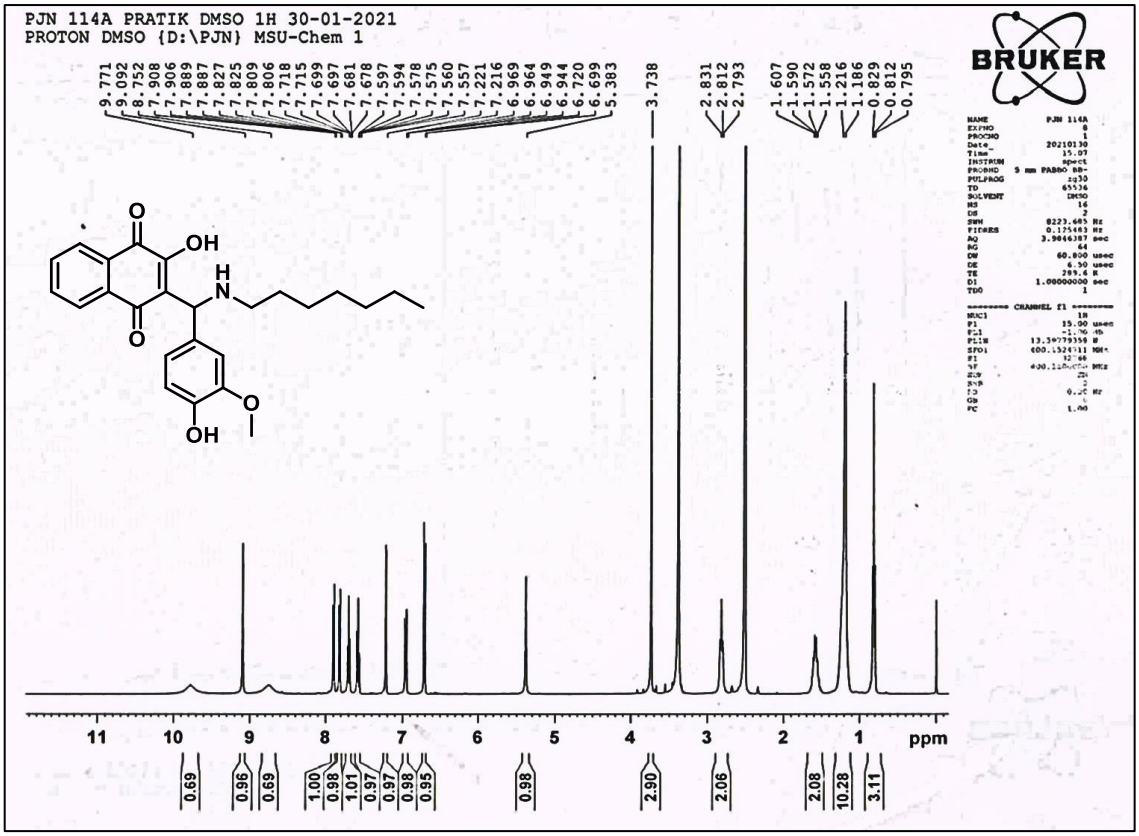

Figure S2.33 ^{1}H NMR spectra of compound **10**

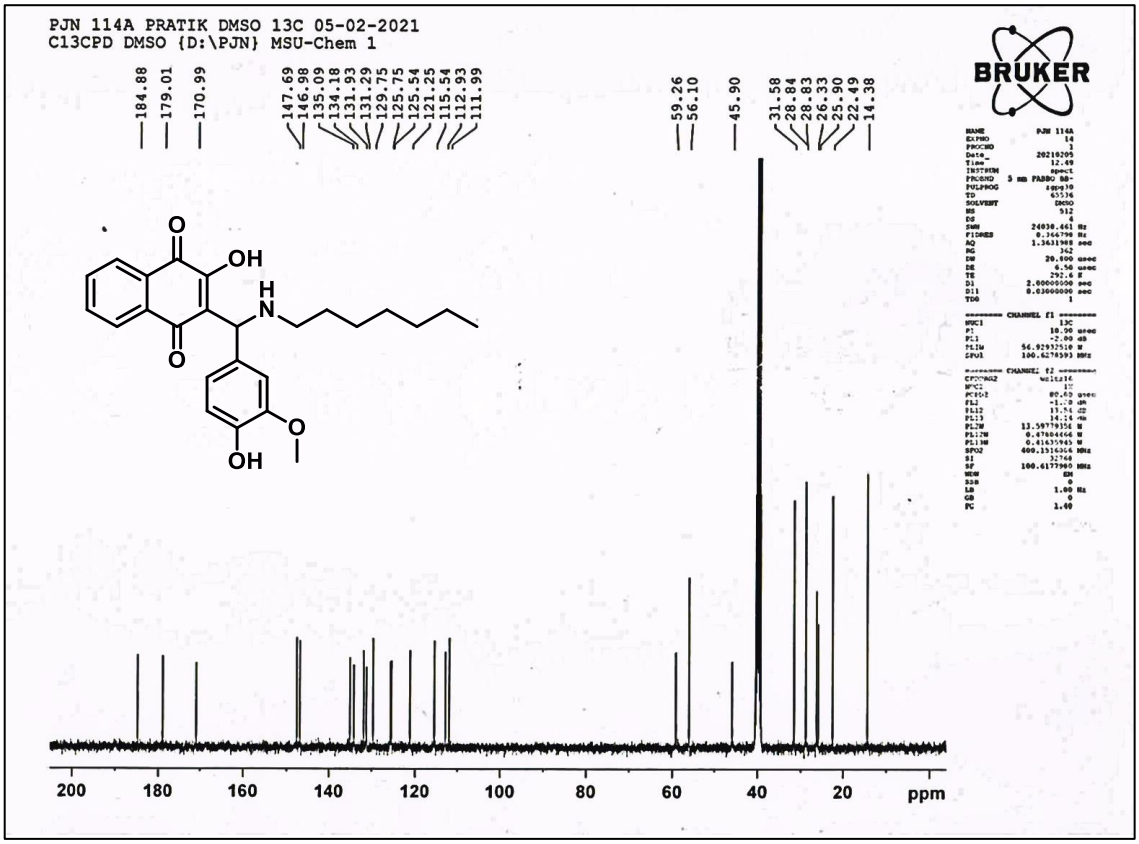

Figure S2.34 ^{13}C NMR spectra of compound **10**

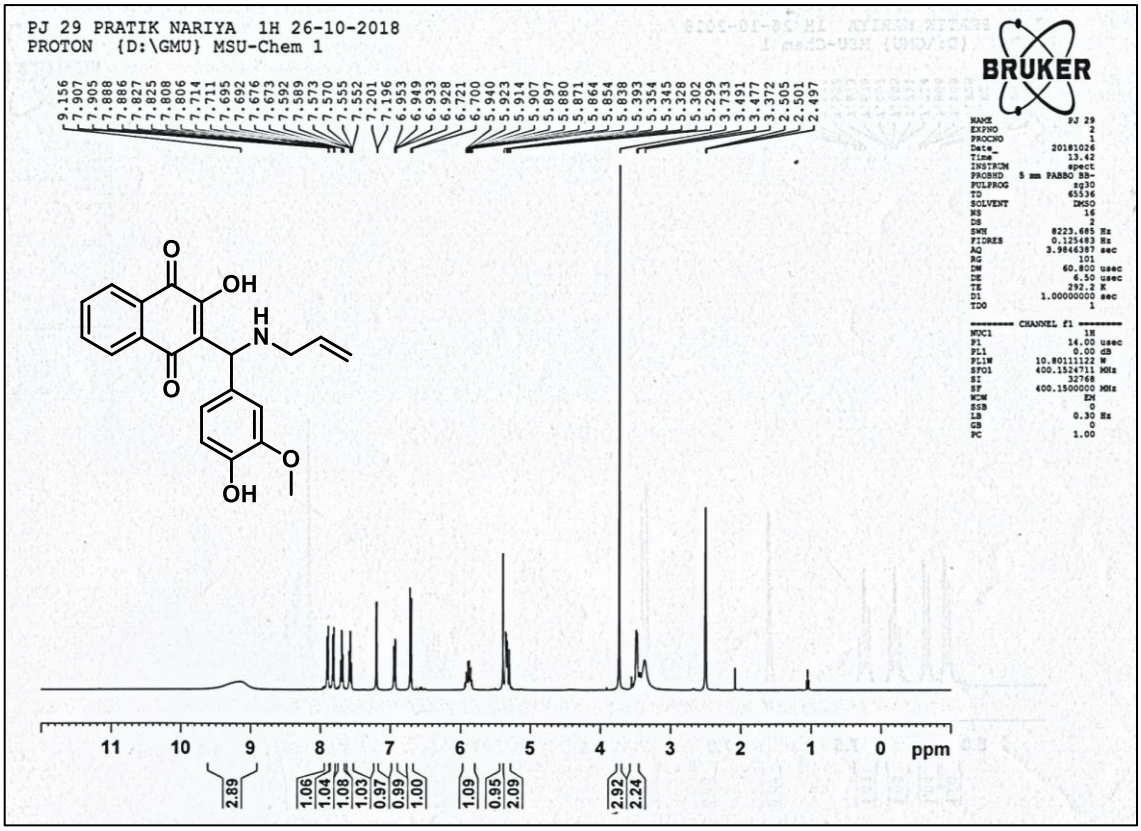

Figure S2.35 ^{1}H NMR spectra of compound **11**

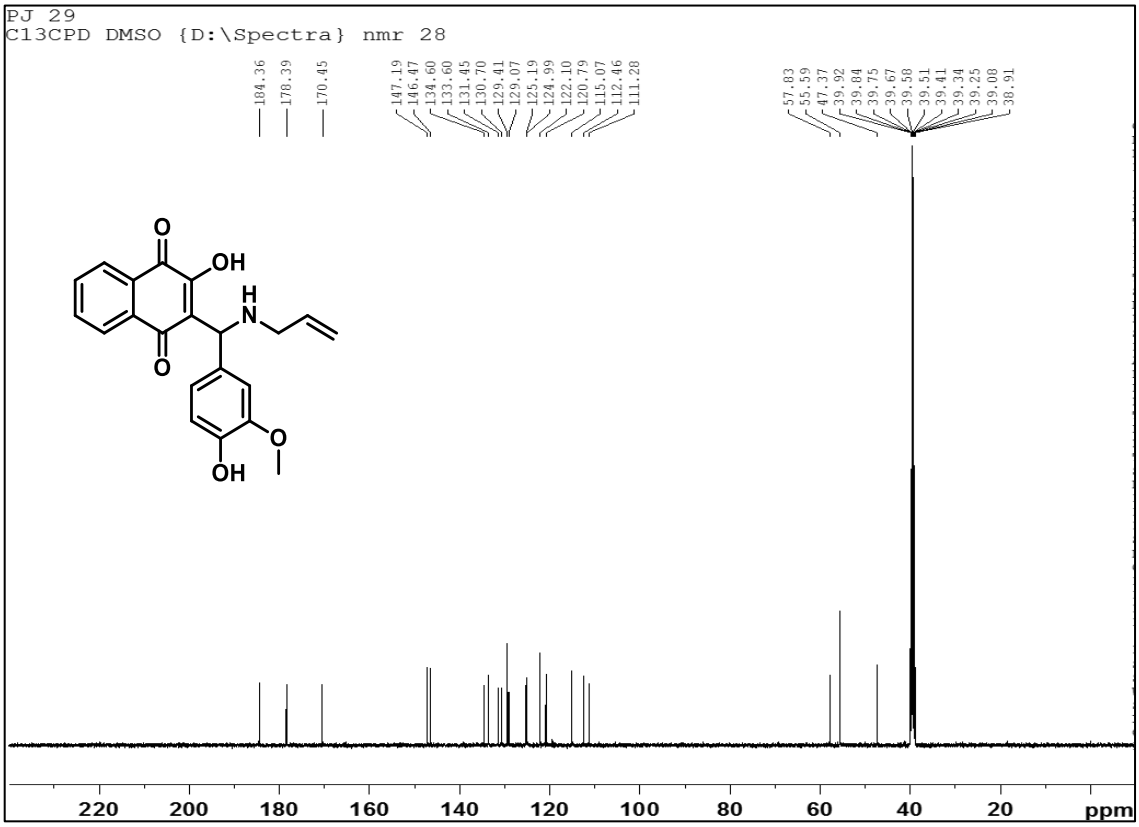

Figure S2.36 ^{13}C NMR spectra of compound **11**

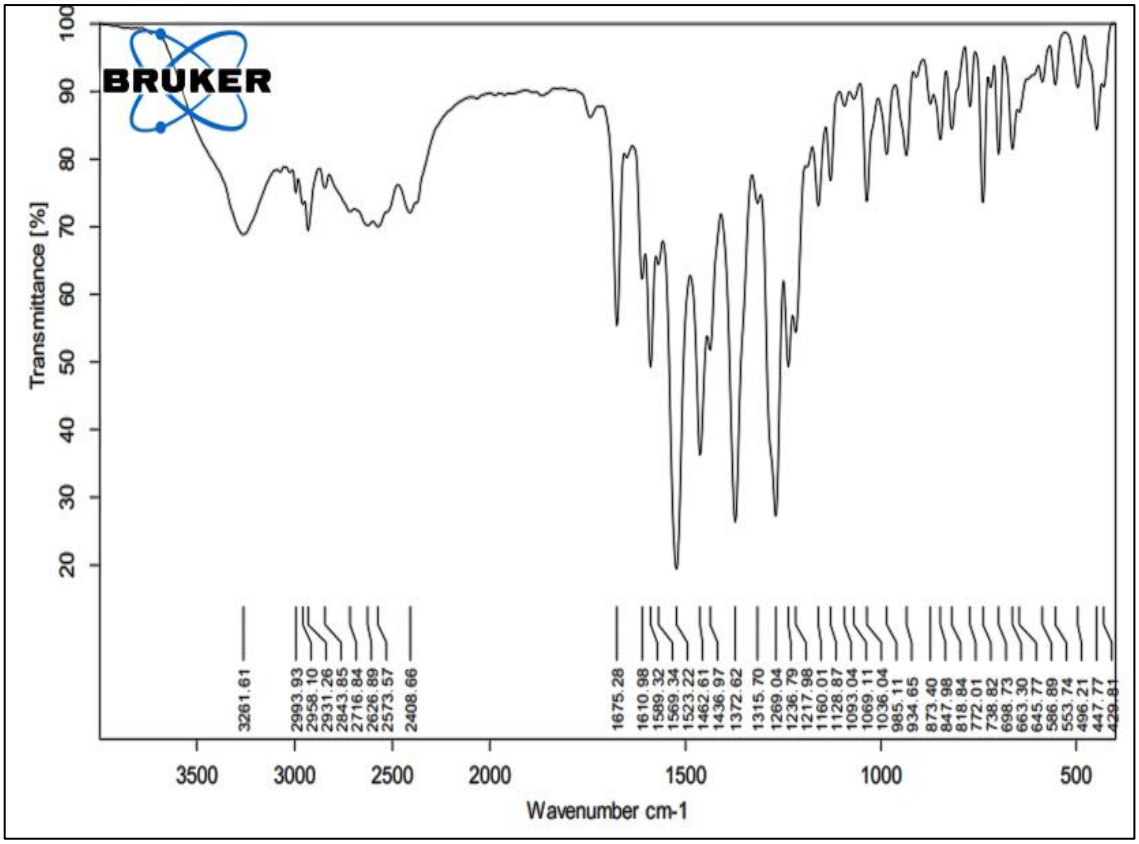

Figure S2.37 FT-IR spectra of compound **11**

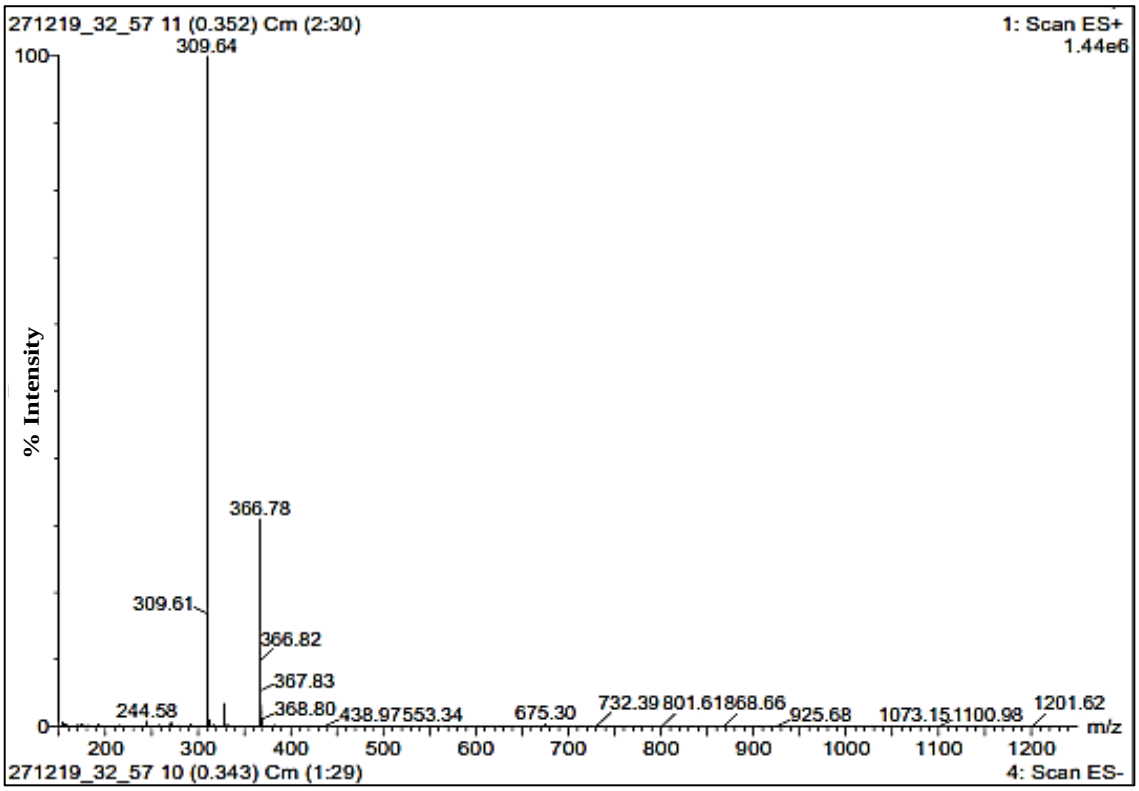

Figure S2.38 ESI-MS spectra of compound **11**

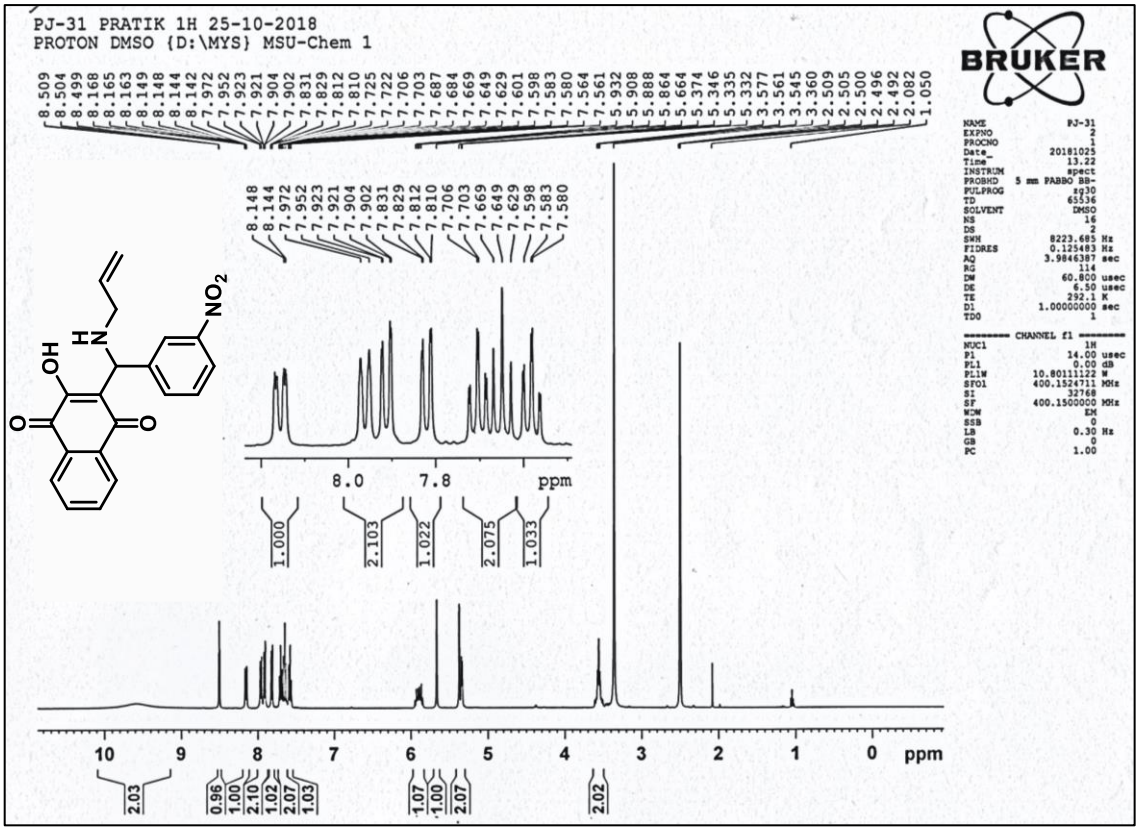

Figure S2.39 ^{1}H NMR spectra of compound **12**

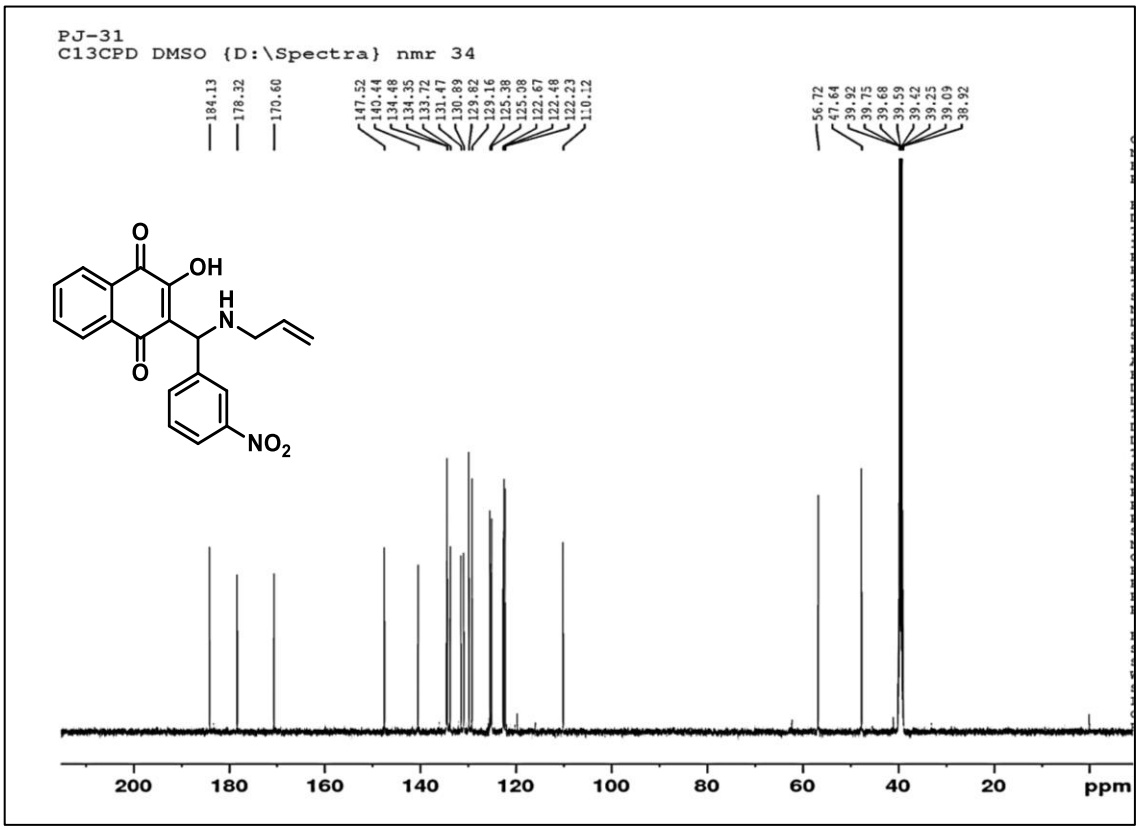

Figure S2.40 ^{13}C NMR spectra of compound **12**

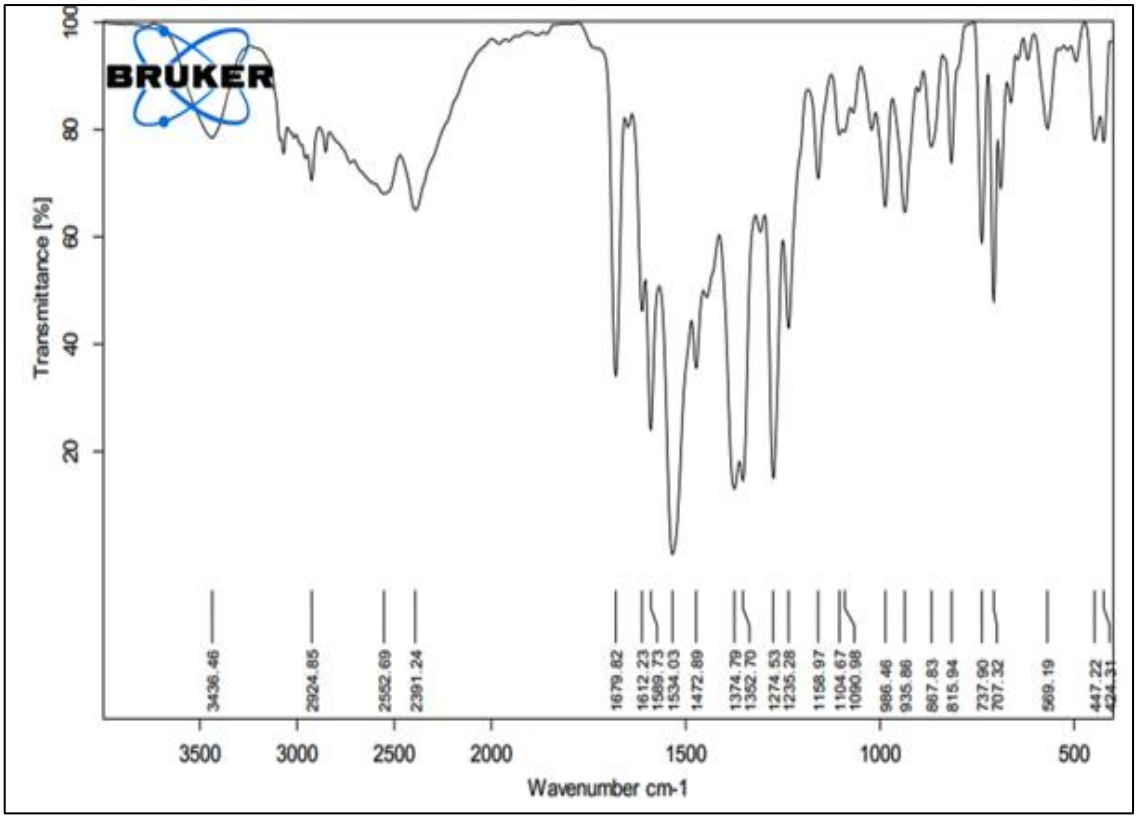

Figure S2.41 FT-IR spectra of compound **12**

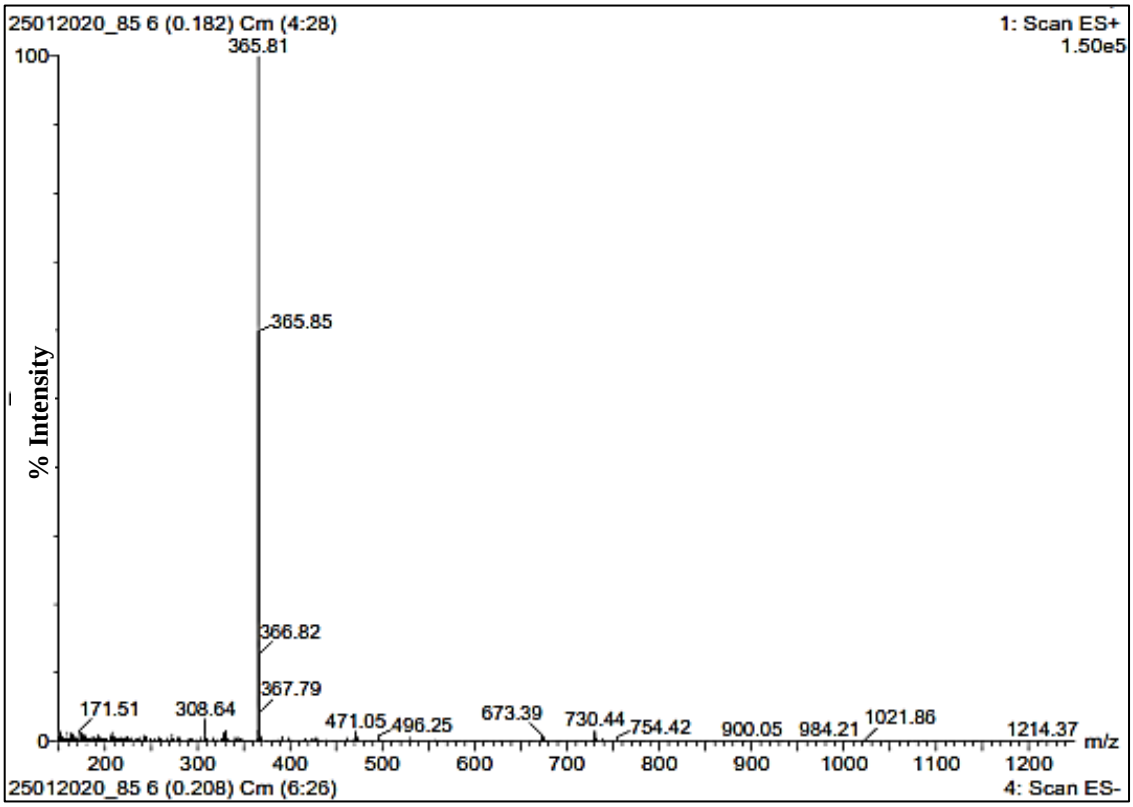

Figure S2.42 ESI-MS spectra of compound **12**

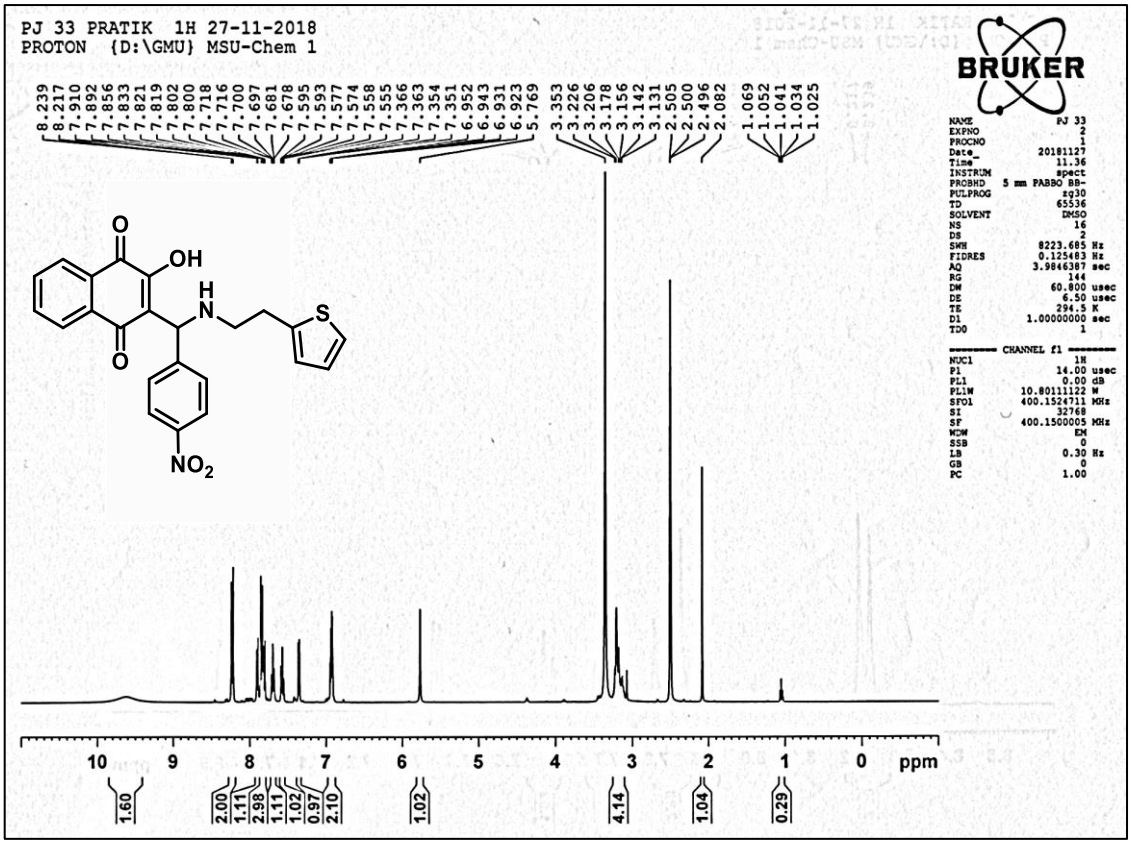

Figure S2.43 ^{1}H NMR spectra of compound **13**

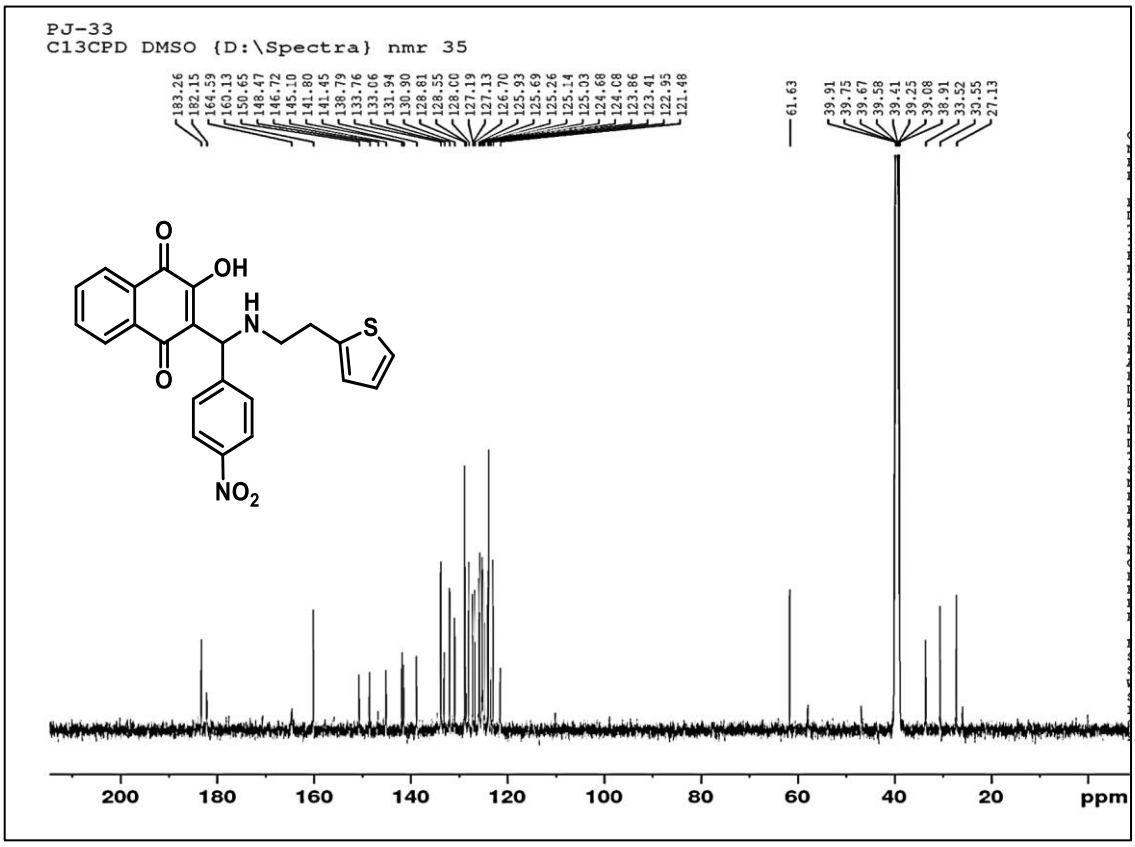

Figure S2.44 ^{13}C NMR spectra of compound **13**

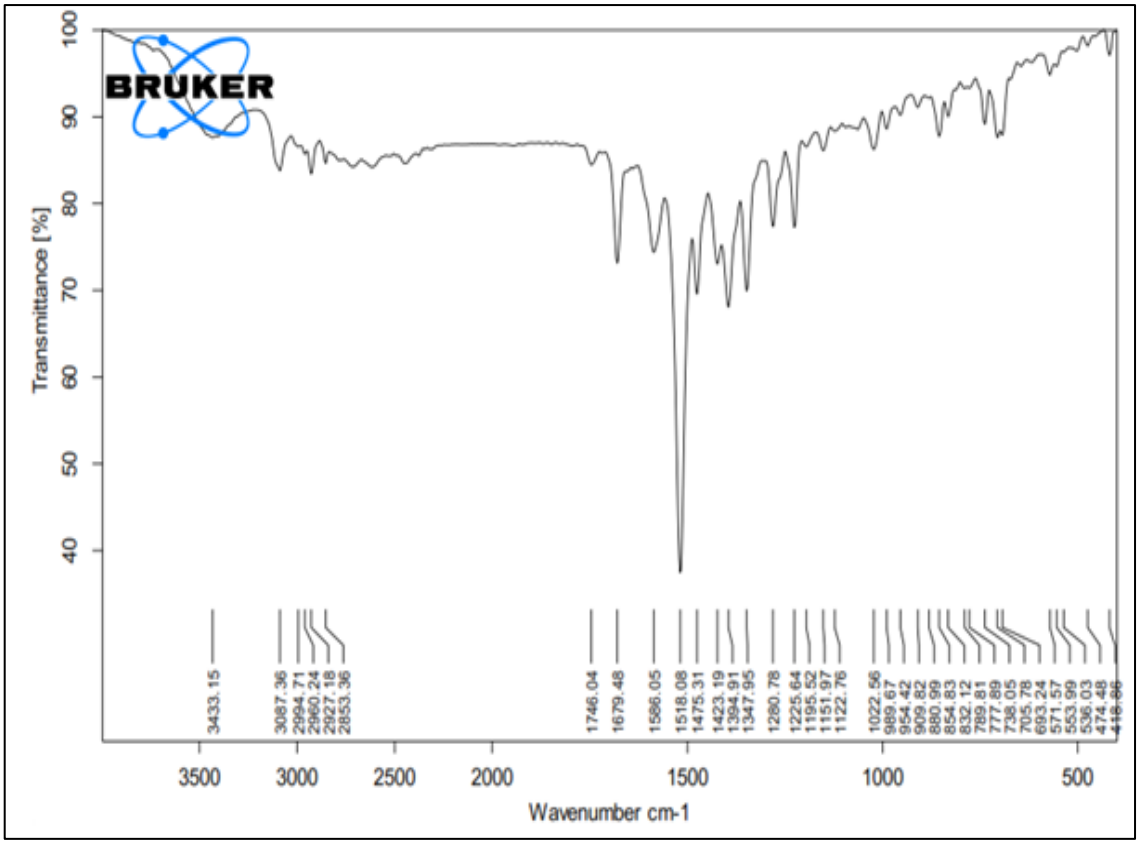

Figure S2.45 FT-IR spectra of compound **13**

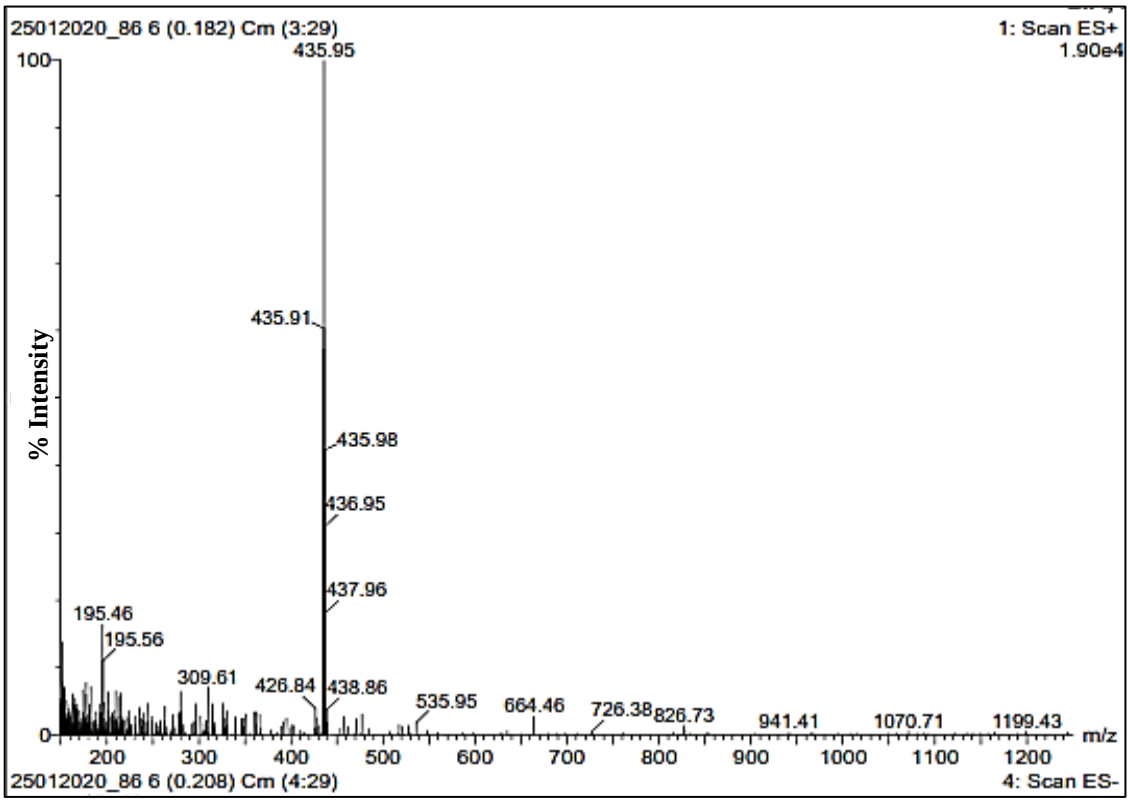

Figure S2.46 ESI-MS spectra of compound **13**

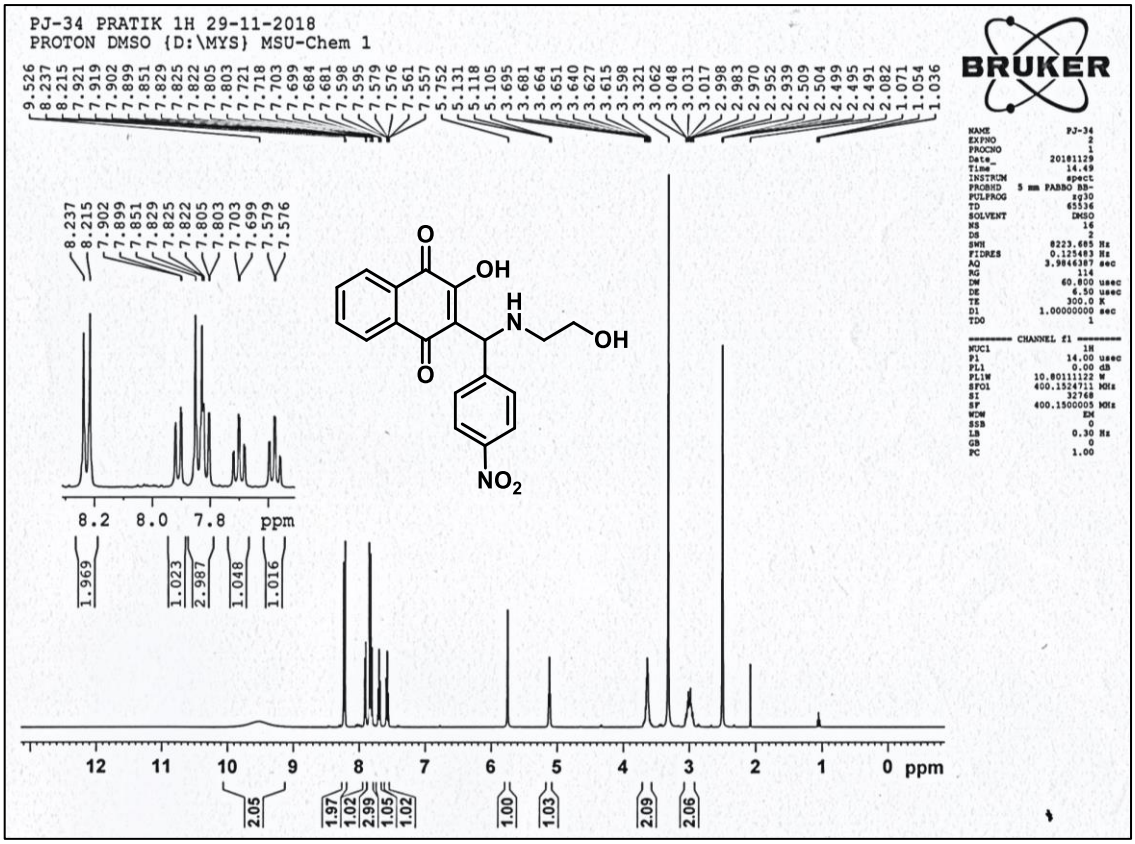

Figure S2.47 ^{1}H NMR spectra of compound **14**

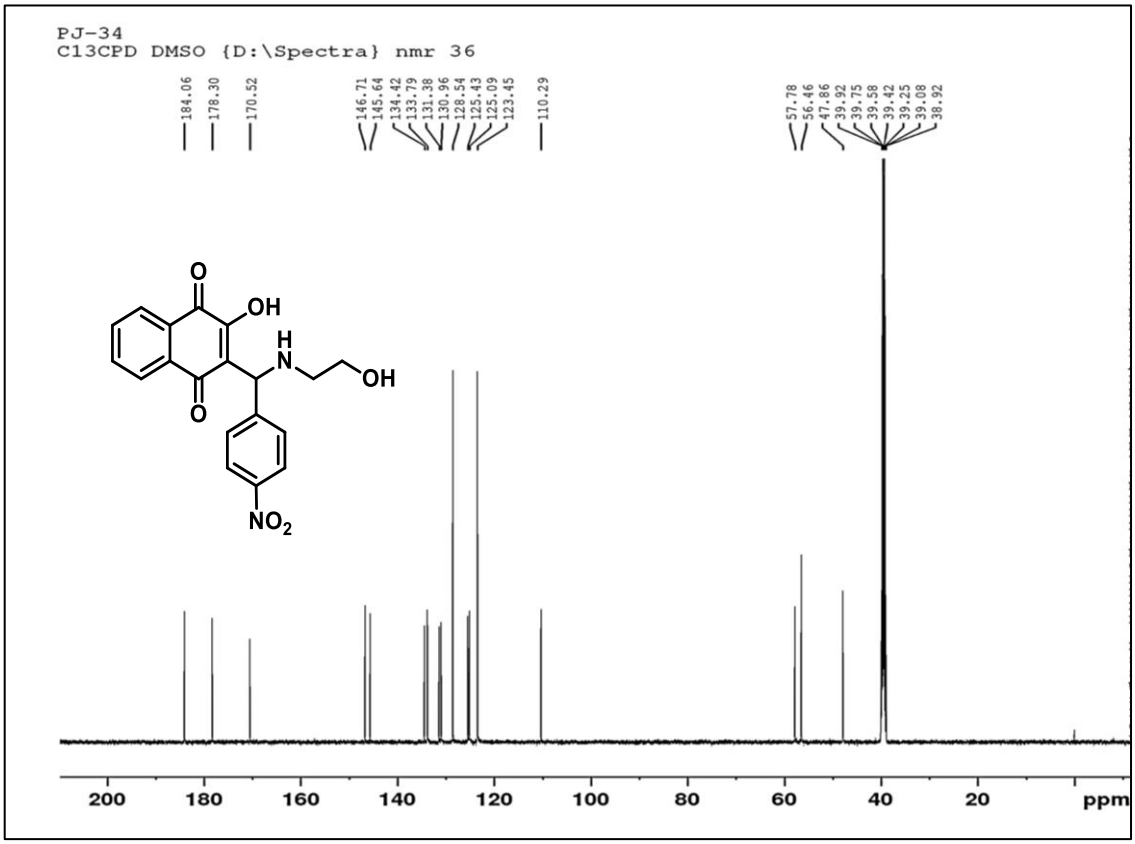

Figure S2.48 ^{13}C NMR spectra of compound **14**

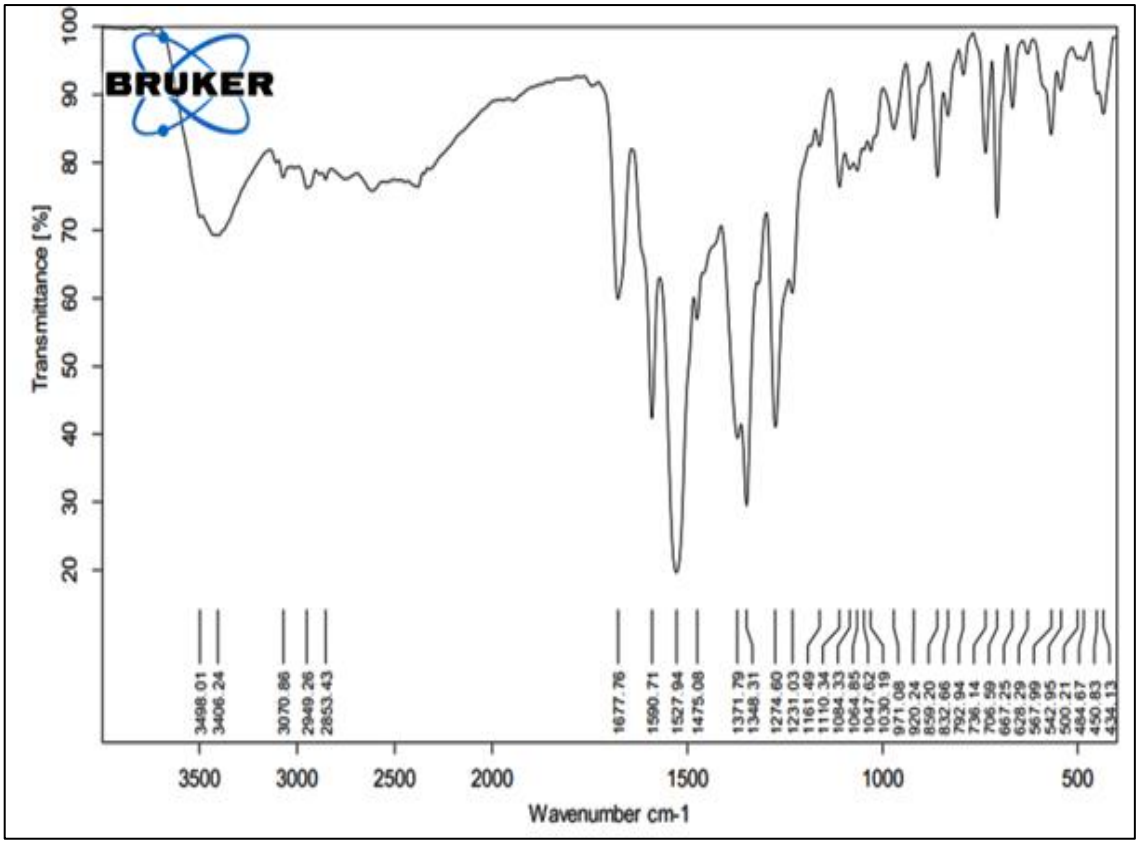

Figure S2.49 FT-IR spectra of compound **14**

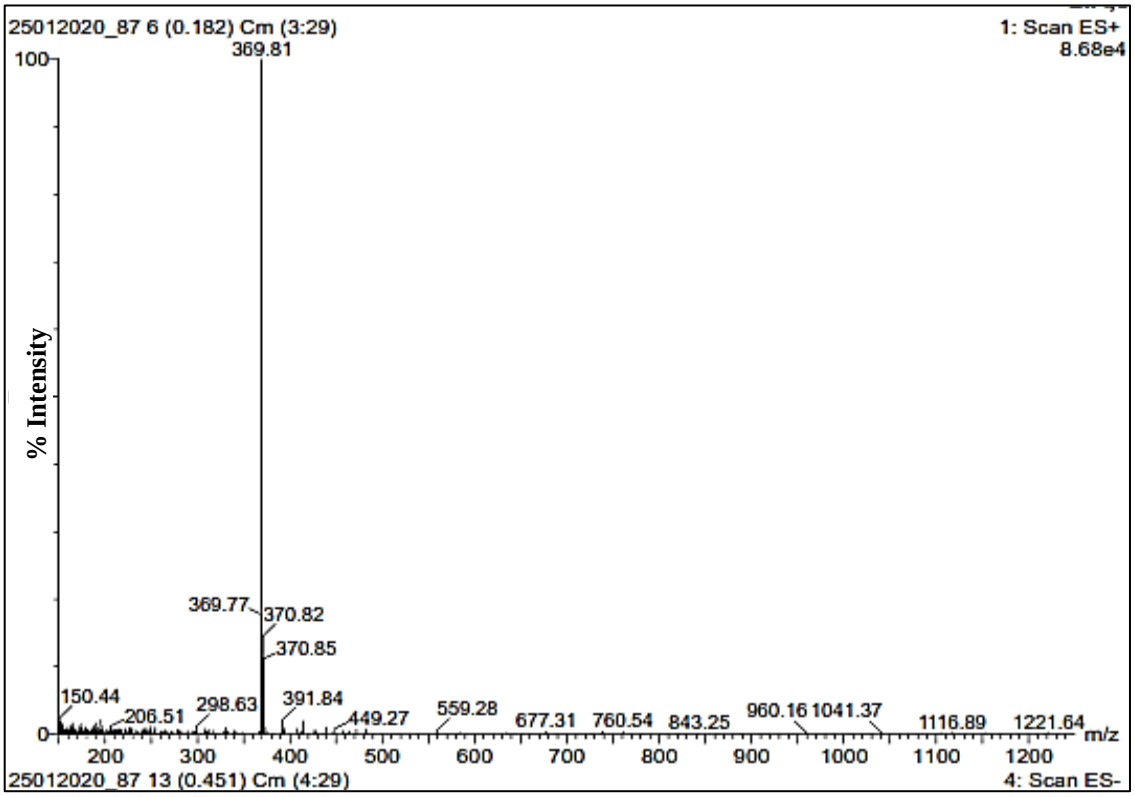

Figure S2.50 ESI-MS spectra of compound **14**

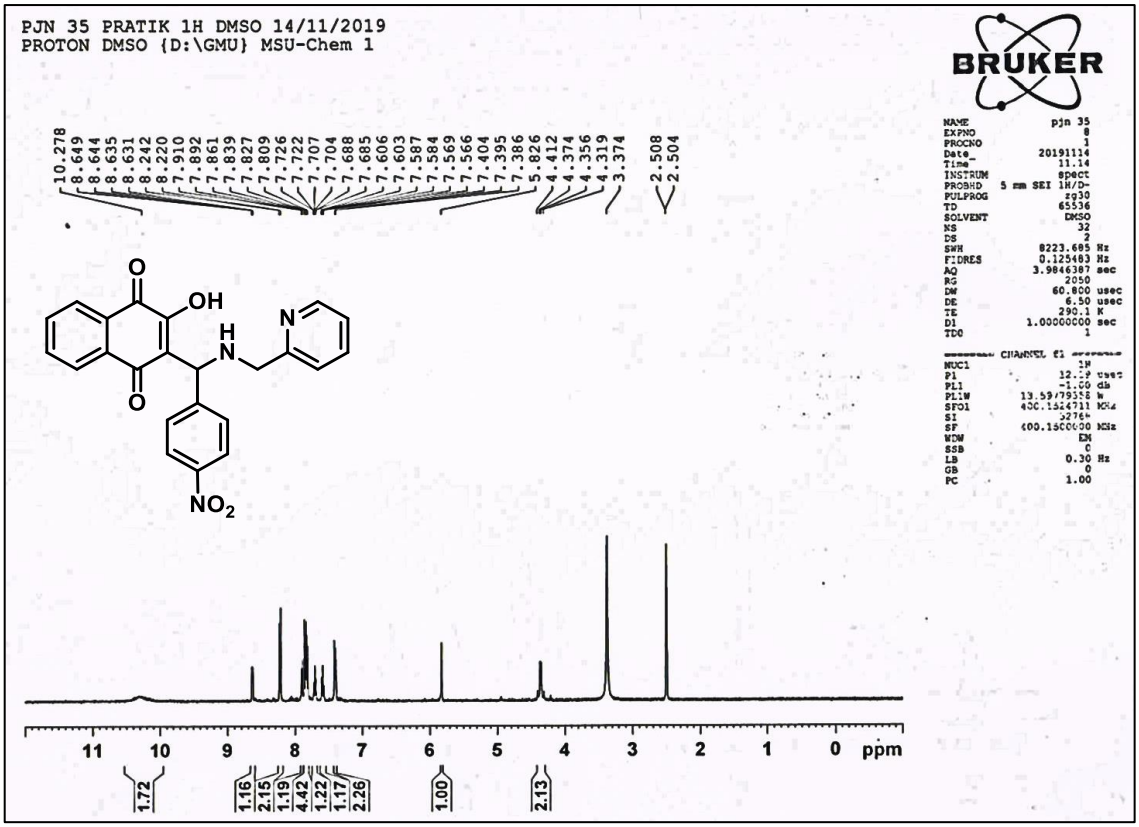

Figure S2.51 ^{1}H NMR spectra of compound **15**

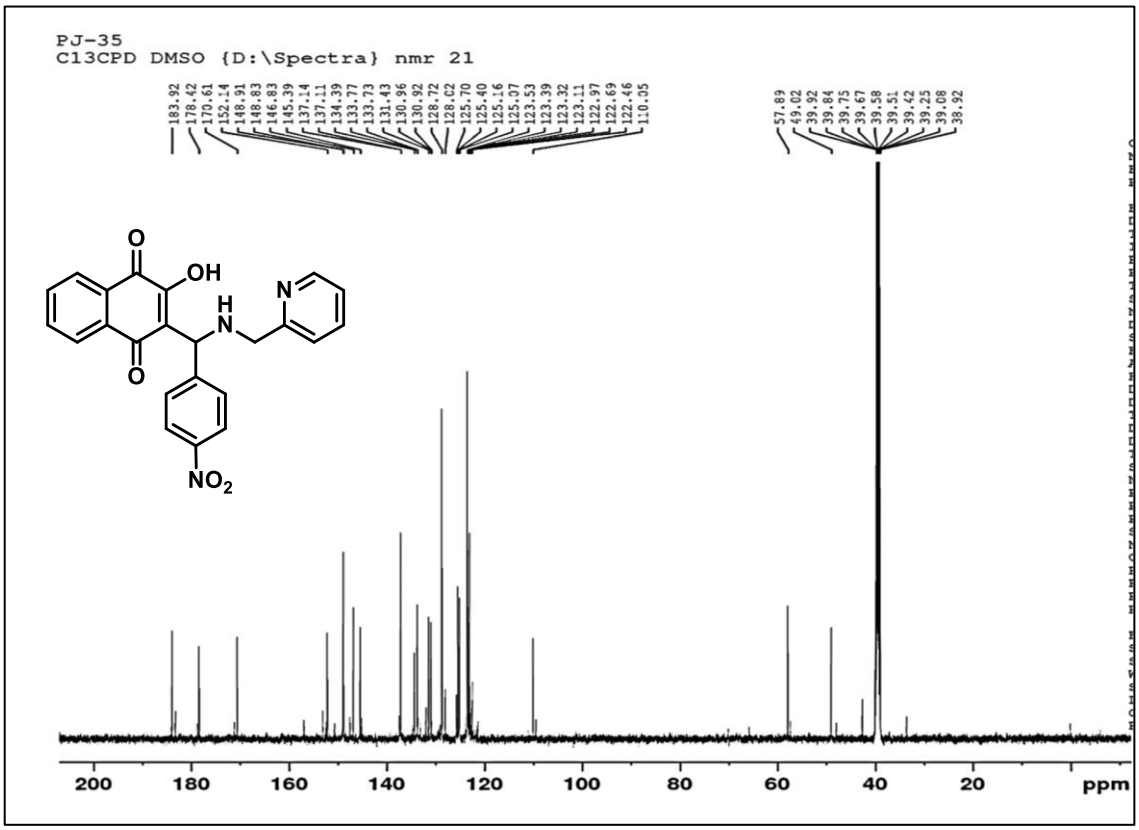

Figure S2.52 ^{13}C NMR spectra of compound **15**

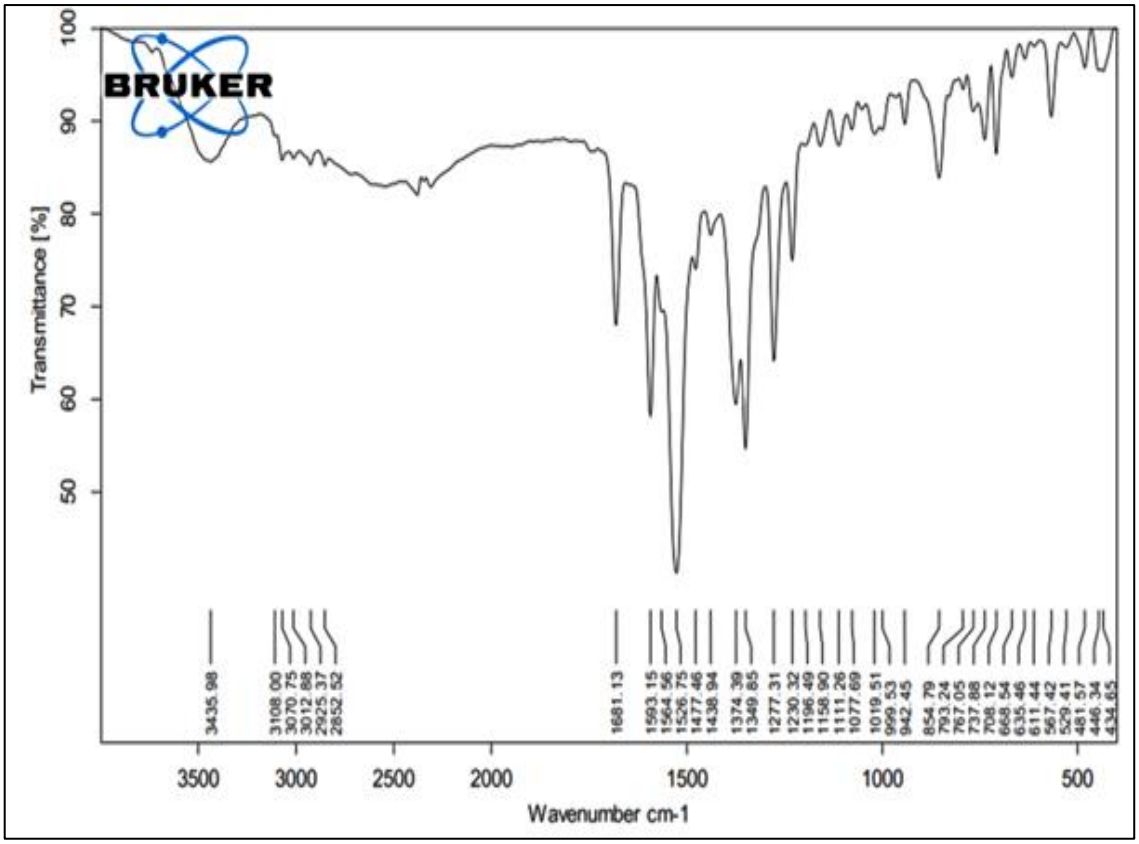

Figure S2.53 FT-IR spectra of compound **15**

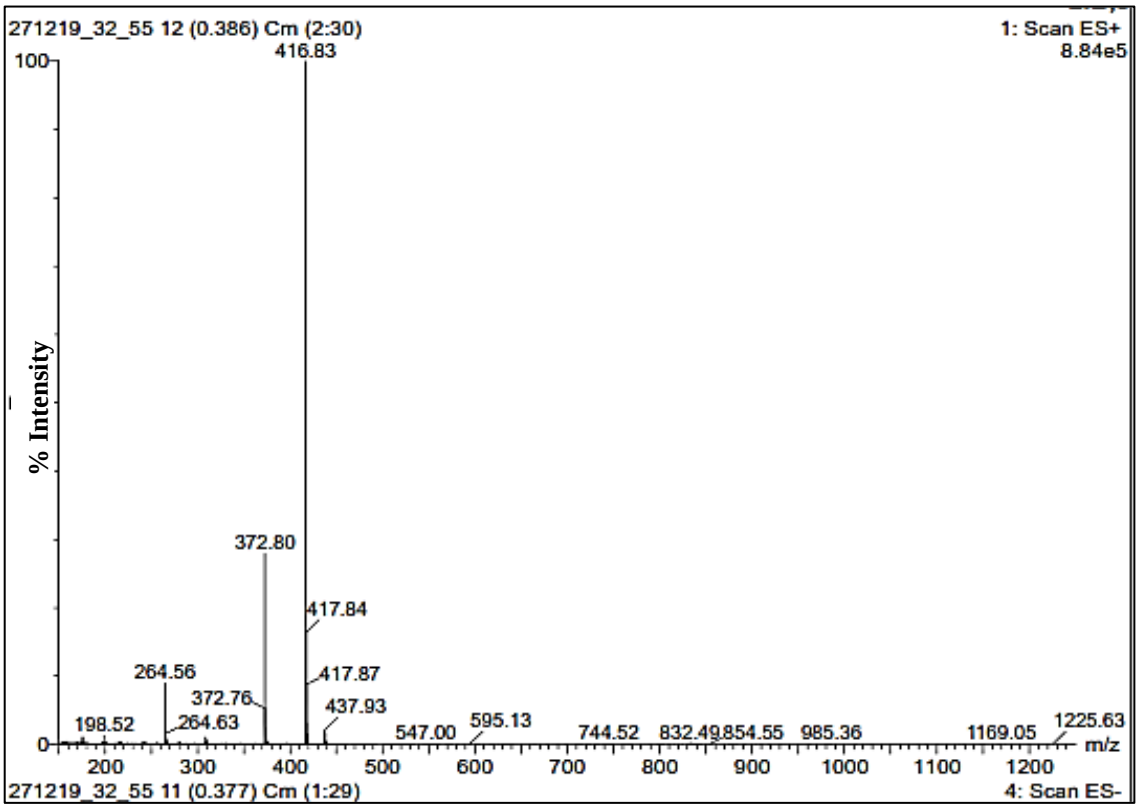

Figure S2.54 ESI-MS spectra of compound **15**

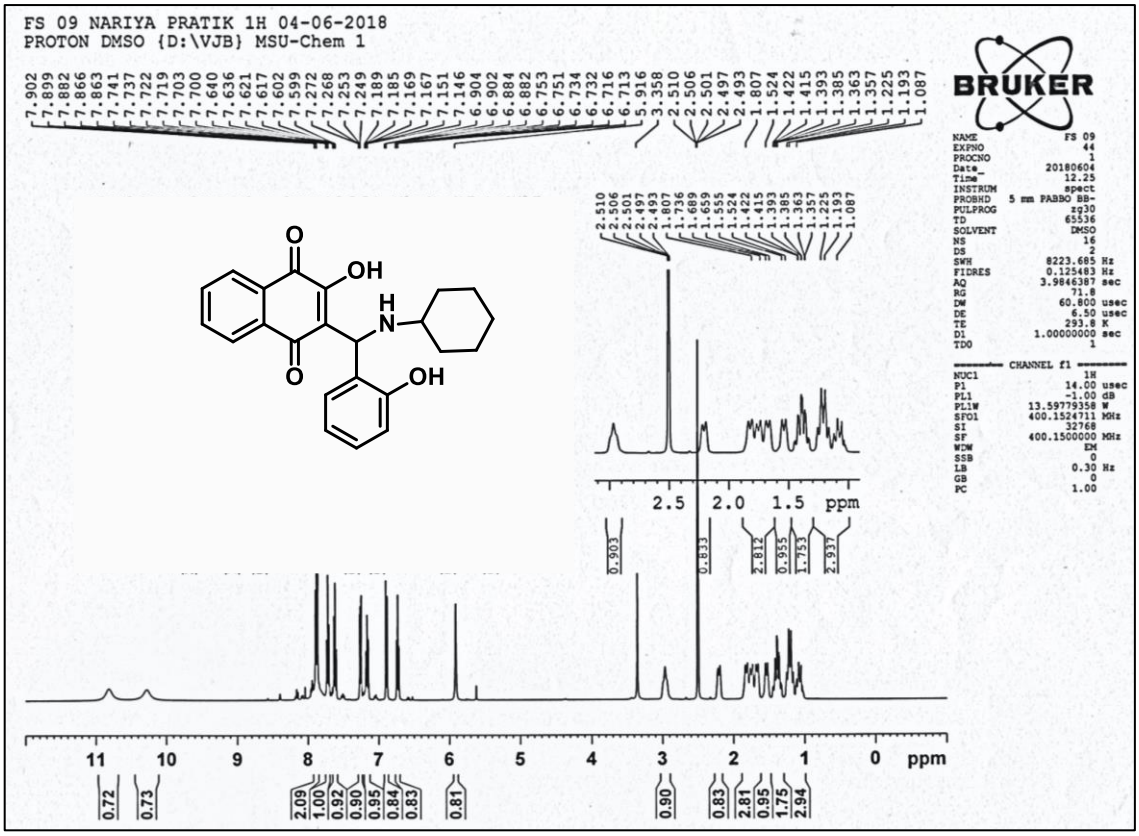

Figure S2.55 ^{1}H NMR spectra of compound **16**

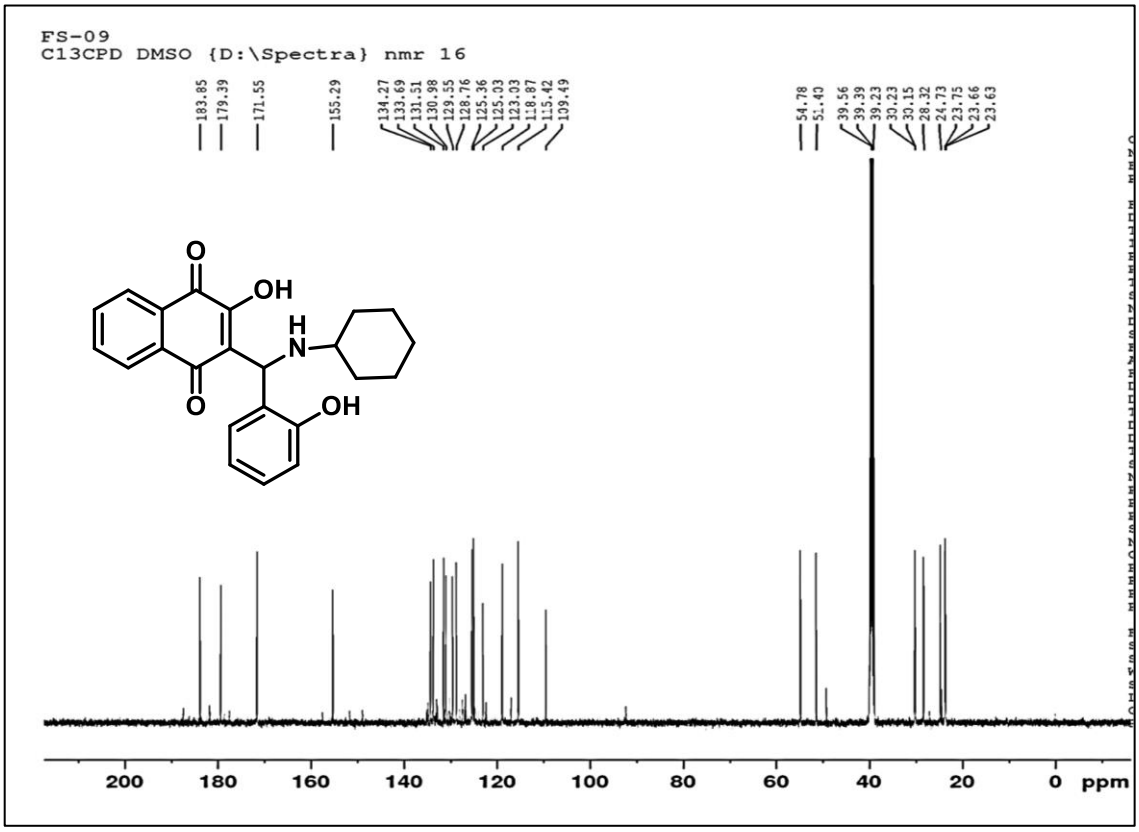

Figure S2.56 ^{13}C NMR spectra of compound **16**

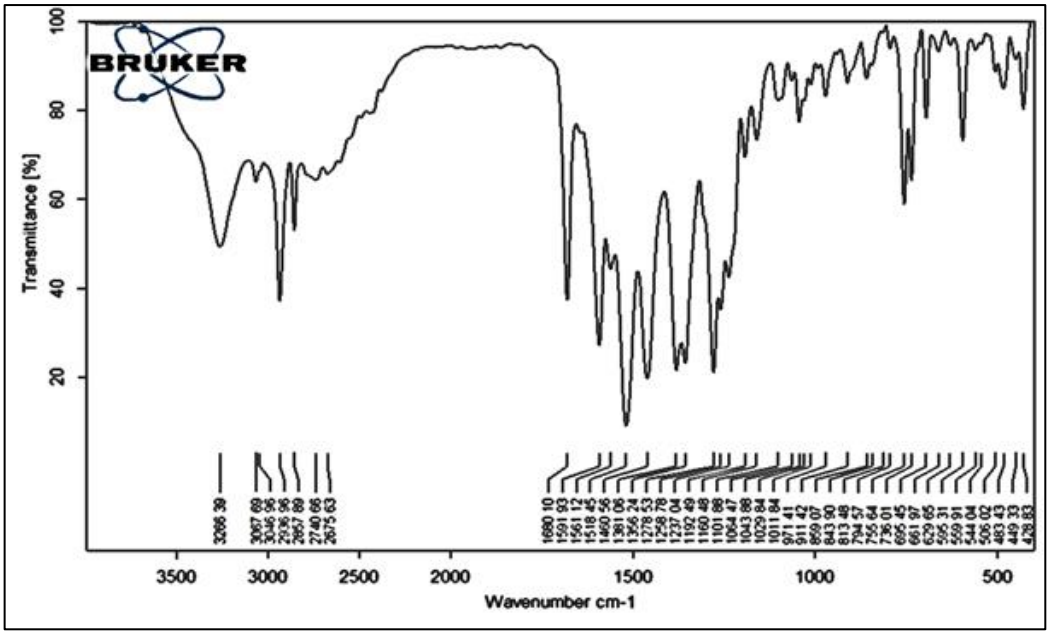

Figure S2.57 FT-IR spectra of compound **16**

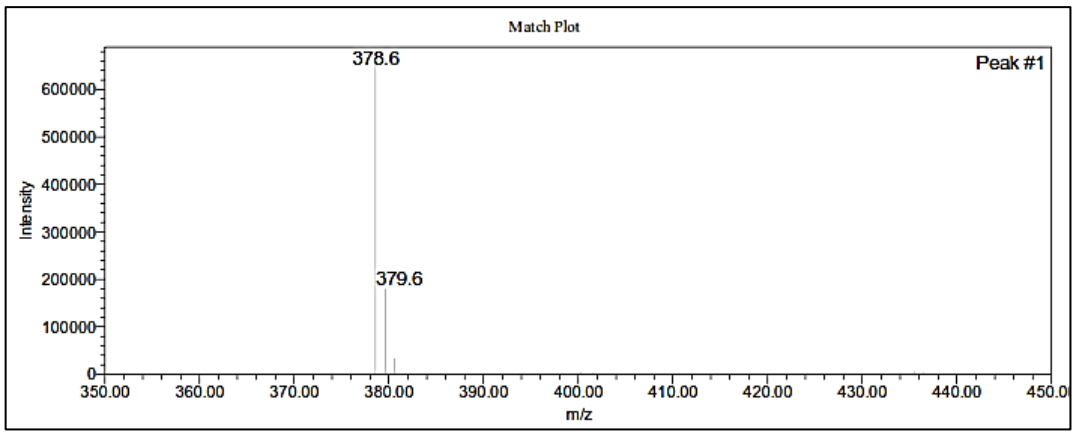

Figure S2.58 ESI-MS spectra of compound **16**

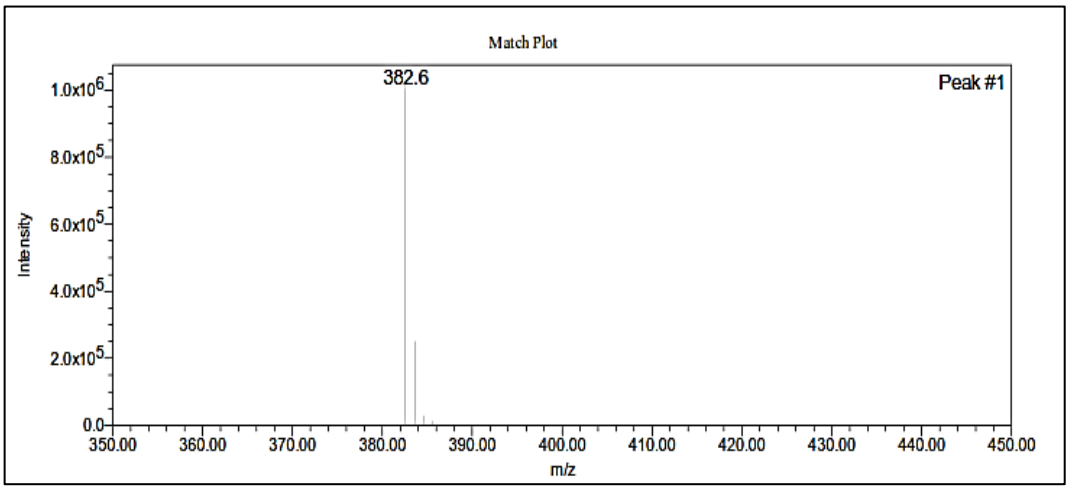

Figure S2.59 ESI-MS spectra of compound **17**

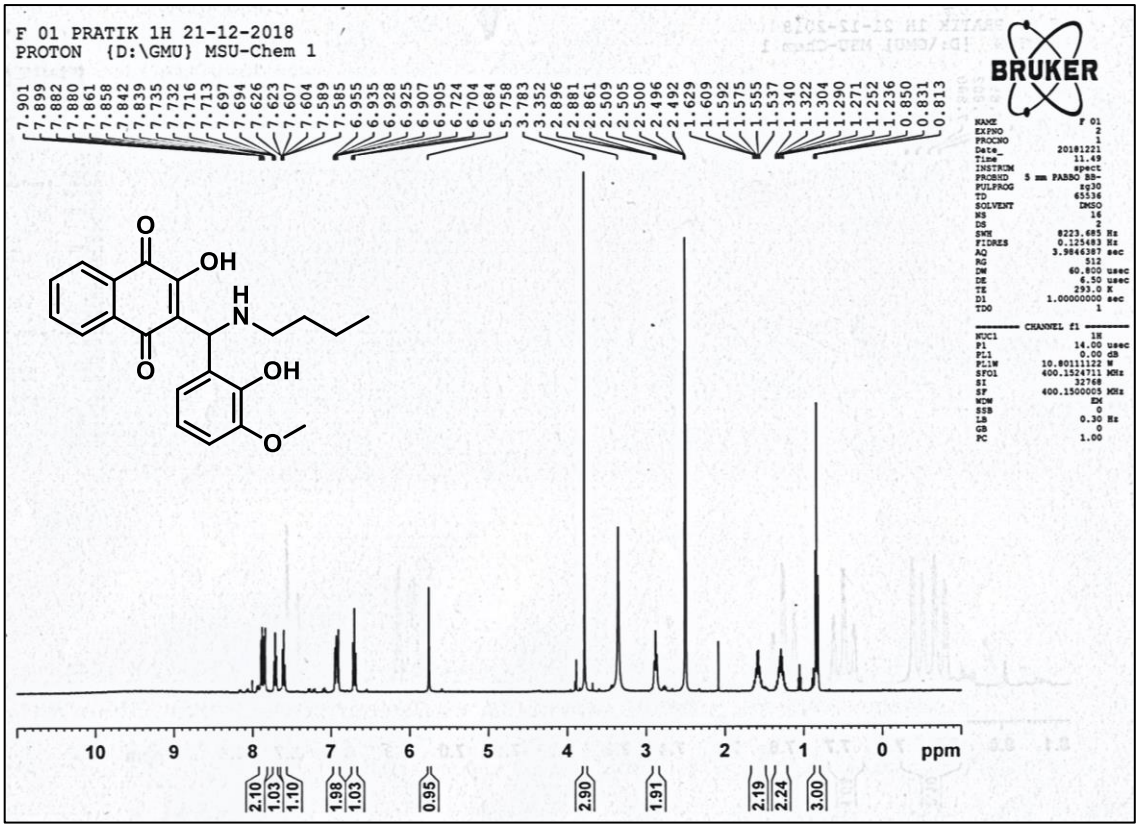

Figure S2.60 ^{1}H NMR spectra of compound **17**

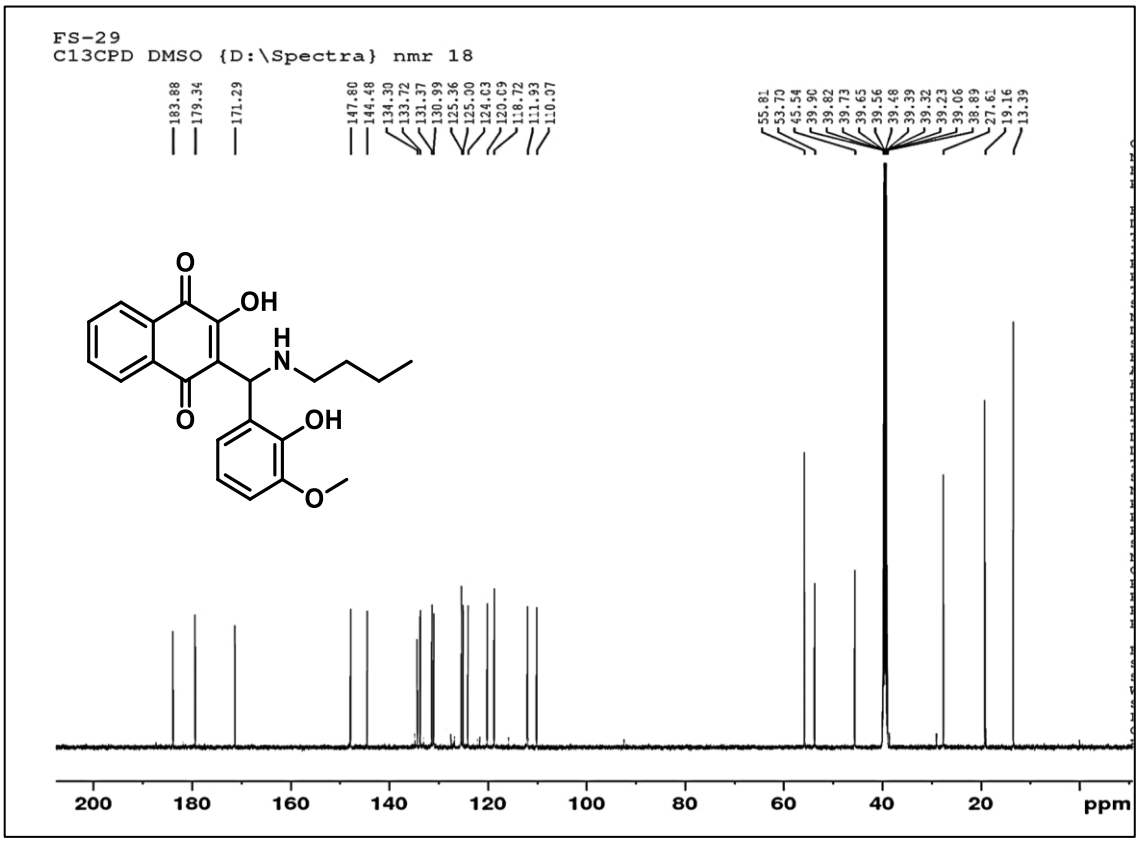

Figure S2.61 ^{13}C NMR spectra of compound **17**

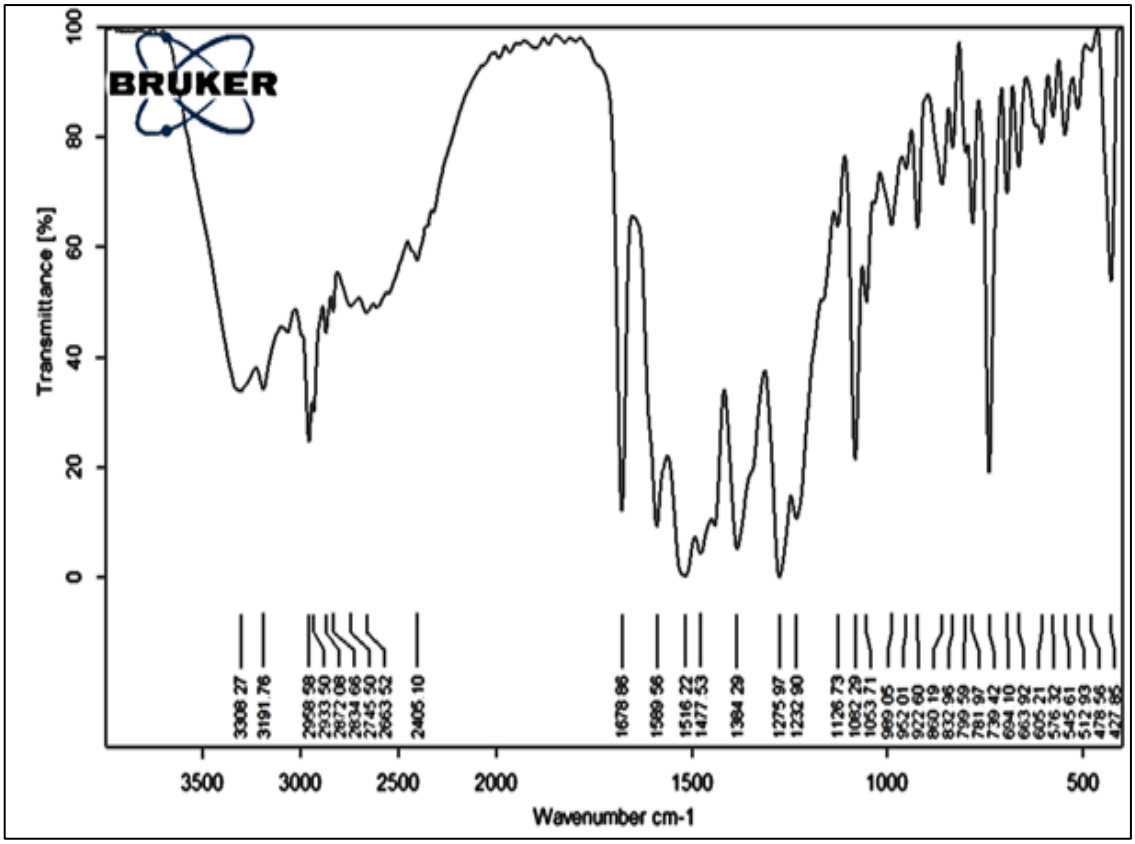

Figure S2.62 FT-IR spectra of compound **17**

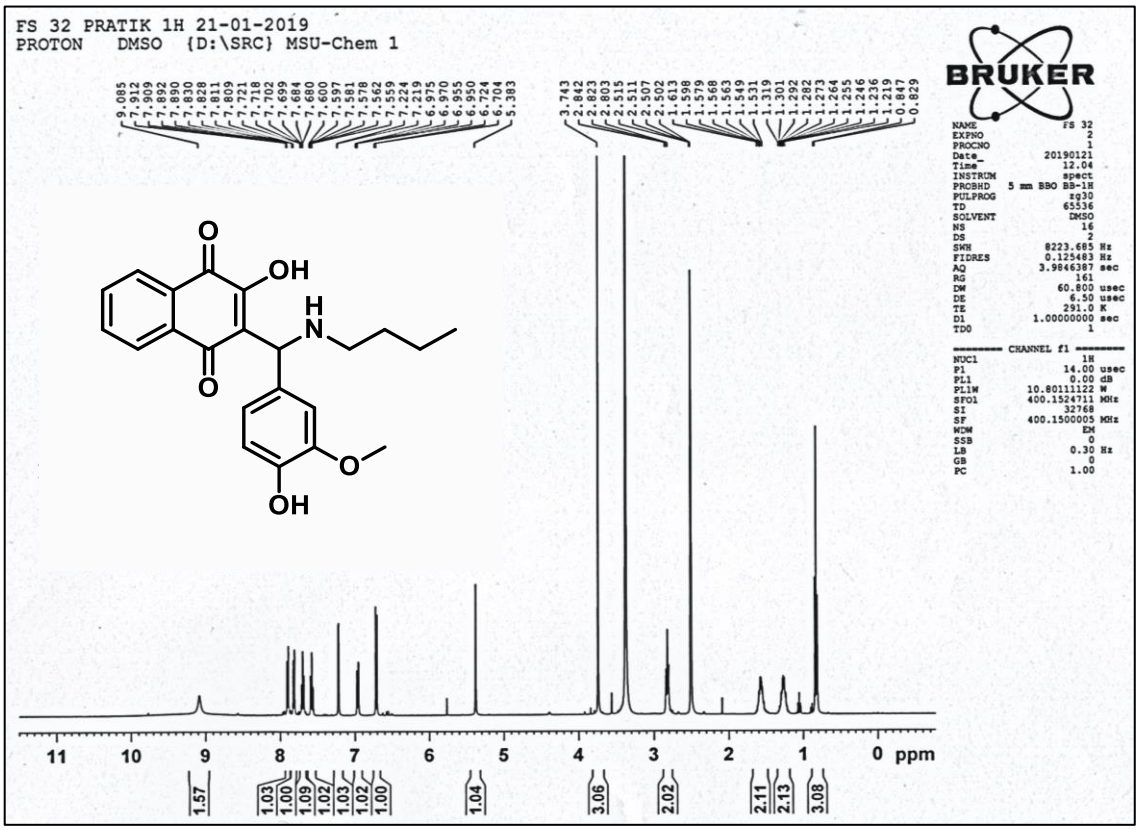

Figure S2.63 ^{1}H NMR spectra of compound **18**

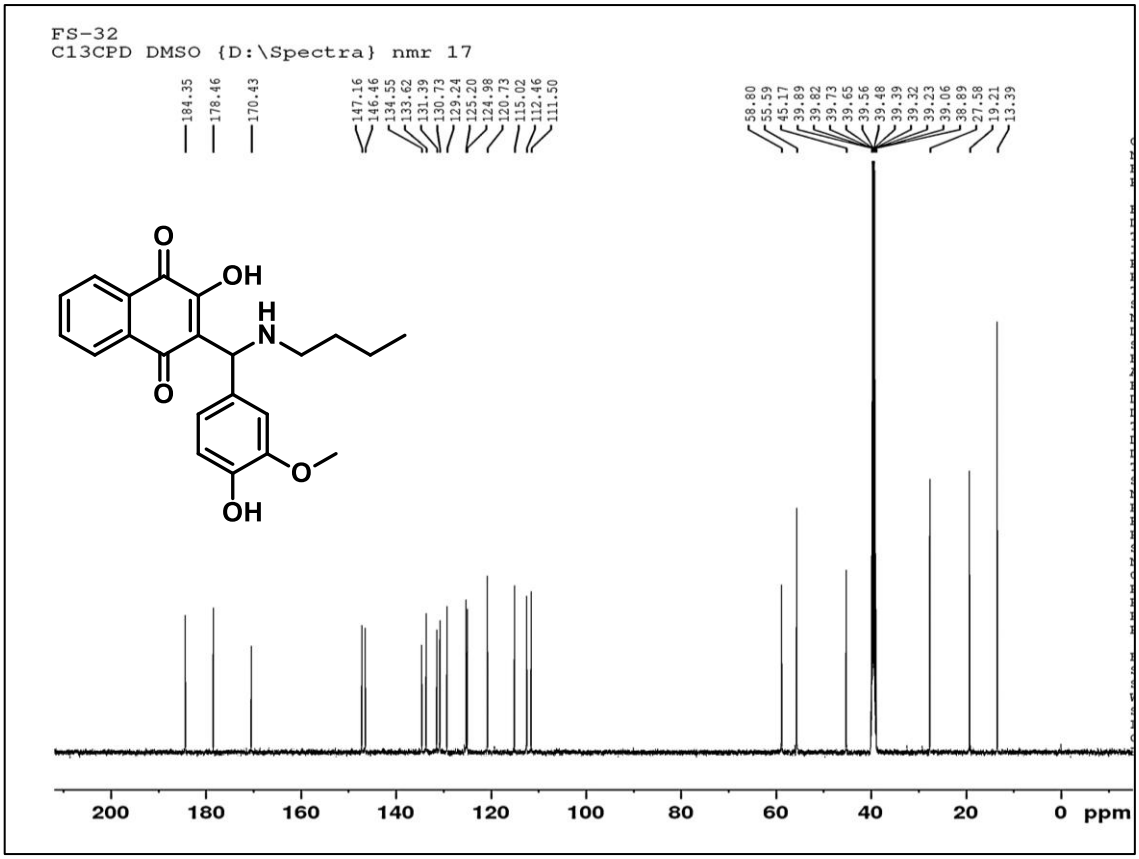

Figure S2.64 ^{13}C NMR spectra of compound **18**

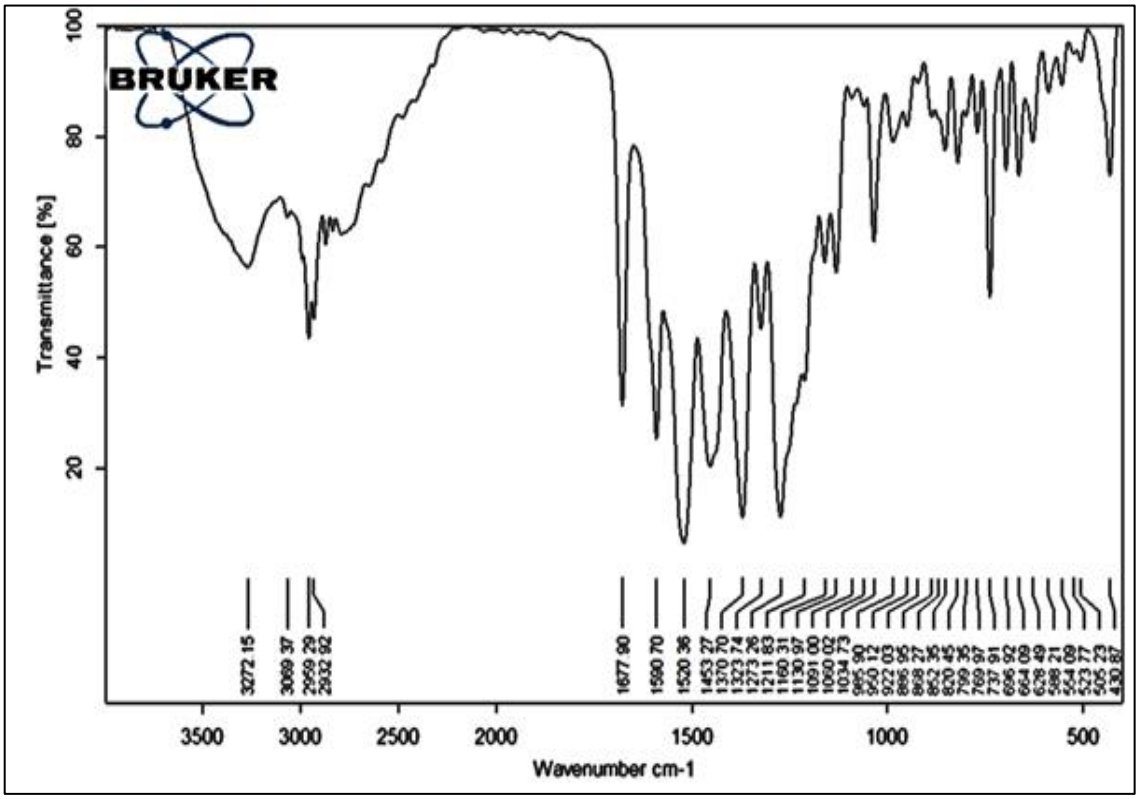

Figure S2.65 FT-IR spectra of compound **18**

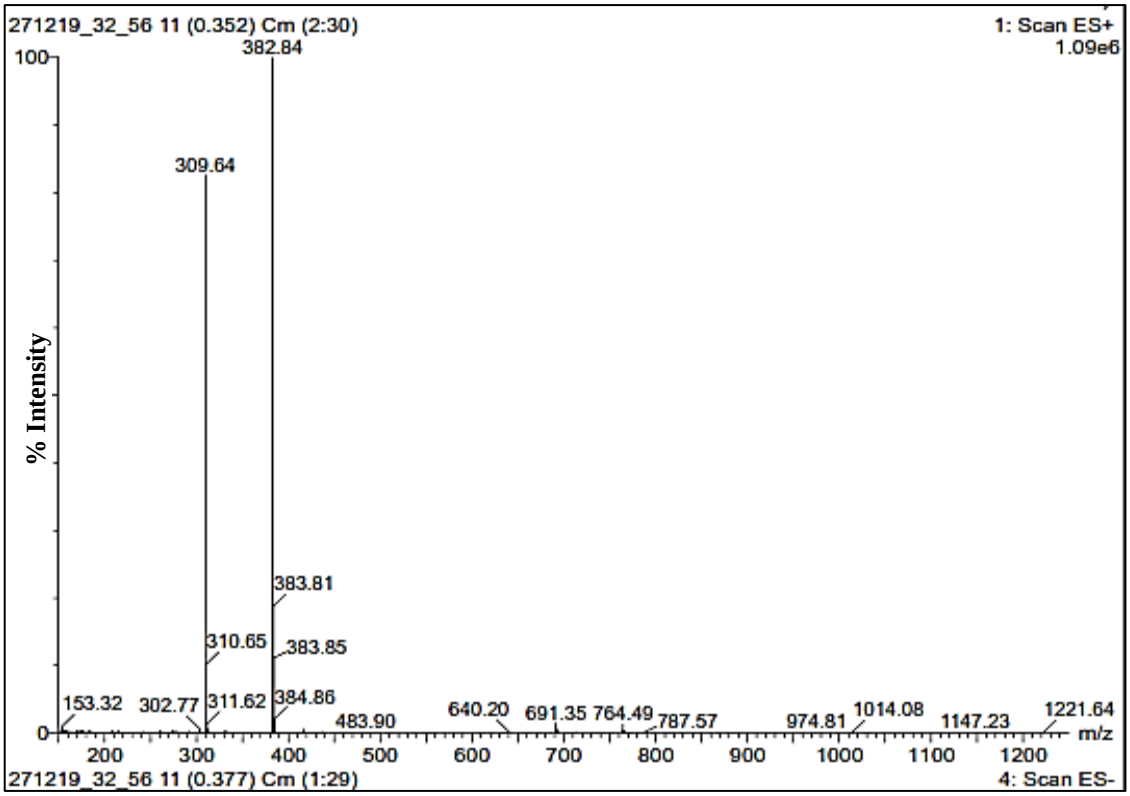

Figure S2.66 ESI-MS spectra of compound **18**

2.6 References

1. Wellington, K. W. Understanding cancer and the anticancer activities of naphthoquinones-a review. *RSC Adv.* **5**, 20309–20338 (2015).
2. Kumar, B. S. *et al.* Synthesis of pharmacologically important naphthoquinones and anticancer activity of 2-benzyllawsone through DNA topoisomerase-II inhibition. *Bioorganic Med. Chem.* **25**, 1364–1373 (2017).
3. Sreelatha, T. *et al.* Synthesis and SAR study of novel anticancer and antimicrobial naphthoquinone amide derivatives. *Bioorganic Med. Chem. Lett.* **24**, 3647–3651 (2014).
4. Jordão, A. K., Vargas, M. D., Pinto, A. C., da Silva, F. de C. & Ferreira, V. F. Lawsone in organic synthesis. *RSC Adv.* **5**, 67909–67943 (2015).
5. Baiju, T. V. *et al.* Quinonoid compounds via reactions of lawsone and 2-aminonaphthoquinone with α-bromonitroalkenes and nitroallylic acetates: Structural diversity by C-ring modification and cytotoxic evaluation against cancer cells. *Eur. J. Med. Chem.* **151**, 686–704 (2018).
6. Anaissi-Afonso, L. *et al.* Lawsone, Juglone, and β-Lapachone Derivatives with Enhanced Mitochondrial-Based Toxicity. *ACS Chem. Biol.* **13**, 1950–1957 (2018).

7. Ahmad, A. *et al.* New ferrocene modified lawsone Mannich bases with anti-proliferative activity against tumor cells. *J. Saudi Chem. Soc.* **21**, 105–110 (2017).
8. Tandon, V. K., Yadav, D. B., Chaturvedi, A. K. & Shukla, P. K. Synthesis of (1,4)-naphthoquinono-[3,2-c]-1H-pyrazoles and their (1,4)-naphthohydroquinone derivatives as antifungal, antibacterial, and anticancer agents. *Bioorganic Med. Chem. Lett.* **15**, 3288–3291 (2005).
9. Neves, A. P. *et al.* Exploring the DNA binding/cleavage, cellular accumulation and topoisomerase inhibition of 2-hydroxy-3-(aminomethyl)-1,4-naphthoquinone Mannich bases and their platinum(II) complexes. *J. Inorg. Biochem.* **119**, 54–64 (2013).
10. Oliveira, K. M. *et al.* Selective Ru(II)/lawsone complexes inhibiting tumor cell growth by apoptosis. *J. Inorg. Biochem.* **176**, 66–76 (2017).
11. Bala, S., Sharma, N., Kajal, A., Kamboj, S. & Saini, V. Mannich Bases: An Important Pharmacophore in Present Scenario. *Int. J. Med. Chem.* **2014**, 1–15 (2014).
12. Al Nasr, I. *et al.* Antiparasitic activities of new lawsone Mannich bases. *Arch. Pharm. (Weinheim).* **352**, 1–9 (2019).
13. Mahal, K. *et al.* Improved anticancer and antiparasitic activity of new lawsone Mannich bases. *Eur. J. Med. Chem.* **126**, 421–431 (2017).
14. da Silva, G. B., Neves, A. P., Vargas, M. D., Marinho-Filho, J. D. B. & Costa-Lotufo, L. V. New insights into 3-(aminomethyl)naphthoquinones: Evaluation of cytotoxicity, electrochemical behavior and search for structure–activity correlation. *Bioorganic Med. Chem. Lett.* **26**, 3537–3542 (2016).
15. Hossain, M., Das, U. & Dimmock, J. R. Recent advances in α,β-unsaturated carbonyl compounds as mitochondrial toxins. *Eur. J. Med. Chem.* **183**, (2019).
16. Filho, J. F. A., Lemos, B. C., de Souza, A. S., Pinheiro, S. & Greco, S. J. Multicomponent Mannich reactions: General aspects, methodologies and applications. *Tetrahedron* **73**, 6977–7004 (2017).
17. Neves, A. P. *et al.* Novel aminonaphthoquinone Mannich bases derived from lawsone and their copper(II) complexes: Synthesis, characterization and antibacterial activity. *J. Braz. Chem. Soc.* **20**, 712–727 (2009).
18. Oramas-Royo, S. *et al.* Synthesis and cytotoxic activity of metallic complexes of lawsone. *Bioorganic Med. Chem.* **21**, 2471–2477 (2013).
19. Soni, J. Y., Sanghvi, S., Devkar, R. V. & Thakore, S. Synthesis and evaluation of

novel quinuclidinone derivatives as potential anti-proliferative agents. *RSC Adv.* **5**, 82112–82120 (2015).

20. Das, M. *et al.* B-Cyclodextrin Based Dual-Responsive Multifunctional Nanotheranostics for Cancer Cell Targeting and Dual Drug Delivery. *Carbohydr. Polym.* **206**, 694–705 (2019).
21. Upadhyay, K. K. *et al.* Carbon monoxide releasing molecule-A1 improves nonalcoholic steatohepatitis via Nrf2 activation mediated improvement in oxidative stress and mitochondrial function. *Redox Biol.* **28**, 101314 (2020).